UNIVERSITA' DEGLI STUDI DI PADOVA

NORTHUMBRIA UNIVERSITY OF NEWCASTLE

TESI DI LAUREA MAGISTRALE IN INGEGNERIA ELETTRICA

DESIGN AND REALIZATION OF A BIDIRECTIONAL EV BATTERY CHARGER FOR V2G AND G2V PURPOSES

RELATORI: **PROF. GHANIM PUTRUS**

PROF. ROBERTO TURRI

LAUREANDO: **ALBERTO SGARBOSSA**

ANNO ACCADEMICO 2013/2014

" Love is not love Which alters when it alteration finds, Or bends with the remover to remove:
O no! it is an ever-fixed mark That looks on tempests and is never shaken;
It is the star to every wandering bark, Whose worth's unknown, although his height be taken.
Love's not Time's fool, though rosy lips and cheeks Within his bending sickle's compass come:
Love alters not with his brief hours and weeks, But bears it out even to the edge of doom.
If this be error and upon me proved, I never writ, nor no man ever loved".

W. Shakespeare

Contents

Abstract

The continuous development of electric drive systems and battery technology has made the Electric Vehicle technology (EV) a more competitive option in the market with conventional vehicles. Among other merits, EVs can also provide ancillary services to support the grid (acting as controlled loads or energy storage units) in order to provide supply/demand matching to level the daily load profile and contribute to voltage and frequency control. The large deployment and wide spread of EVs in the future will provide the opportunity for this support to be implemented on a large scale, and the positive effects on the grid will be increased linearly as a function of the amount of vehicles connected to it.

The EV needs to be connected to the grid via a smart interface controller. Using the EV as a controlled load only (G2V), a controller which handle unidirectional power flow is required, whilst according to the implementation of V2G mode (EVs supply power to the grid) the converter is required to have bidirectional capability. The research described in this dissertation deals with the development of a bidirectional battery charger which allows bidirectional power flow during battery charging (G2V) and during the flow of battery's stored energy to the grid (V2G), based on control signals from the grid and battery management system (BMS). The regulatory standards on power quality influence the topology and the control system of the converter.

The topology and the control strategy adopted for the bidirectional battery charger will be introduced and analysed with the support of the Simulink software. After the tests conducted on the model, the battery charger will be physically realised and connected to the grid by the use of the dSPACE platform, in order to verify the correct functioning of the device. This tool is necessary to control the physical system already built, implementing the signals coming from the Simulink model, acting as an interface between the logic world of the software and the physical world of the converter. The most relevant results in the real physical world, checked with the use of an oscilloscope, will be then analysed.

1. Introduction

The spreading of electrical mobility into a vehicle market which is mostly dominated by thermal mobility can be explained with basically three reasons: there are, indeed, some issues dealing with *internal combustion engine* (ICE) that can be investigated. The **first problem** posed is in terms of ecology: mitigation and elimination of polluting emissions is an objective followed by the most of the world's countries. Greenhouse emissions have a strong impact on health and environment, and the thermal mobility is the most important cause of it. The **second problem** deals with economy: despite of their high energy density, which made them very useful in traction field, fuels derived from oil are non-renewable resources, and it is demonstrated that the costs for them will inevitably increase with time, so consequently the traditional traction costs will become higher year after year. The **final problem** deals with the fact that an electric motor can guarantee a higher efficiency than an ICE; the highest efficiency of an ICE can be evaluated to be around 33%, whilst the efficiency of an electric motor can be evaluated to be around 90%. However, electrical traction cannot overcome completely all these problems: for example, the power which nowadays charges the battery of the vehicle can't be fully produced by renewable sources of energy (environmental issue), and producers will go on using oil for power production in the future. The spreading of EVs can be a valid alternative to mitigate mobility issues. At the same time, it can give important advantages to the same grid, according with electrical energy production and distribution [1].

The meaning of the term *electrical vehicle* (EV) can be analysed in a deeper way, since different kinds of topology are defined with these words [2]. An **electrical vehicle** is a fully or partially propelled by an electric motor vehicle, which is fed by electric or electric-related energy sources. If there is full electric propulsion, the vehicle is called *purely electric vehicle* (PEV). If the energy source is a battery, the acronym (BEV) is used; if it is a fuel cell, instead, the PEV is called (FCEV). **Hybrid electric vehicles** (HEV) are vehicles where one of the energy sources is electricity and the other one is commonly a fossil fuel. Two different types of hybrid electric vehicles can be found: HEV and *Plug-in HEV* (PHEV). Although they are both hybrid vehicles, only PHEVs have the possibility of being connected to the grid using a battery charger, whilst HEVs' battery is not accessible. This is a very important characteristic, since the design and the size of the entire electric system of the two different vehicles will be different. For instance, EV technology presents an excellent way to reduce oil consumption for traction, by the use of the regenerative braking, which contributes to decrease the total amount of losses of the vehicle.

An aggressive introduction of efficient HEVs in the national market will only slow the increase of fossil fuels demand, but this won't reverse the trend of a mobility which is still strongly dependent from fossil fuels. PHEV technology, instead, extends the capability of the HEV, since oil consumption can be massively substituted by the use of the electricity. The possibility to charge the battery from the utility grid (at home or in electrical station) almost frees the vehicle from the need of fossil fuels, because the main energy carrier would be the power which is stored in the battery, and the oil will be considered as an auxiliary energy carrier. The vehicles considered in this work are the ones which can be connected to the grid by the use of a plug: this means that the battery charger considered in this dissertation will be suitable for PHEV and BEV technology, and it will basically act as an interface between the grid and the battery.

Before considering the grid point of view, even the **vehicle side** has to be analysed. This analysis is important because the design of the battery charger will vary in function of the characteristics of the vehicle. Two different topologies can be faced considering (for instance) a PHEV, which are series (Fig. 1 a)) or parallel (Fig. 1 b)) drivetrain architectures. For the improvement of the system, the design of a more developed battery charger can be introduced, if the same architecture will admit it . For instance, the winding of the electric motor can be used as inductors [3] [4] [5], or the battery charger, if it is composed by a three phase AC/DC converter, can be also used to run the same electrical motor. This means that the battery charger will not deal just with the battery, but

it can have a crucial role with regards to the whole EV's circuitry; the cooperation between charging and traction modes is becoming stronger and stronger, to allow the possibility of getting different functions starting from the same components.

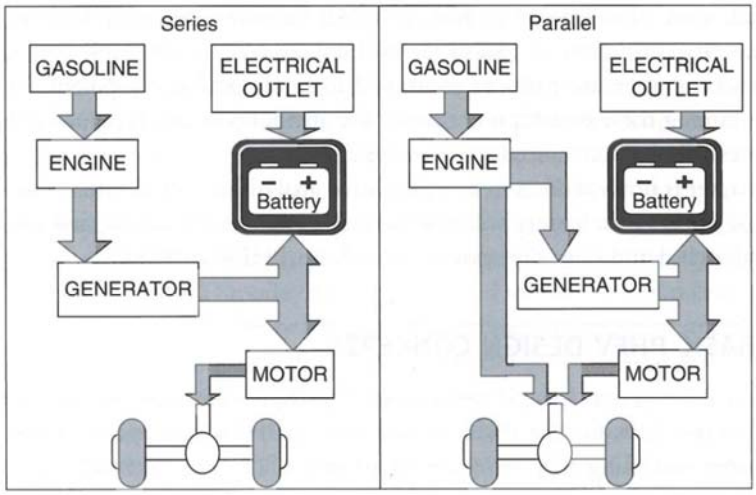

Figure 1 – Series and parallel drivetrain architecture for PHEVs [6]

An overview of the impact of the spreading of the electrical mobility from the **grid side** can be now analysed from the infrastructures point of view. In fact, the prediction of a high spread of the electrical mobility introduces modifications in the customers' usage of the grid. At the same time, the grid manager needs to be sure that the same grid is able to supply properly and in any instant the power required from entire previous original loads (houses, offices, and working places) whit the addition of these new EV loads. Will the current electric power infrastructures be able to match the increased demand of power brought by PHEVs? If the EVs will be considered as pure loads which cannot be piloted, the grid will face many difficulties; but whether the EV will be considered as "smart loads", whose energy flow can be modulated, the grid won't suffer from their spreading, and it will have instead some benefits from it.

Figure 2 describes "load duration curves" under different assumptions made on the penetration of EVs (considered as "smart loads"). A hypothesis on the percentage of EVs' spreading can be picked up, and in one year the power demanded to the grid for feeding all the loads is registered, hour by hour.

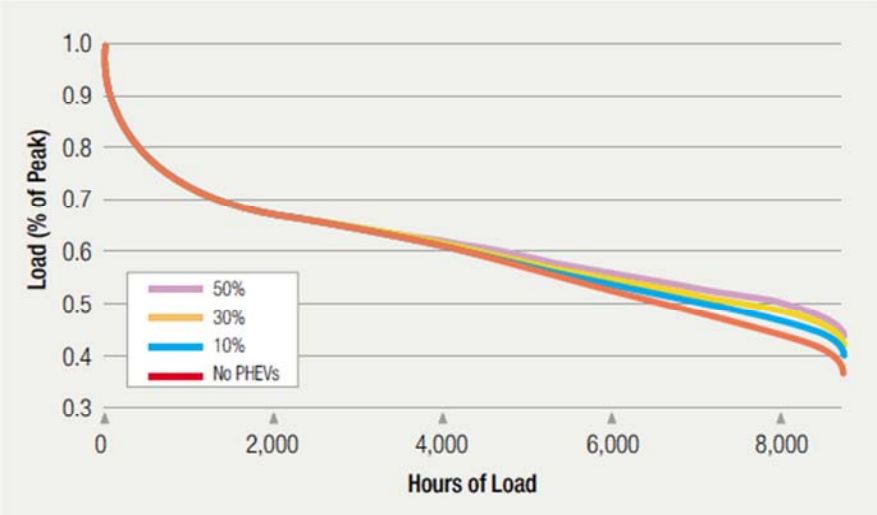

Figure 2 – Load duration curve with several hypothesis on the EVs spreading [7]

The load profile is then built in such a way that the peak power can be found at the extreme left and the lowest power peak is in correspondence of the extreme right, and all the other values are ordered according to this criterion. In this way, when a point of the profile is selected, the graph says that the power required by customers during the year has been equal or higher than the value that the same point shows in the vertical axis, for an amount of hours which is identified by the abscissa of the selected point. It's now possible to notice that new loads (EVs) do not contribute to the system's higher peak. Even in the case in which EVs are still pure loads (the power flow inversion from vehicle to the grid is not yet applied), the grid doesn't have any overload problem and, as a matter of fact, electric industry can sell more electrical energy without increasing the maximum power peak required to power plants. This is one of the most important advantages that the EV technology coupled with smart charging can bring to the grid.

The idea of the **power inversion** can be now considered: the power flows from the grid to the battery (*vehicle-to-grid*, V2G) when the battery is discharged and needs to be recharged after traction mode; but the bidirectional battery charger will be able to take back part of the energy stored in the same vehicle's battery when it is full and deliver it to the grid (*grid-to-vehicle*, G2V) [8]: the EV in this way is transformed to an "energy storage system" for the grid, in a way to furnish important ancillary services. The main services brought by this kind of system are, in fact, supply-demand matching, overcoming of difficulties associated with intermittent nature of renewable energy such as wind and PV, and voltage-frequency control. However, relevant advantages for the grid can be achieved only with significant spreading of the technology and also thanks to smart grid capabilities.
Here a classification of V2G applications is analysed more in detail.

- Virtual Power Plant: the whole EV's fleet can be seen as a virtual power plant, which can be employed in order to balance power supply and demand. In this way the power generated by traditional plants can be decreased during determined periods of time. The clear aim of this strategy is to replace the power that power plants should produce using the energy stored in EVs during peak periods, when the production is more expensive. In this way generation will become cheaper and there will be decrement of pollution. This model can be also used as a support of renewable energy sources, thanks to the possibility to store energy. Unfortunately a great lack of the system is pointed out: the real chances to set up a virtual power plant are low, due to the fact that battery capacity is not so high yet, and there's the need of lot of EVs all parked together and connected to the grid to have a power that can be useful for the grid.

- Application in Micro Grids: V2G can be used for services in micro grids and autonomous islands, supplying active or reactive power to grid. In particular, applications in these contexts assume particular stress, because in such grids power comes in many cases from renewable energy. EVs can reduce the uncertainty of renewable energy resources, thanks to their ability on storing energy.

- Utilizing as V2B/V2H: EVs can be used to meet demand in peak hours, but the flow of energy can be carried out not only for vehicles to the whole grid, but from vehicles to single buildings (V2B) or to houses (V2H). Actually, there is strong interest in public charge locations such as shopping centre or places of work, where vehicles can be connected when they are parked. Equipping car park with a proper smart controller makes possible the use of energy stored in batteries, smoothing the load curve of the same building. One of the best advantages in this application is surely the fact that it is easier to control than the virtual power plant, because the number of vehicle to be controlled is definitely lower.

The most promising markets for V2G power flow are those services that electric industry calls ancillary services. These are services that the grid needs twenty-four hours per day, seven days per week; for this project there is the necessity of a great penetration of EVs, and every time a big amount of vehicles has to be available. Among the others, there is a specific ancillary service, very important for the grid: the frequency regulation. In particular, EVs are well suited to provide this service thanks to their fast and accurate response to operator's signals, and usually not a prohibitive energy request is made. Nowadays, frequency regulation services are supplied by

electric generators, which are switched on or off in function of an automatic signal, which deals with the mismatch between supply and demand. If demand is greater than generation, regulation up is required and the signal will induce generators to increase the power delivered to the grid, and vice versa. The new idea which can help these generators is to use the energy stored in the batteries of the vehicle, when this solution is possible. This means that regulation up is equal to the discharge of the battery; regulation down is equal to the charge of it. An issue that comes directly from this service is that storage resources providing frequency regulation are basically related to the random nature of the same regulation service: a prolonged period of regulation down, for example, could charge completely the battery pack of the vehicles. In this case, the fleet would be unable to receive power from regulation and provide services to the grid (this depends on the severity of the disease and the global capacity of the storage units which are connected). That's why the grid operator should know, on average, the portion of regulation reserve that is available for ancillary service from storage resources; at the same time, the grid manager needs in any instant an adequate number of EV composing the fleet: a minimum power threshold has to be always guaranteed.

With the word "V2G" it is implied the flow of active power from vehicle to grid; adding this mode to the traditional "G2V", the active power flow is represented with continuous charge and discharge cycles of the battery, and this can reduce the same battery's lifetime. This is an important disadvantage of the entire application. Consumers can disagree and not allow the carrying out of these operations. However, there is an application in which the battery's cycles of charge and discharge are not engaged: this is the case of **reactive power** operations [9]. On board chargers are able to provide applications such as reactive power compensation and voltage regulation without the charging or the discharging of the battery. The reactive power which is absorbed in correspondence of the load side is transmitted from the generation system to the load through transmission and distribution networks: this causes the increment of energy losses and the decrement of the efficiency of the system. EVs can supply this reactive power locally without forcing the grid to generate it and send it through the network; consumers owning an EV that carries an on board battery charger can negotiate with the utility grid to allow the usage of the same charger for grid support, compensating the reactive current, also for other consumers close to him that haven't an EV (Fig. 3). The generation of reactive power in correspondence of the common coupling point provides an increased efficiency of the system and decreases also the transformer's overloading. The importance of this reactive compensation stands on the fact that all can be made despite of the state of charge of the battery; converters are almost always able to supply reactive power.

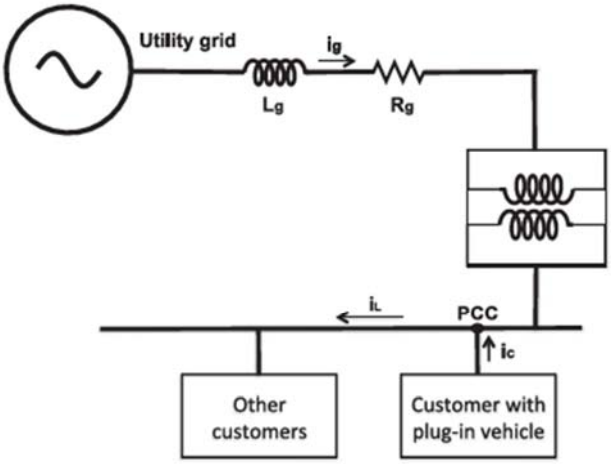

Figure 3 – Reactive power regulation with EV connected to the PCC [9]

The effective realization of a model like this in the real world is still not so easy, because lot of parameters are able to influence the spreading of electrical mobility, which are not linked only to technological issues. First of

all, fuel price can be a strong variable that influences consumers. This price is subjected to frequent fluctuations, and it's demonstrated that lower prices correspond to reduction of EV's purchases and vice versa. Also the gap between consumer's expectations and performances of an electric vehicle has to be considered; but the most important issue is related to the fact that there is difference between power markets: for some countries, V2G would not be so much beneficial from the economical point of view. Barriers of different natures are present and still strong: consumer's behaviour, economic incentives, cultural and social contests have here great importance. Government supports are needed to overcome these non-technical issues, trying to create the background for making the electrical traction a strong and reliable system.

Setting aside the requirement for all this kind of non-technical issues, the proposed work means to design a battery charger which can be suitable for G2V and V2G modes in order to overcome all the technological obstacles that can interfere with the effective bidirectional power flow from the EV point of view. After the analysis of the role of each single component of the device, a block scheme will be built, in order to check the stability of the system, and the proper controller will be applied. The last step will consist in the practical realization of the device in the laboratory.

2. The Bidirectional Converter

This chapter deals with all the battery charger's fundamental characteristics that make it suitable for the achievement of the bidirectional power flow [10].

All the different options to build an electric vehicle which can support both traction mode and the grid pass through the necessity to design a bidirectional battery charger. The power has to be allowed to flow from the power supply to the battery for the reload of the same battery, and from the battery to wheels or to the same grid. Even in case of braking there should be the opportunity to convert kinetic energy into electric energy through the electric motor (regenerative braking). Figure 2.1 shows the block scheme of the battery charger, where thick lines represent the power flow and fine lines represent the data flowing from each block to the controller and vice versa The proposed configuration consists into two different main blocks. The first one is a DC/DC bidirectional converter, which has to link the battery and a capacitor, called DC link; the second one will be the AC/DC converter, which will be connected at one side to the capacitor, and at the other side to the grid. By the use of some relays, if the battery charger is designed for a three phase power supply, the same converter will be able to run the motor and perform even traction mode (dashed line).

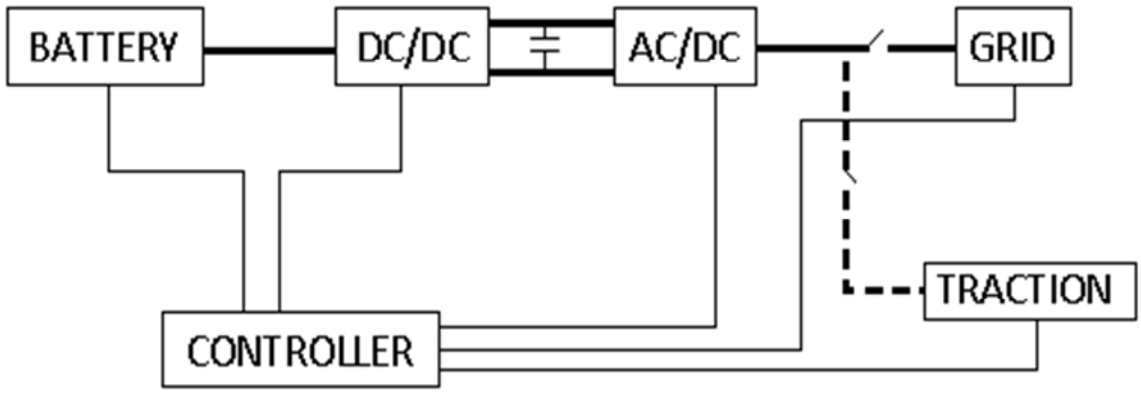

Figure 2.1 – Block scheme of the battery charger

Every single block has to be linked with the controller through data flow wires for monitoring, control and safety purposes. In this way indeed the controller is able to recognize the state in which every block is in any instant of the working mode (data flowing from the circuit to the controller), but at the same time it can pilot the DC/DC converter and the AC/DC converter in function of all the information which it gets from the circuit (data flowing from the controller to the circuit). This is important because every part of the system has to run both in function of the other parts composing the system and in function of some internal parameters, which can be for instance the SOC or the temperature of the battery, and in function of some external parameters, like the amount of active power required by the grid in case of emergency. All the thick lines represent the bidirectional power flow: if grid-battery system is involved, V2G and G2V modes correspond to the two modes that can be applied, and the power flowing consists both of active and reactive power; whether the system composed by electric motor (instead of the grid) and battery is involved, the two modes which produce two opposite power flows are traction mode and regenerative braking mode.

2.1 AC/DC Converter

2.1.1 – H BRIDGE CONVERTER

The AC/DC converter is the heart of the battery charger system [11] [12]. It works as a rectifier when the power flows from the grid to the battery and as an inverter when the flow is reversed: this makes the bidirectional requirement always verified. The full bridge inverter (H Bridge) is the most used configuration in standard industrial applications, thanks to its simple topology and low number of switching devices and elements needed for its realization; fig 2.2 depicts the circuitry of the design.

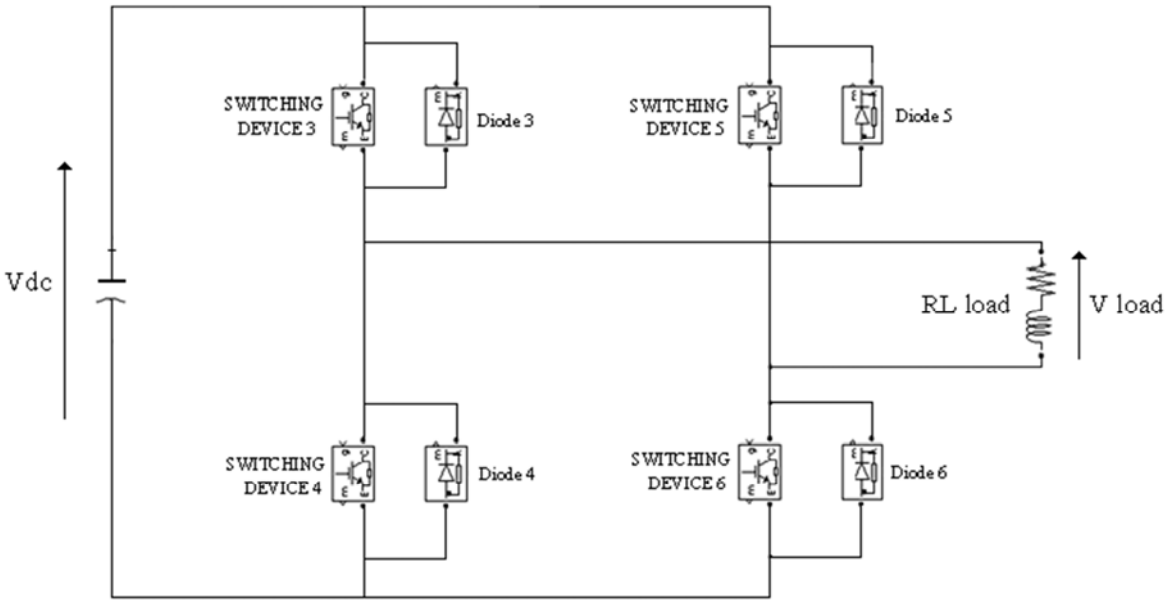

Figure 2.2 – Single phase H bridge converter

Diodes are necessary to avoid any damage which can be produced after the instantaneous opening of switching devices installed in an inductive circuit: indeed, from the nature of the load, the current step coming from the sudden opening could be able to generate an overvoltage, which is able to break the same circuit.

From the physical point of view, two switches of the same arm can't be both closed: this situation indeed means the creation of a short circuit that damages the devices of the circuit. Dead times have to be introduced when the system will be physically realised: basically, although one switch has already been opened, there is still the need of waiting few moments before closing the other one of the same arm, for being sure that the first one is really opened and no short circuit risks are present. This limitation does not depend on the control strategy but on the topology of the circuit. There aren't any other limitations to be kept in mind regarding the way the switching devices are fired; so many control techniques can be applied. For the achievement of the bidirectionality of the system, the converter has to be based on controllable switching devices: many possibilities on the choice of these can be picked up, but uncontrolled devices (diodes) or semi controlled ones (thyristors) can't be used.

From battery's charging and discharging point of view, single phase and three phase topology can both be used because, basically, the converter works charging or discharging the battery by the connection between this and the grid; the use of a single phase battery charger (using one phase and neutral conductor) or a three phase battery charger (using all the three phases) achieves the same global result. The differences between the two topologies stand on a higher power flow, which means lower time for charging the battery, and a more complex system, considering the three phase case. Also, whether a single phase battery charger will be considered, inside the vehicle two different converters are needed to be installed, one single phase dealing with the charging of the battery (V2G and G2V modes) and one three phase for traction mode. If the three phase battery charger solution is brought on, the topologies of the battery charger's converter and traction's converter are the same and the converter can do both the operations.

The use of only one power electronic device to achieve many different modes can be a great advantage in terms of investments and in terms of lighter weight of the power electronic block inside the vehicle. The three phase solution brings more stress to the same AC/DC converter, since it will have to satisfy both traction mode and the charging of the battery. For this reason, the converter used for all these purposes needs an appropriate choice of the size of the switching devices, and the heavier losses of energy, coming from an intensive use, have to be properly disposed in order not to overheat the system. For the next step dealing with the realization of the control strategy either a single phase converter or a three phase converter can be considered; the choice for this dissertation regards a single phase one.

2.1.2 - CONTROL METHODS

The square wave control method is the simplest one: according to this technique, referring to fig. 2.2, which shows a single phase H bridge converter connected to a general RL load , the DC constant voltage input can produce, in correspondence of the AC output, only two possible values: $+V_{dc}$ or $-V_{dc}$. In this way a voltage square wave is obtained in output, and its fundamental is a sine wave which can be matched with the one of the grid.
The advantage coming from an easy control does not balance the disadvantages: the harmonic content is very high, and frequency is the unique parameter that can be controlled: fundamental and harmonics amplitudes can't be piloted and the peak value of the fundamental is always constant and equal to $(4/\pi)* V_{dc}$. Analysing the frequency spectrum, harmonic amplitudes are $1/u$ times the fundamental amplitude, where u is the harmonic order. The following equation shows harmonic orders present in the system

$$u = 6k +/-1 \tag{2.1}$$

with $k=0, 1, 2, 3\ldots$ This spectrum can be an issue from the grid point of view (although the system composed by the battery charger and the battery would not suffer from any problem): a filter should be required for making suitable the connection to the grid. A better control technique can be applied: the *pulse width modulation* (PWM) is introduced.

The theoretical idea of PWM starts from the assumption that the reference wave furnished in input can be reproduced in output according to a proper switching technique of AC/DC converter's switching devices. The hypothesis is to divide time into very small periods, called switching periods T_s. In each of them the value of the reference input is close to be a constant, and the converter is asked to produce an output constant value which approximates it. The voltage level required, however, varies period by period, whilst the voltage at the DC side of the converter is fixed. This problem is overcome by the combination of the two voltage levels allowed during the switching period to produce a mean value close to the reference. This means that if the voltage that has to be produced in a determined period is assumed to be $u'(t)$, the same quantity can be written as

$$u'(t) = \frac{1}{Ts} * (\mathrm{V_{dc}} * \mathrm{T_{on}} - \mathrm{V_{dc}} * \mathrm{T_{off}}) \quad (2.2)$$

Where T_{on} is the fraction of the switching period in which positive voltage is applied and T_{off} the remaining fraction in which negative voltage is applied. The following equation can be written

$$u'(t) = \mathrm{Vdc}\ (2\delta - 1) \quad (2.3)$$

Here the symbol δ is the ratio between T_{on} and T_s and is called duty cycle.
How can be seen by the equation, the variation of the required voltage u'(t) produces the variation of the duty cycle applied in a determined period to the converter. This idea will be implemented by the use of the following method, called Sinusoidal PWM (SPWM).

The SPWM technique uses a sine wave as the input signal: the frequency and the amplitude of the output waveform created by the converter can be modified according to the variation of this reference signal, $V_{control}$ (Fig. 2.3 a)). The technique is based on the comparison between the reference signal and a triangular carrier signal, which is called $V_{triangle}$. The output of the control will be high (assuming unit value) or low (assuming nil value) if $V_{control}$ assumes higher or lower values than $V_{triangle}$; this kind of square waveform produced is used for the firing of the switching devices. If the output is high, for instance, switching device 3 and 6 of fig. 2.2 will be closed, and the voltage through the load will be equal to V_{dc}. If the output is low, switching devices 4 and 5 will be closed and the voltage becomes $-V_{dc}$. In this way, the waveform produced will be the one shown in fig. 2.3 b) and despite of a profile which has only two values, if the Fourier analysis is carried on, a sine wave with the same amplitude and frequency of the control signal can be distinguished.
Two parameters are fundamental, and they need to be analysed properly since the profile of the output waveform depends from them.

The first parameter is the modulation index m, which is defined as

$$m = \frac{Vcontrol}{Vtriangle} \quad (2.4)$$

where $V_{control}$ is the amplitude of the control reference signal and $V_{triangle}$ the amplitude of the triangular carrier signal. The peak amplitude of the fundamental of the output sine wave produced is

$$V_{fundamental} = m * V_{dc} \quad (2.5)$$

If m<1 is applied, the peak amplitude is reduced: this is the way in which the amplitude of the output voltage can be modified. On the other hand, when the modulation index reaches and overcomes $m=1$, the equation is not true anymore and the working region is not linear. This happens because the reference signal exceeds the amplitude of the triangular signal and in this way a proper SPWM piloting of the switches cannot take place. The higher the overmodulation is the closer to square wave modulation control the output voltage becomes, so the amplitude of the fundamental is not $m * V_{dc}$ anymore, but according to the continuous increments of m, it keeps on going close to $\frac{4}{\pi} * V_{dc}$. The modulation index is a parameter which influences the amplitude of the output fundamental, and at the same time even the harmonic distortion.

The second parameter, which is the frequency modulation ratio, is introduced.

$$m_f = \frac{f_s}{f_1} \quad (2.6)$$

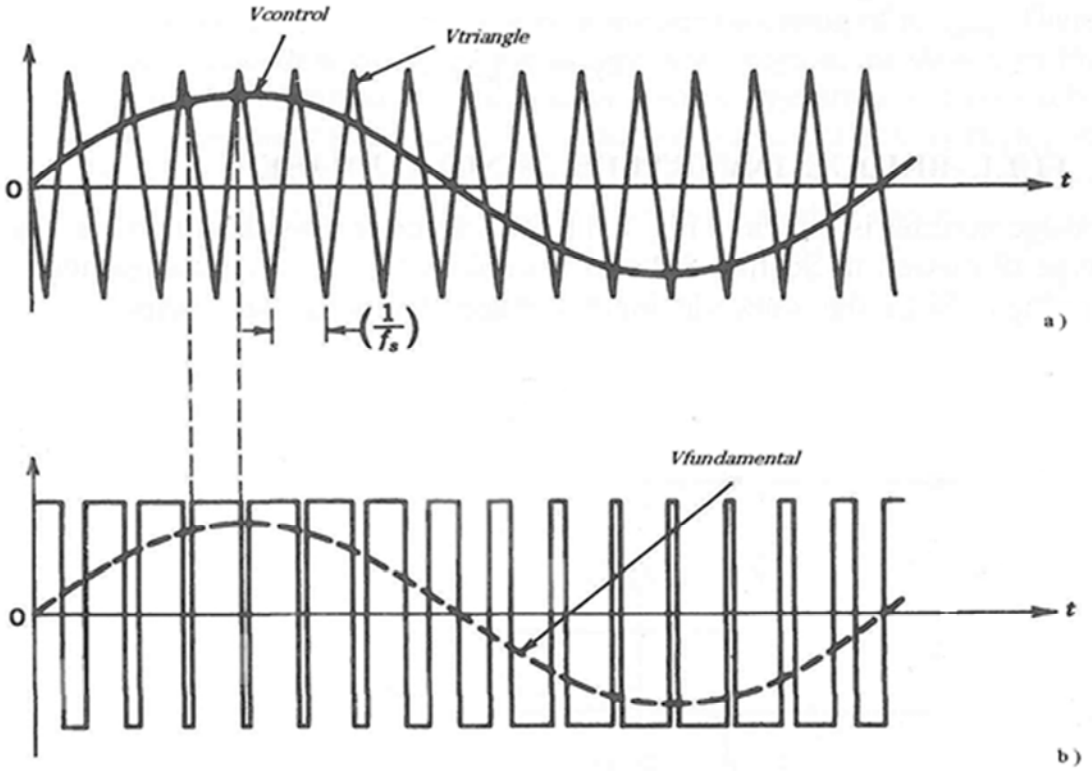

Figure 2.3 – SPWM technique: a) comparison between control signal and triangular carrier signal b) control signal for switching devices and resultant fundamental waveform produced in output (two different standards) [3]

f_S is the frequency of the triangular signal, whilst f_1 is the desired fundamental frequency of the inverter voltage output, so the frequency of the reference signal. It is necessary for a proper work of the entire system that the triangular carrier signal and the sine wave intersect at least twice every single period of the triangular signal, and this happens if the slope of the triangular signal is higher than the maximum slope of the sine. This means that the following equation has to be verified

$$m_f > \pi * \frac{m}{2} \tag{2.7}$$

In this way, if the two parameters' boundaries are respected, the created system works properly. What can be still an issue for the grid is the distortion of the profile of the wave, so harmonic analysis can be now carried on. The harmonics in the inverter output voltage waveform appear as sidebands, centred on the switching frequency and its multiples, that is, around harmonics m_f, $2m_f$, $3m_f$, and so on, and this general pattern holds true for all values of m in the linear range. Because of the relative ease in filtering harmonic voltages at high frequencies, it is desirable to use a high frequency for the triangular carrier signal, except for a disadvantage: inverter's losses in correspondence of switching devices increase proportionally with the switching frequency f_S. The AC/DC converter will use a 20 [kHz] triangular carrier frequency, and the reference signal frequency is 50 [Hz]. For the improvement of the harmonic spectrum, usually the triangular carrier signal frequency which is frequently used is three times a multiple of the fundamental frequency.

2.1.3 – SPECTRUM ANALYSIS

Since the AC/DC converter acts as the interface between the battery charger and the grid, it is important to analyse its harmonic spectrum in order to check if the connection to the grid can be realised without the application of any filter. Rigorous standard implies to keep the total amount of harmonics below a fixed threshold, and because of this the analysis of the power exchanged with the grid has to be always monitored and its quality improved. It is possible to study the voltage sine wave produced by the converter with the fast Fourier transform (FFT) analysis, with the aim of a better awareness of the characteristics of the sine wave built by the converter. The following figures show the analysis that can be carried on with the *Simulink* platform using the option "*Powergui*".

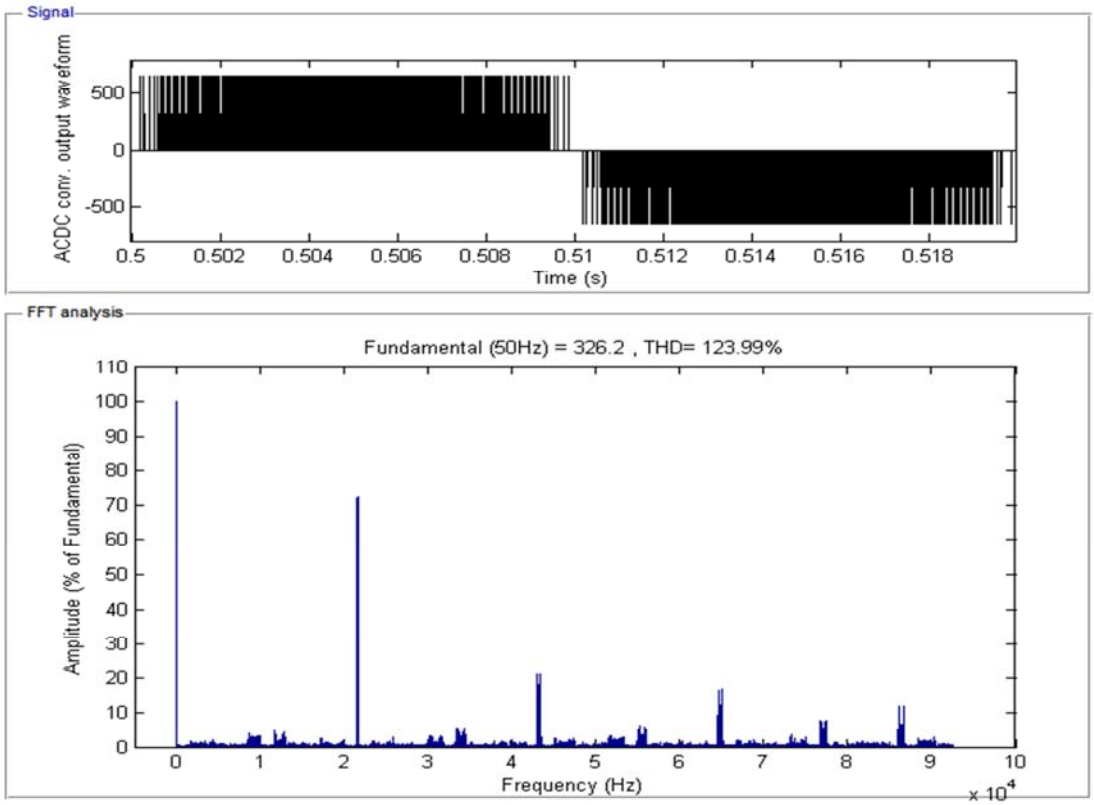

Figure 2.4 – Spectrum of the voltage at the AC side of the AC/DC converter

As can be seen, the graph depicted in fig. 2.4 shows the spectrum of the voltage waveform produced in correspondence of the AC side of the AC/DC converter without any filter connected to its output; the Fourier transformation is applied to one voltage period and the amplitude of each harmonic is compared to the fundamental, whose amplitude in percentage is 100. The switching frequency is 20 [kHz], so this means that harmonics will be related to this value. The fundamental frequency is equal to 50 [Hz] as what expected, and in correspondence of frequency values of 20 [kHz], 40 [kHz], 65 [kHz], 80 [kHz] the harmonics amplitude is relevant. The concept of THD (*Total Harmonic Distortion*) can be now introduced.

$$THD = \frac{\sqrt{\sum_{h=2}^{\infty} {Y_h}^2}}{Y_1} \tag{2.8}$$

This parameter should be taken in consideration, because national standards avoid the connection of the AC/DC converter to the same grid if the value does not stand under a fixed threshold, which can be around 5% for a LV-MV network. How can be seen, the software calculation may seem not to be suitable for the connection to the

grid, showing a THD value equal to 123,99 %. How can be seen by THD definition, all the harmonics are introduced to the sum independently from their order. This means that high order harmonics, although they don't create problems on the grid's current, are very influent with regards to the TDH calculation. If a different "harmonic window" is considered, so from DC to 2500 [Hz] (gap often considered) (Fig. 2.5), the calculation will give back a value which is suitable for the connection to the grid without the application of any filtering device.

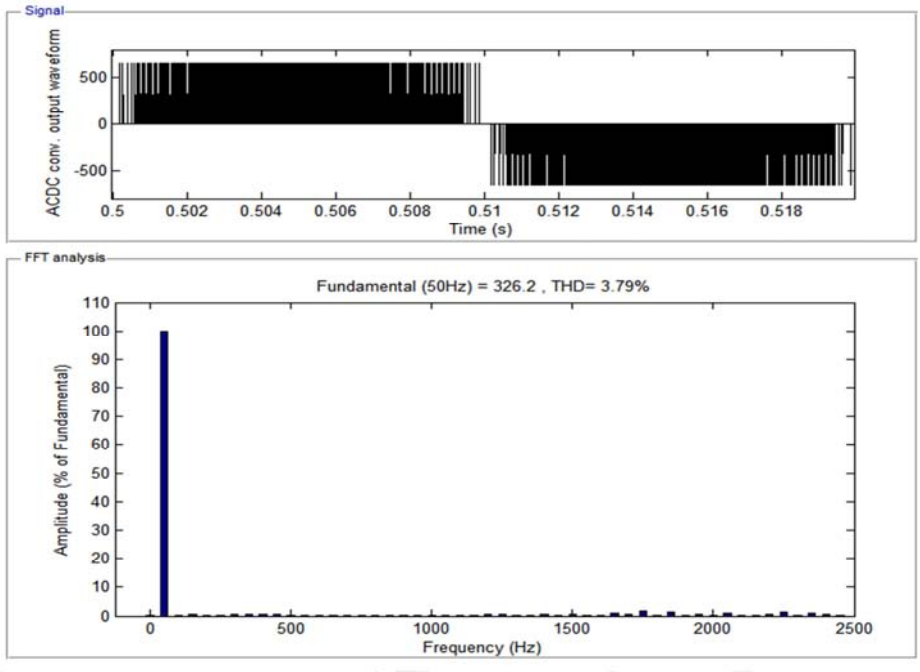

Figure 2.5 – Reduced voltage spectrum at the AC side of the AC/DC converter

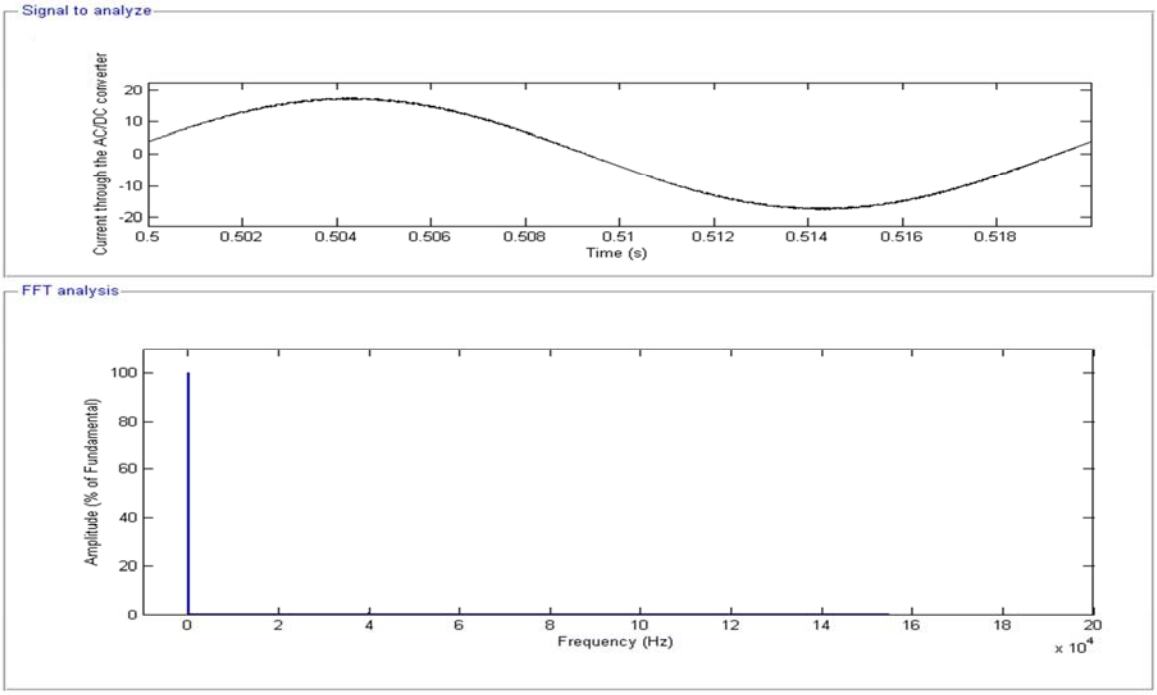

Figure 2.6 – Spectrum of the current flowing through the grid and the AC/DC converter

It can be seen how the reduced window adopted for the calculation of the voltage THD generates a result which is completely different from the previous one: the value passes from 123.99% to 3.79%. This means that the distortion was duty of high order voltage harmonics. The spectrum of the current which flows from the grid to the AC/DC converter can be analysed too. Figure 2.6 depicts the current shape analysis.

As can be seen, the current sine wave is smooth and whether the spectrum is studied, it can be seen that high frequency voltage harmonics don't affect the current profile: after the fundamental all the harmonics present can be considered negligible, and this comes from the fact that the grid is represented as an inductive load. In this way all the high order voltage harmonics don't generate high order current harmonics and the current profile is close to be perfectly sinusoidal.

2.1.4 – SWITCHING DEVICES CHOICE

The switching devices which can be applied to the system can be both MosFETs and IGBTs. Which device is more suitable? Many different aspects can be considered.

- Voltage levels: IGBTs can support higher voltage applications
- Power losses: for high current applications, IGBT's losses will be less than MosFEt's losses
- Costs: IGBTs are less expensive than MosFETs
- Switching Frequency: IGBTs are slower than MosFETs: their best performances are given at 20 [kHz] or less; some particular IGBTs can reach switching frequency of about 100 [kHz], but not higher.

Since the system works with a switching frequency of 20 [kHz] and it deals with high voltages, the best choice will be that one of using IGBTs.

2.2 DC/DC Converter

The DC/DC converter is a bidirectional device which is installed in such a way to connect the battery and the AC/DC converter, and the link between these two power electronic devices consists in a capacitor, called DC link, grafted in parallel [12] [13].

The importance of a synchronised run of the two converters is relevant: the DC/DC converter has to guarantee that the same amount of power which flows through the AC/DC converter has to be furnished by the battery, in such a way that the system is always in equilibrium from the power point of view. **Is the DC/DC converter necessary for the battery charger's operations required?** Theoretically, the battery charger is able to fulfil V2G, G2V and traction mode without the application of a DC/DC converter and only by the use of the AC/DC converter. Although it is not necessary, the DC/DC device is installed leading to some important advantages.

The advantages achieved with the series connection of AC/DC and DC/DC converter are explained in the following paragraph. The first deals with different SOCs of the battery: when the battery is exhausted and needs to be charged, its voltage can be the half of the rated voltage at unity SOC. The variation of the battery voltage value influences the peak of the sine wave produced by the AC/DC converter, and this in turn influences the amount of active and reactive power absorbed by the system. Deep differences between the two fundamental magnitudes are equal to strong variations of active and reactive power. The AC/DC converter is able to modulate the amplitude of the output sine wave produced according to the variation of its modulation index; however the peak of the sine wave produced can be only reduced from the maximum value and not increased. This is the

possible limitation that a DC/DC converter will be able to overcome. In this way a complete decoupling between the voltage through the battery and the DC side of the AC/DC converter is achieved. If the scheme of a battery charger using both DC/DC and AC/DC converter is applied, a wider range of voltage through the capacitor can be reached, ensuring a more flexible system, and this will be basilar for the achievement of reactive power regulation.
The second benefit deals with the fact that the DC current which feeds the battery can be smoothed by an inductor, improving the quality of the power absorbed by the battery (preventing it from ripples that can impact on its life time). At the DC side of an AC/DC converter there is indeed a direct current flow, but the current is not continue: in fact it does not assume instantaneous values effectively close to its mean value. The presence of an inductor is required.

The assumption made for this work is that the voltage of the battery is always lower than the voltage through the capacitor. The ratio between these two voltages is a value which is almost fixed (equal to 1-2): the parameter which gives power bidirectionality will be the sign of the mean value of the current. Many alternatives to the chosen circuit, which is analysed in the following section, can be proposed for the design of a DC/DC converter. Their analysis is completed in Appendix 1.

2.2.1 – BIDIRECTIONAL DC/DC BOOST CONVERTER

The scheme of the bidirectional boost converter is shown in fig. 2.7 [14]. The number of switching devices is minimal (two) and only one of them is commutating during each mode, whilst the other one is always off. Two diodes are needed to complete the scheme.

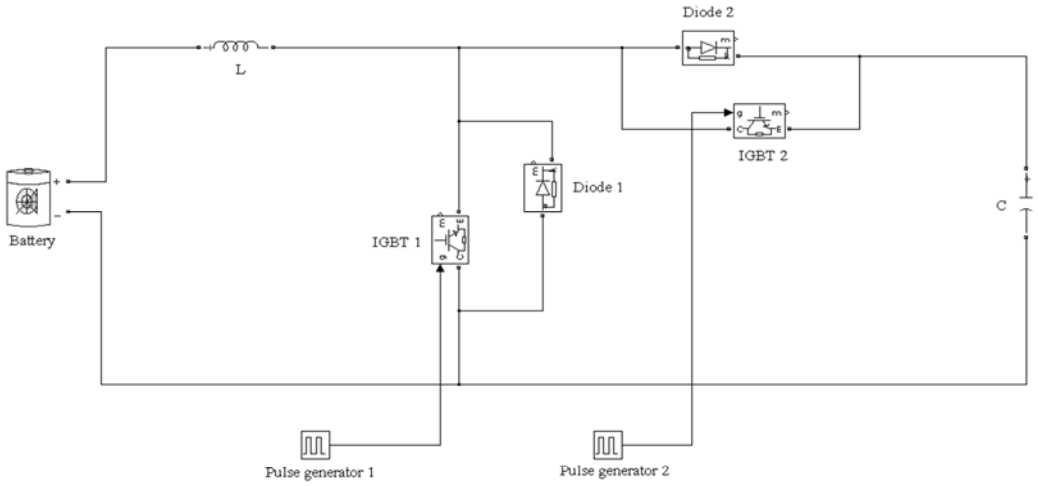

Figure 2.7 – Bidirectional boost converter

If the power is considered to flow from the grid to the battery, the commuting device is IGBT2 whilst IGBT1 is always open. When it is open, the same circuit is open and no current flows and feeds the battery; when the switching device is instead closed, the resultant mesh will make the current to flow naturally from the higher potential (capacitor) to the lower one, charging the battery. The value of the duty cycle applied to the switching device determines the amount of current (active power) which flows from the grid side to the battery. A duty cycle close to unit means that for almost all of the switching period the mesh is made by capacitor, inductor and

battery, and a high current will flow. If the duty cycle is close to be nil, for almost all of the switching period the capacitor is not connected to the battery and inductor system, so less current will flow.

If the power is supposed to flow from the battery to the grid, the commuting device will be IGBT 1. The current will flow in the opposite way as the former case studied. When IGBT 1 is closed, in fact, the battery charges the inductor, which stores energy. When the switching device changes its state, the diodes force the current to flow through diode 2 and battery (inductor) energy is transferred from one side to the other of the converter. Even in this case the duty cycle value is directly proportional to the amount of active power flow. If the duty cycle is high and close to unit, it means that for most of the time the inductor is charged and when the switch commutes lot of energy will flow; if it is low, negligible energy is transferred from the battery to the AC/DC converter.

2.3 – The chosen topology

The bidirectional converter which will be considered for this dissertation consists of a bidirectional boost converter (DC/DC converter) and a single phase H bridge converter (AC/DC converter). This is the topology which will be now considered in order to do the next step, which is the design of the control strategy of the system. The whole battery charger topology is shown in fig. 2.8.

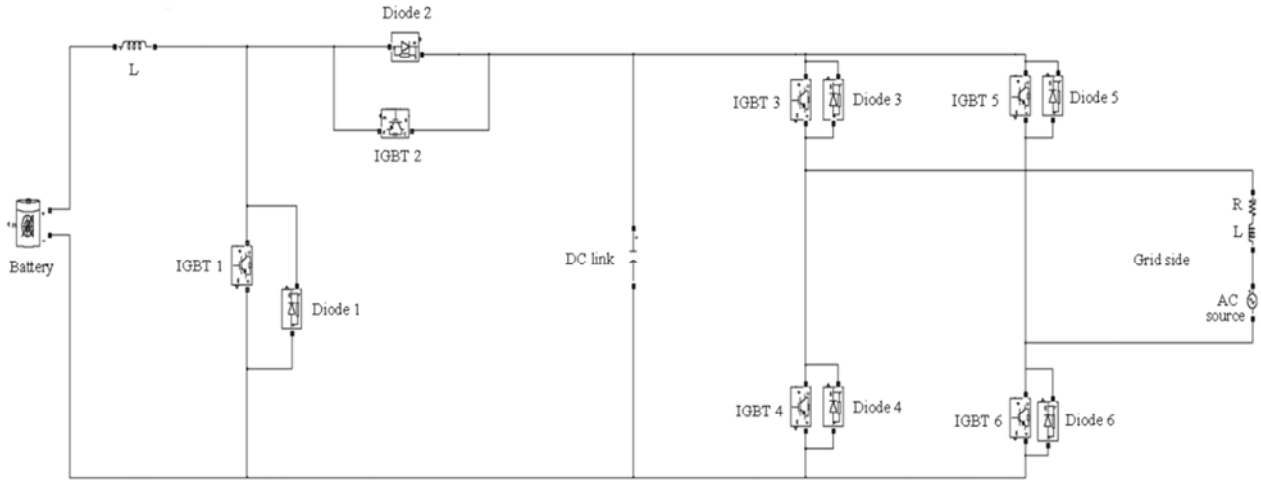

Figure 2.8 – The whole configuration: Battery, DC/DC converter, AC/DC converter, grid

3. Active and Reactive Power

The way in which the battery charger, focusing on its AC/DC converter, absorbs or delivers active and reactive power when it is connected and synchronized to the grid, and the parameters which are able to impact on the exchanged power, are fixed in this chapter. The second section of the chapter shows how this power flow will impact on the battery charger electrical parameters' dynamic.

3.1 – The Grid Model

The structure of the grid can be roughly represented as an inductive-resistive load, but the resistive part is always assumed smaller than the inductive reactance. This is not always true, specially whether LV systems are considered. However, under this assumption, the following equations are the same for every voltage level, from the transmission to the distribution networks; the voltage becomes a parameter which is strongly connected to inductive reactance. The achievement of the control of voltage drops or over voltages passes through the regulation of the reactive power, whilst the control of the frequency will mostly depend on the active power flow. For a better analysis of the system and prove the connection active power and phase angles and reactive power and voltage amplitudes, a section of the grid is considered, and Thévenin theorem is applied. The result is that of a scheme made by an ideal voltage source and an R-L load connected in series (Fig 3.1); the analysis can be made according to it.

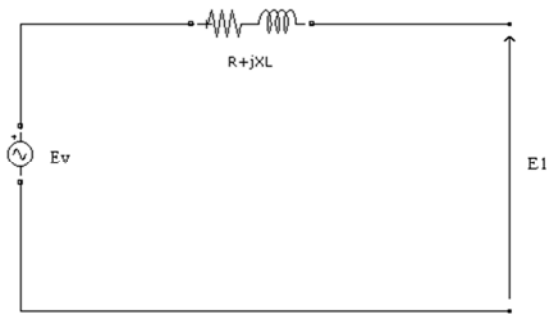

Fig. 3.1 – Scheme of the grid

$$\Delta E \cong |Ev| - |E_1| = RI\cos\varphi + XI\sin\varphi \tag{3.1}$$

$$3E_1 * \Delta E \cong (3E_1 * I\cos\varphi * R) + (3E_1 * I\sin\varphi * X) \tag{3.2}$$

$$3E_1 * \Delta E = RP + XQ \tag{3.3}$$

Where P is the active power flow and Q is the reactive power flow. Since $E_1 \cong Ev - \Delta E$,

$$3(Ev - \Delta E) * \Delta E = RP + XQ = 3Ev * \Delta E - 3\Delta E^2 = M \tag{3.4}$$

M can be considered as an auxiliary parameter which will be useful for the next step.

If the equation which describes M function of ΔE is plotted, and the variable term is assumed to be ΔE, the result is the parabola shown in fig. 3.2, which matches the abscissa axis in 0 and Ev. The value of Ev is assumed to be 230 [V].

Since the aim is to make the grid working around its rated voltage, all voltage drops and over voltages have to be limited. This means that the analysis will be conducted looking at the left side of the plot, where ΔE is close to 0 or, anyway, is a percentage of the rated voltage Ev.

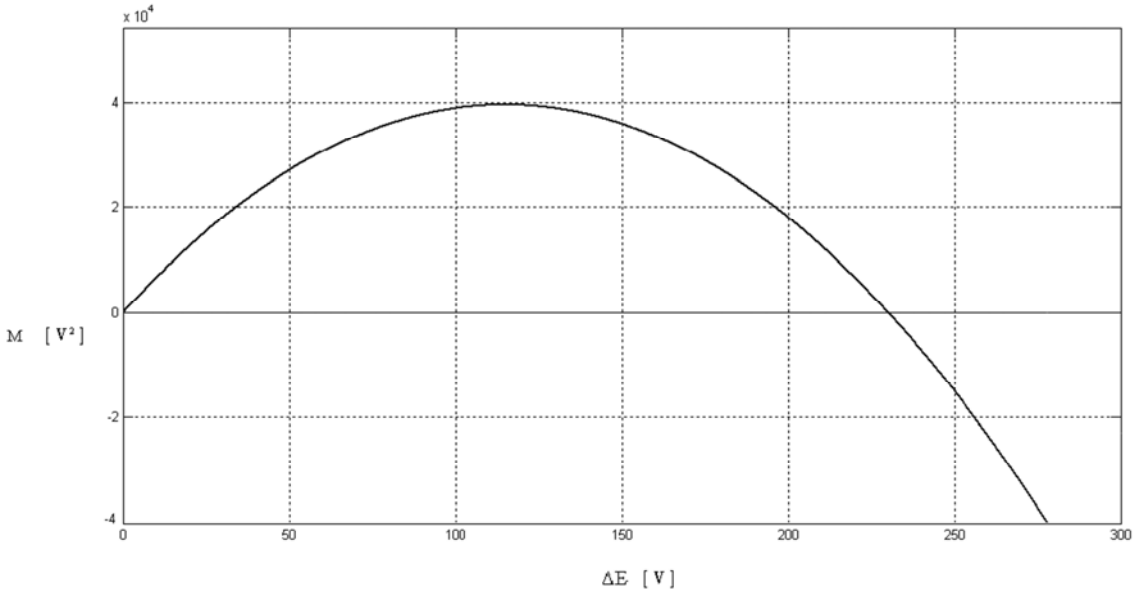

Figure 3.2 – Relation between the parameter M and the voltage drop ΔE

Assuming that the voltage drop will be always less than 50 [V] (precautionary parameter), a close-to-linear relation between x and y axis, so between M and ΔE, can be found. This means that positive values of M deal with voltage drops, negative values of M deal with over voltages, and in this way the new fictitious parameter M can be replaced by ΔE parameter for the next equations.

$$M = RP + XQ \tag{3.5}$$

$$\frac{M}{X} = \frac{RP}{X} + Q \tag{3.6}$$

$$Q = \frac{M}{X} - \frac{RP}{X} \tag{3.7}$$

Since the assumption is that of a model where X is greater than R, the second term of the (Eq. 3.7) presents a relatively low value, and as a consequence of this, a pure variation of active power will not influence in a deep way the reactive power exchanged; on the other hand, a variation of the parameter M produces a relevant variation of Q, which will be amplified in case of low values of X in absolute term (parameter which depends on the grid). This means that, theoretically, when the converter will run and it will be subjected to a relevant variation of active power, the results will have to show a limited variation of reactive power exchanged. The variation of the reactive power exchanged, according to the variation of the active power flow, will get smaller and smaller whether the R parameter will get closer to nil value or the ratio between R and X will be considered negligible.

The case of the grid approximated to a pure inductance as in fig. 3.3 is analysed. The vectors defining magnitude and phase of the input and output voltages and currents are those represented in the picture. Considering a two-axis domain, the hypothesis is that the vector V_i leads the vector V_o, and the angle between the two (phase angle) is called θ. The vector V_i is represented coincident with the real axis, whilst the vector V_o that lags the first can be found in the fourth quadrant, because the angle θ is assumed not to be greater than 90°.

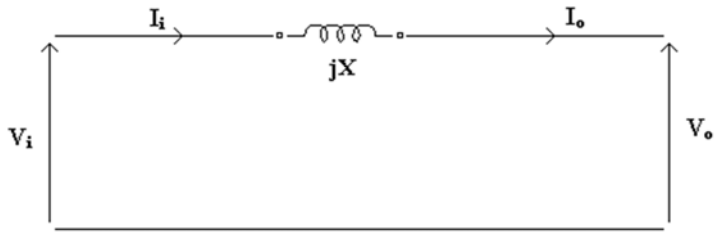

Figure 3.3 – Scheme of the grid modelled as a pure inductance

$$\boldsymbol{S_O} = \boldsymbol{V_O} * \boldsymbol{I_O}^* \tag{3.8}$$

$$\boldsymbol{S_O} = \boldsymbol{V_O} * \frac{\boldsymbol{V_i}^* - \boldsymbol{V_O}^*}{-jX} \tag{3.9}$$

$$\boldsymbol{S_O} = \frac{\boldsymbol{V_O} * \boldsymbol{V_i}^*}{-jX} - \frac{{V_O}^2}{-jX} \tag{3.10}$$

$$\boldsymbol{S_O} = \frac{V_O * V_i * e^{-j\theta}}{-jX} - \frac{{V_O}^2}{-jX} \tag{3.11}$$

$$\boldsymbol{S_O} = \left(V_O * \frac{V_i}{X}\right) * e^{j\left(\frac{\pi}{2} - \theta\right)} - \frac{{V_O}^2}{X} * e^{\frac{j\pi}{2}} \tag{3.12}$$

The two vectors can be seen as the voltage produced by the battery charger and the voltage of the grid. Let's make the hypothesis that the system is working in G2V mode: active power has to flow from the grid to the vehicle. Vectors with the subscript letter "i" deal with the grid and the ones with the subscript letter "o" deal with the AC/DC converter when the connection with the grid is realised. In function of the values of the parameters of the battery charger (SOC, duty cycle, voltage through the capacitor…) the controller creates a sine wave through the AC/DC converter, which is the V_o vector. Splitting the equation, its real and imaginary part will furnish respectively the active and reactive power, that are considered flowing from the grid to the battery charger (V_o lags V_i).

$$P_O = Re(\boldsymbol{S_O}) = \frac{V_O * V_i}{X} * \cos\left(\frac{\pi}{2} - \theta\right) = \frac{V_O * V_i}{X} * \sin(\theta) \tag{3.13}$$

$$Qo = Im(\boldsymbol{So}) = \frac{Vo * Vi}{X} * \sin\left(\frac{\pi}{2} - \theta\right) - \frac{{V_O}^2}{X} = \frac{Vo * Vi}{X} * \cos(\theta) - \frac{{V_O}^2}{X} \tag{3.14}$$

If the magnitude of the vector which defines the voltage of the grid is assumed to be constant, the active power depends on the magnitude of the voltage and the phase angle in correspondence of the AC/DC converter. Real working situations deal with phase angles values "θ" which are relatively small. For this reason some simplifications can be conducted, and the following equations show P and Q when the phase difference between the two vectors V_i and V_o is equal or less than 11°.

$$P_O = \frac{V_o * V_i}{X} * \sin(\theta) \cong \frac{V_o * V_i}{X} * \theta \tag{3.15}$$

$$Qo = \frac{Vo * Vi}{X} * \cos(\theta) - \frac{{V_o}^2}{X} \cong \frac{Vo * Vi}{X} - \frac{Vo^2}{X} \cong Vo * \frac{Vi - Vo}{X} \tag{3.16}$$

These simplified equations (Eq. 3.15, Eq. 3.16) highlight what mentioned before, so how the parameter that mostly influences active power flow is the angle phase, whilst the reactive power is mostly influenced by the difference between the two voltage amplitudes. However, the dependence of the reactive power from the angle phase and of the active power from the difference between the amplitude of the two voltages is still present and not always negligible.

3.2 – AC/DC Converter Connected to the Grid

The following section analyses the way in which the electrical parameters of the battery charger's AC/DC converter are subjected to modifications when a not nil power flow takes place (the DC/DC converter block is not considered at the moment). Two different cases will be studied: the AC/DC converter connected to the grid is fed by an ideal DC source and by a pre-charged capacitor. The aim of the following test is to check how power flow impacts especially on the capacitor, in order to infer how the control system should be projected.

3.2.2 – IDEAL DC SOURCE

An ideal DC voltage source, which always maintains the same voltage independently from the current through it, is used as the feeder for the H bridge converter. The AC side is connected to the grid, which is modelled as a voltage source in series with an RL load, as can be seen in fig. 3.4. The grid parameters are fixed too: the source is assumed to be ideal and the peak amplitude is set to $\sqrt{2} * 230$, according to the Italian standard for LV single phase domestic plants.

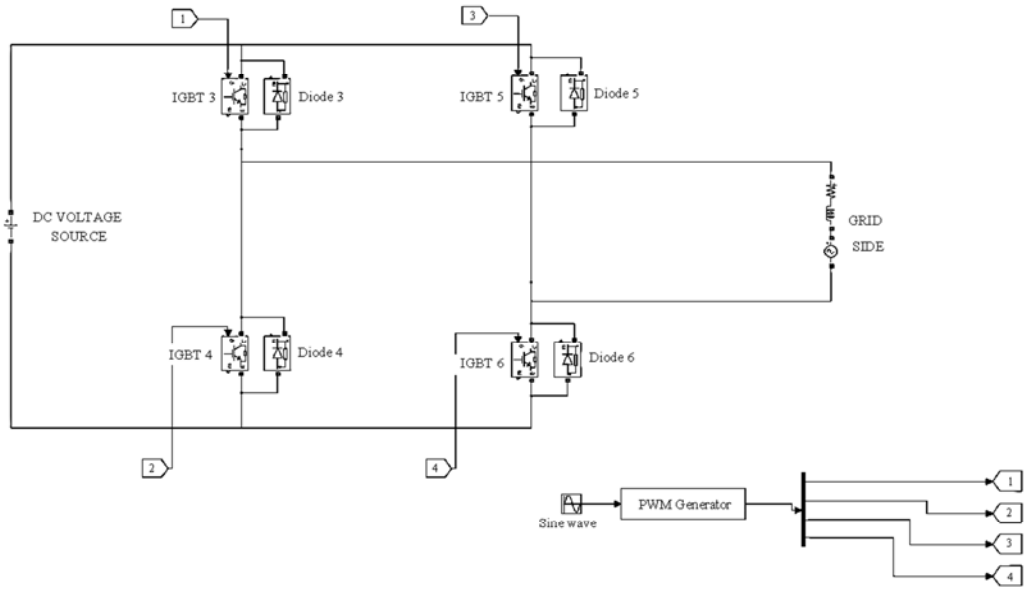

Figure 3.4: scheme of the AC/DC converter interfaced to the grid

The followings are the results depicting the active power flow that can be found changing the phase angle of the sine wave produced by the AC/DC converter with respect to the grid sine wave. As can be seen from fig. 3.5 and fig. 3.6, after some ripples due to transient state, the power delivered or absorbed by the grid (and as a consequence absorbed or delivered by the DC source) reaches a constant value. The active power and the reactive power are calculated by the software by the use of the block "Active and Reactive Power", which uses (Eq.3.17 and Eq. 3.18).

$$P = \frac{1}{T} * \int_{t-T}^{T} V(\omega t) * I(\omega t) dt \tag{3.17}$$

$$Q = \frac{1}{T} * \int_{t-T}^{T} V(\omega t) * I\left(\omega t - \frac{\pi}{2}\right) dt \tag{3.18}$$

P and Q are calculated by the software averaging the VI product over one cycle of the fundamental frequency. The real physical case is not perfectly copied but just approximated, because total harmonic distortion is not nil and the presence of harmonics that bring reactive power are not considered in the calculation although they are present. The difference between these results and the proper calculation considering all the harmonics is anyway negligible.

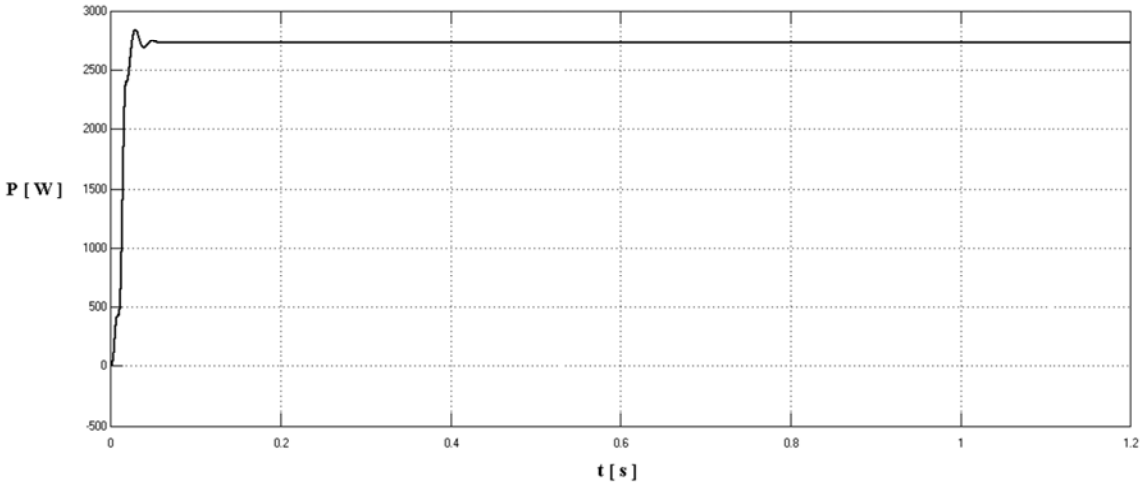

Figure 3.5: Active power from AC/DC converter to grid with phase angle equal to -10° (grid absorption)

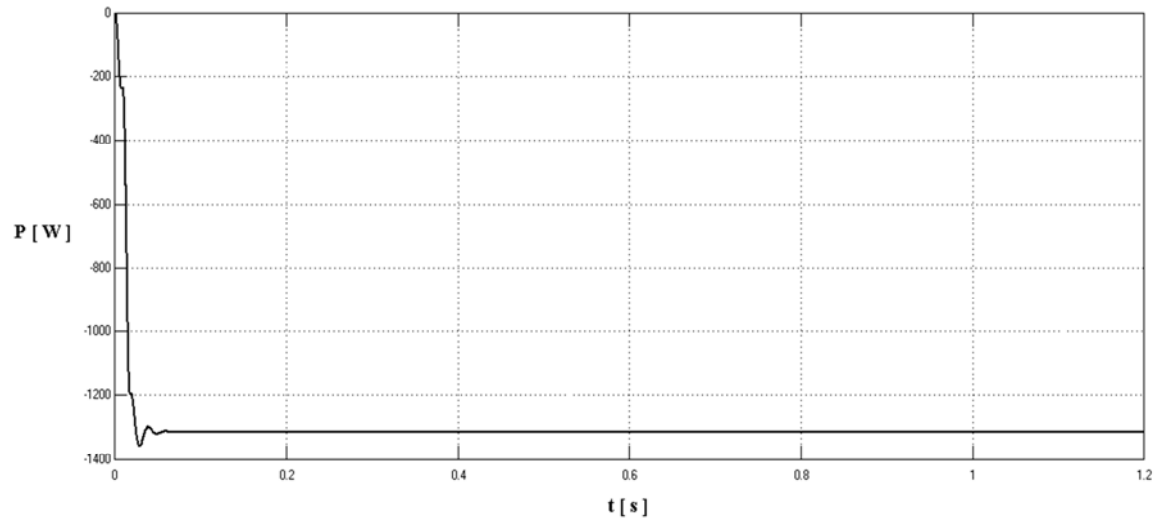

Figure 3.6: Active power from the grid to AC/DC converter with phase angle equal to +5° (grid delivery)

Figures 3.5 and 3.6 show a positive or negative active power which flows from grid to the AC/DC converter; according to the convention used, active power is considered positive if it flows from the DC source to the grid.

Another aspect of the simulation needs to be analysed, and it deals with the transient state which is generated during the first instants, when the grid synchronization is completed and the converter is connected to the grid. If the amplitude of the fundamental produced by the AC/DC converter is equal to the amplitude of the fundamental of the sine wave of the grid, the transient state regarding the active power is limited: fluctuations and overshoot are not present and the system reaches easily the steady state as in the figures. If the matching is not verified, the system reaches instead the steady state after not negligible and unwanted transient states and overshoots. The voltage level needed in correspondence of the AC/DC converter in such a way to avoid active power fluctuations during the transient state can be easily calculated: if the converter is working inside the linear region (modulation index less or equal to unit), the peak amplitude of the fundamental sine wave produced will be *m* times V_{dc}. The following equation will be then solved

$$m * V_{dc} = \sqrt{2} * 230 \tag{4.3}$$

to calculate the appropriate value of *m* to apply (it can't be lower than a fixed term) in function of the voltage V_{dc}. As an alternative, *m* can be considered as a fixed value and V_{dc} can be modified by the control scheme of the system, since it is the voltage that can be found through the capacitor.

The reactive power flow according to the application of an ideal DC source can be also studied. Eq. 3.18 is applied and fig. 3.7 and 3.8 depict transient and steady states of this parameter according to different values of the phase angle. After some fluctuations due to the transient state, when the steady state is reached a constant reactive power exchanged value is achieved.

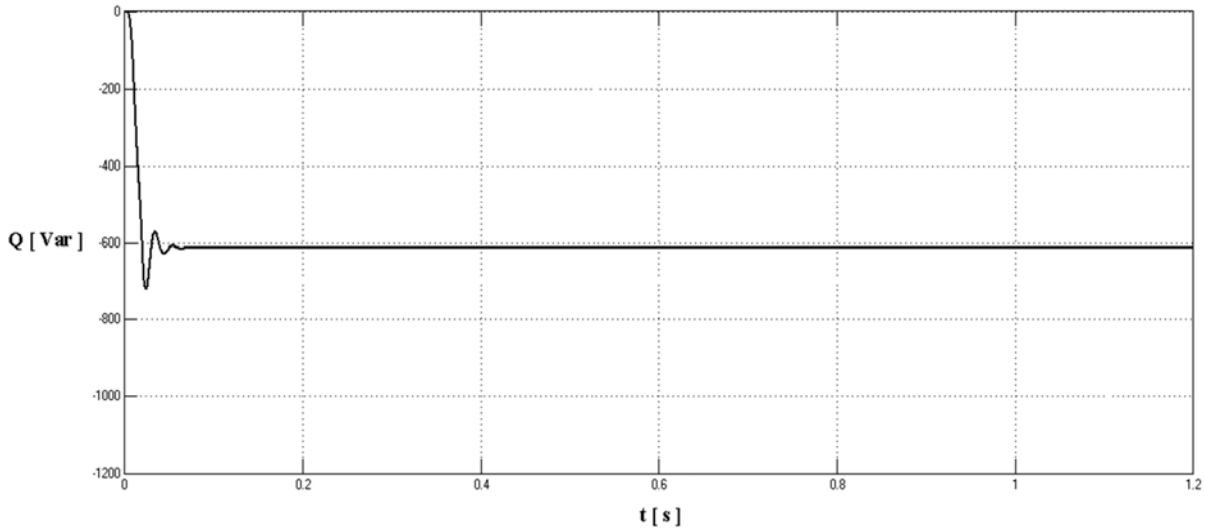

Figure 3.7 – Reactive power exchanged with phase angle equal to -10°

These two examples represent the profiles of the reactive powers exchanged as a consequence of the modification of the phase angle of the sine wave produced by the AC/DC converter with respect to the sine wave of the grid. Since the reactive power profile is not affected in a relevant way by this parameter, the variation that will take place won't be so deep, but at the same time non negligible. The method which can be used for modifying the reactive power profile without affecting the active power flow will be that of varying the voltage

in correspondence of the DC source. If this is not allowed, any control on the reactive power exchanged can't be implemented and this parameter won't be controlled.

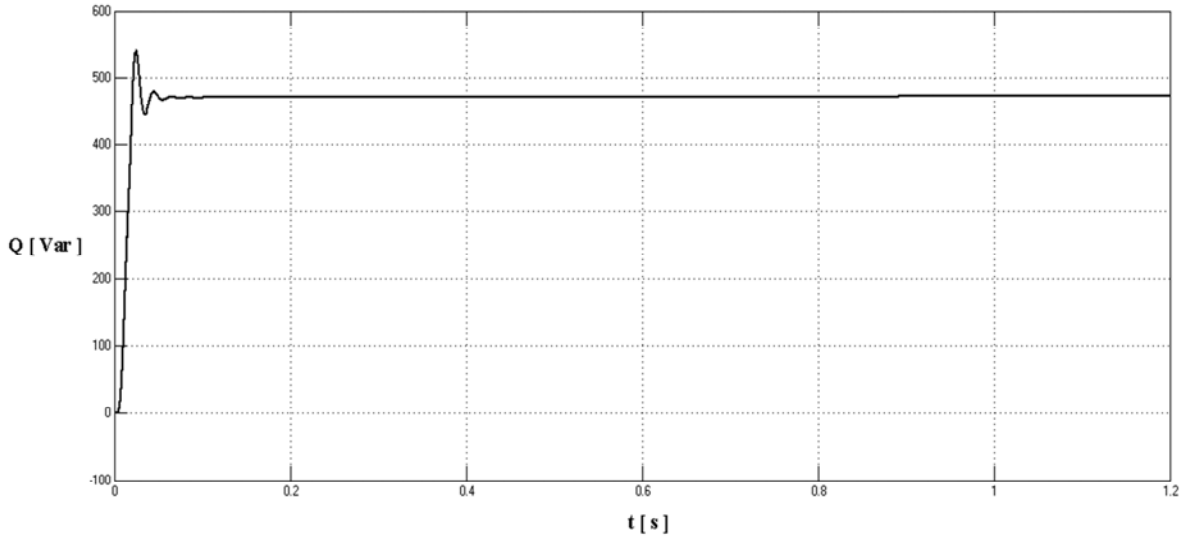

Figure 3.8 – Reactive power exchanged with phase angle equal to +5°

3.2.2 – NON IDEAL DC SOURCE: PRE-CHARGED CAPACITOR

The modification of these power profiles according to the application of a non-ideal DC source to the AC/DC converter is now analysed. The source is not able to keep the voltage constant independently from the current absorbed or delivered: this means that power flow influences the voltage through it. This analysis is conducted because the battery charger is not equipped with an ideal source at its DC side, but with a capacitor which is storing a certain amount of energy. If the capacitor will deliver part of its stored energy or absorb a certain quantity of energy, a consequent variation of the voltage through it will take place, and the variation of this amplitude will affect the amplitude of the sine wave produced by the AC/DC converter. As a consequence, both the active and the reactive power exchanged (Eq. 3.13, Eq. 3.14) will be modified, although the value of θ is fixed. The variation of reactive power will certainly be deeper than the variation of active power. The following fig. 3.9 and fig. 3.10 show the evolution of two of the three most important parameters, which are the active power delivered by the AC/DC converter and the voltage through the capacitor at DC side.

The active power flow (Fig. 3.9), after the achievement of a temporary steady state, is subjected to a linear decrement, and the relation between voltage and power is linear too. The voltage through the capacitor is equal to 650.5 [V] at t=0, feeding the converter is such a way that initially the two waveforms have both the same amplitude; but its voltage decreases during the simulation due to the fact that a costant energy flow is taking place.

The speed of the voltage variation deals with two parameters. The first one is the active power flow: the most it is consistent, the most the variation will be fast. The second one is the capacity of the device: considering a fixed active power flow and a fixed voltage through it, if the capacity is high more energy is stored into the capacitor; the voltage through it will change in a slower way than considering a lower capacity capacitor. Here the simulation is run for V2G, but the profiles of the two parameters considered are basically the same for a reversed active power flow (G2V): in this case, the analysis will find an active power flow which progressively increases, and the voltage through the capacitor will increase too, because it will store energy coming from the grid. For

this reason, this situation can be dangerous, and safety devices controlling the voltage through it are applied to the real circuitry.

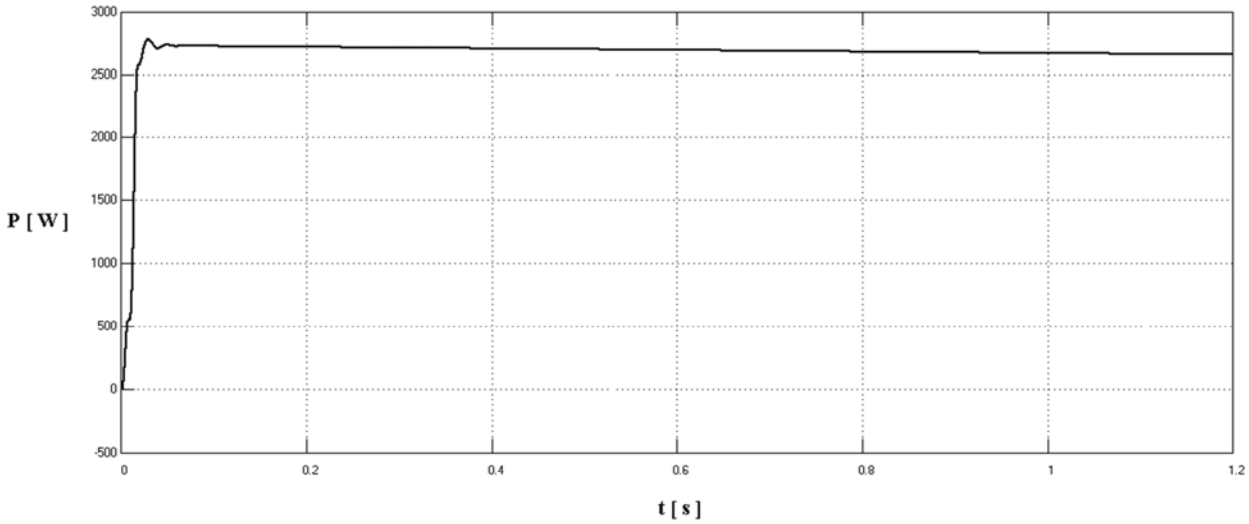

Figure 3.9 – Active power delivered by the AC/DC converter to the grid

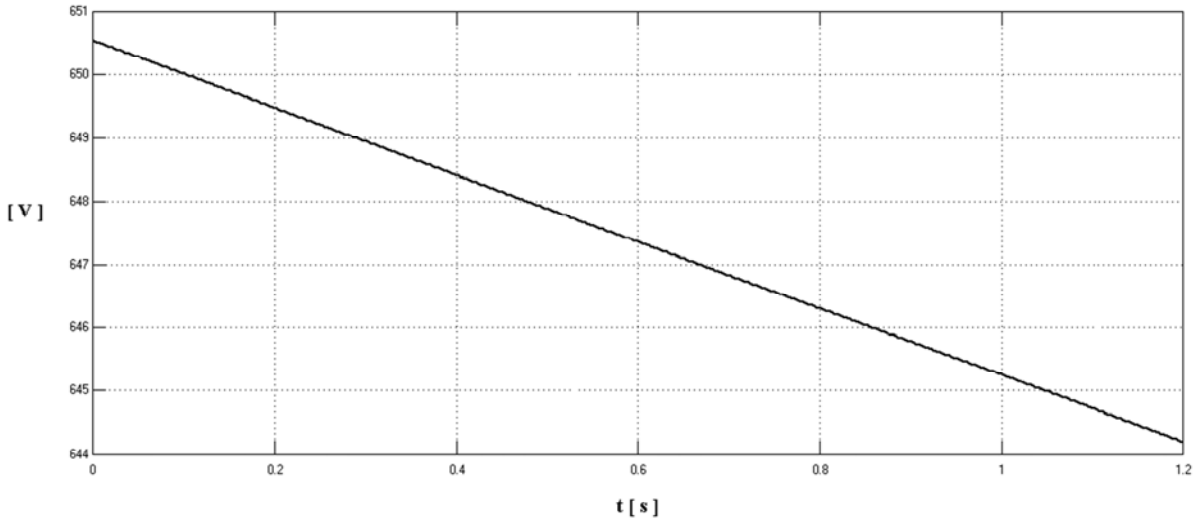

Figure 3.10 – Voltage through the capacitor while active power is delivered

How deep the variation of reactive power exchanged by the two systems is, considering this situation? The following fig. 3.11 shows the profile of the reactive power exchanged, and it is easy to see that the variation of the voltage of the capacitor, which seems to be not so relevant (decrement of less than 7 [V] from the initial value of 650.5 [V] during the time window considered), influences in a strong way this parameter. In the first simulation the reactive power exchanged by the two systems with an ideal DC source was around 620 [Var] (negative value) (fig.3.7). With the usage of a non-ideal DC source, the variation of the voltage at the DC side brings the reactive power exchange to be subjected to an increment of around 15% in less than 1.5 seconds with respect to the previous simulation.

In addition to this, if the active power flow is reversed, so from the grid to the DC source (charging mode), it can be demonstrated that the capacitor is subjected to an increment of the voltage through it (instead of a decrement), and the reactive power depicted in the graph even changes its sign, becoming positive.

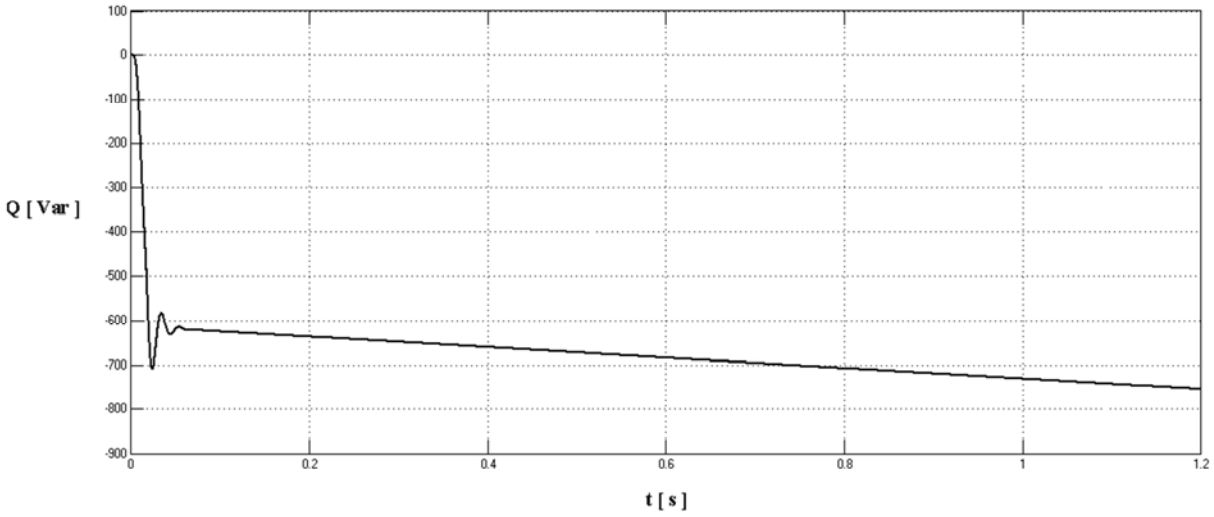

Figure 3.11 – Reactive power exchanged between the AC/DC converter and the grid

The variation of active and reactive power from the rated values, as a consequence of the application of a non ideal DC source, can be now compared. The variation of the active power from its rated value can be found quantifying the difference at t=1.2 seconds between the first simulation (Fig. 3.5), with ideal DC source, and the second simulation (Fig. 3.9), in which the capacitor is used: the variation is of about 70 [W] over 2700 [W], so the variation is of about 2.6%. If the same process is repeated for reactive power, the difference between the two results calculated at the same instant t=1.2 seconds is of about 134 [Var]. Since the steady state reactive power value calculated in the first simulation was 620 [Var], the variation of reactive power is of 21.61%, ten times more than the increment of active power. Thanks to these results, the importance of the DC/DC converter can be better understood: the decoupling between the battery and the AC side can preserve the capacitor from voltage fluctuations, which are able to move the system from the required working point.

If a steady state characterized by a capacitor voltage value different from the rated one is achieved, charging and discharging modes, which deal with active power flow, may not be subjected to such strong variations to make the system not compatible with the charging or the discharging of the battery. As a consequence, the system is able to work in conditions which are more or less close to the rated ones.
A stable active power flow doesn't avoid strong variations of the reactive power exchanged; this variation can be an undesired situation for both the grid and the customer, so a way to control the voltage of the capacitor needs to be implemented. A control block which is able to keep fixed the voltage of the capacitor for the achievement of the steady state needs to be implemented. The concept of the control will be that one of matching exactly input power and output power (power of the battery and power at the DC side of the AC/DC converter), in such a way that the capacitor will be neutral in terms of power exchanged at steady state, and the voltage through it remains constant.

4 – Control Scheme

This chapter deals with the design of a proper control strategy which can pilot the AC/DC and the DC/DC converter, in a way to achieve a steady state where a fixed amount of active power flows through them, charging or discharging the battery of the electrical vehicle. Before designing the control scheme of the system, there is the necessity to fix the input data which determine the battery charger's working conditions. Among all the others, three main inputs are fundamental. The first one deals with the **active power flow**: once this amount is defined, the value of the phase angle θ is calculated and applied to the AC/DC converter, which is then piloted in such a way that the active power flow required is achieved. The second input deals with the **battery's parameters**: in function of the SOC and the temperature, for instance, the control strategy of the battery charger has to be able to modify its working point, in order to avoid damages or dangerous situations. The third input is not an internal input, because it comes from the communication between the EV and the grid manager. This input is able to modify the active power flow, in order to **support the grid** whenever this help is needed and the vehicle is in the right conditions to do it.

The control strategy here introduced will focus on the first and the third input, so the way in which the active power flow can be handled for V2G and G2V modes. For the achievement of a proper control scheme, the first thing to be done is the analysis of the whole system, in such a way to understand how it behaves and in which way the controller has to pilot the switching devices in order to reach the desired steady state. Figure 4.1 shows the global topology of the battery charger, before the application of the control strategy. Voltage and current measurements will be necessary as inputs for the control system, applied as feedbacks. The appropriate control system will be studied first for charging and then for discharging only, because the two configurations in the two different cases are physically different. Starting from a simple and ideal theory, step by step, the issues which affect the battery charger according to its non-ideal working situation will be faced.
The last step will be the one of creating a single control which is able to pilot the battery charger for any working situation.

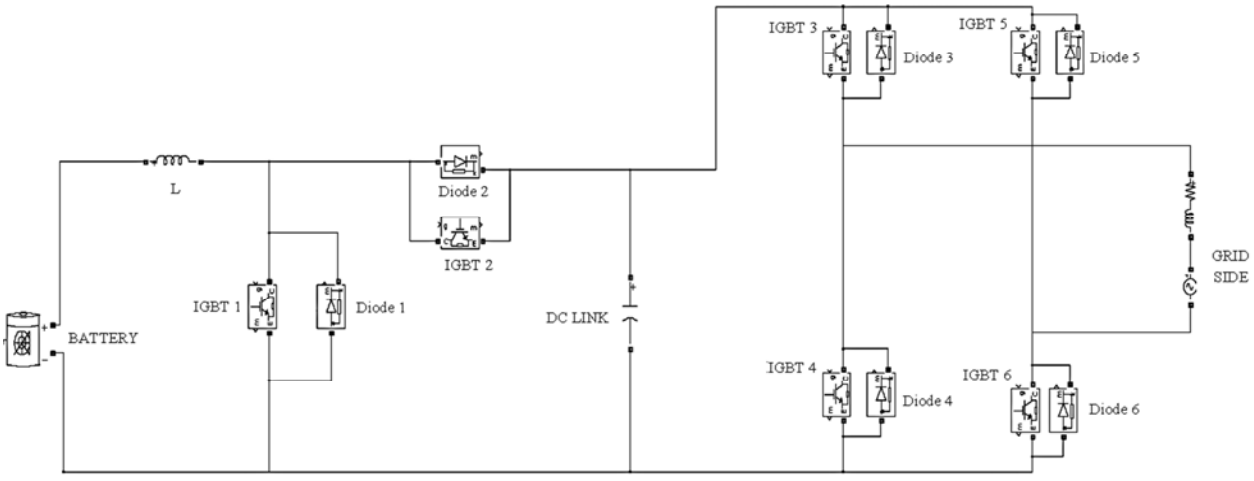

Figure 4.1 – Whole topology of the battery charger

4.1 - Charging Mode (G2V): control strategy

This mode is the one in which the battery absorbs active power from the grid. During charging mode, the energy is stored inside the battery and its SOC grows up till 100%. This normally happens when the owner wants the vehicle to be recharged after the vehicle is driven, but can also happen when the grid produces an amount of active power which is higher than the active power required by all the loads connected to the same grid: the difference between production and absorption can be stored inside the vehicle, so the ancillary service called G2V takes place. **Two hypotheses** are made before running this group of simulations: the first is that the voltage of the battery increases in a negligible way and can be always considered to be constant, the second is that the two converters (AC/DC and DC/DC) don't have any losses.

Charging mode means that the AC/DC converter works as a rectifier. Its four IGBTs will be fired in such a way to build a sinusoidal waveform which lags the waveform of the voltage of the grid. At the same time, the DC/DC converter's fired IGBT will be the one in series with the inductor (IGBT2), whilst the other one will always be open. The active power flow is now assumed to be determined only by the θ angle, assuming that both the voltage produced by the AC/DC converter (V_o) and the voltage at the grid side (V_i) have constant amplitudes. The total amount of power flow will be determined by the relation between the voltages and the phase angle (Eq. 4.1)

$$P = \frac{V_o * V_i}{X} * \sin(\theta) \cong \frac{V_o * V_i}{X} * \theta \qquad (4.1)$$

The active power flow is a parameter which can be set in function of many parameters and it can be increased until the intrinsic limit for a domestic plant is reached. The choice of the proper active power flow will determine the value of the angle phase θ which will then be applied to the AC/DC converter. In other words, a controller will calculate the value of θ to be applied starting from the active power required, implementing (Eq. 4.1), and the IGBTs of the rectifier will be fired according to the value of the θ angle already calculated. This is the reason why the angle phase value is not exactly a real input of the system. In any case, the assumption will be that the angle phase θ is treated as an input for the control of the system, since its correct value is not important for control purposes: what is really important is the way in which different values of θ influence currents and powers.

Now that a fixed active power is absorbed, thanks to the proper control of the AC/DC converter, the control scheme of the system has to be able to fire correctly also the IGBT of the DC/DC converter, in function of the amount of active power flow, because the power absorbed by the battery charger at the AC side has to be equal to the power absorbed by the same battery (the power equilibrium has to be verified). The following is the way in which it is piloted (Fig. 4.2).
A high frequency triangular signal carrier, whose amplitude is between 0 and 1, can be built thanks to the comparison between a proper pulse generator (which creates a square wave) and a constant signal, and an integrator block. The triangular signal obtained is then compared with another signal, which is represented in the figure only with an arrow and the "D" letter, and it is characterised by fixed or variable amplitude, whose nature will be explained in the following paragraph. The comparison between these two signals will produce a positive value whether D is greater than the triangular waveform, a negative value in the opposite case. The following comparator block compares to zero this difference, calculated instant by instant, giving in output the value 1 when the input is greater than 0 and 0 when it is lower; the result will be that of a profile similar to a square wave, but with different extensions of 0 and 1 over each period, depending on the D signal's value. This "square wave" signal is now assumed to be **the signal which pilots the IGBT**. A high value of D determines an extension of 1 greater than the extension of 0, and the duty cycle (ratio between the amplitude of D signal and triangular carrier signal) of the switch will be high and close to unit (or 100%), with the meaning that the switching device state will be more closed than open in that switching period. The control system uses this

simple technique for achieving the control of the DC/DC converter. Now two opposite operations can be considered for a better awareness of what happens physically inside the battery charger's DC/DC converter.

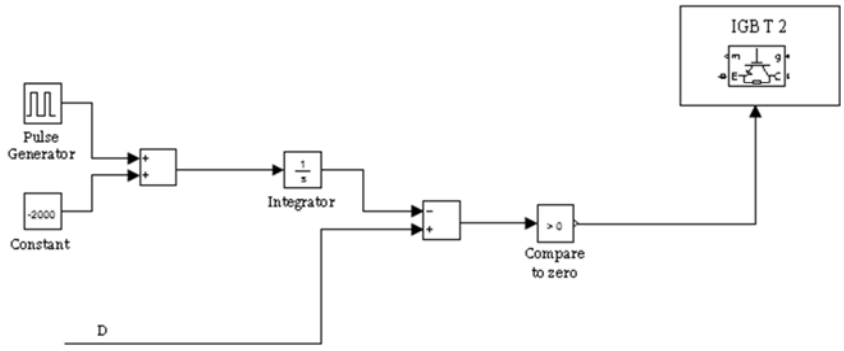

Figure 4.2 – Control scheme for the firing of the DC/DC converter's IGBTs

If the duty cycle is equal to 100%, the switching device is always short circuited and the current coming from the rectifier is free to feed the inductor and the battery without any limitations from the DC/DC converter, no "power filters" are applied between battery and grid. The opposite situation is that of duty cycle equal to 0%. This is the case in which nil current flows through the inductor and the battery. All the intermediate values of the duty cycle deal with intermediate values of currents from the rectifier to the battery: it is easy to infer that more average current inside the battery is equal to more power absorbed and more energy stored inside it.

The following scheme is the control scheme of the system, which uses the principle already explained for setting to the right value the power absorbed by the battery which is coming from the grid (Fig. 4.3): this important step will face the way in which the **duty cycle D is calculated**.

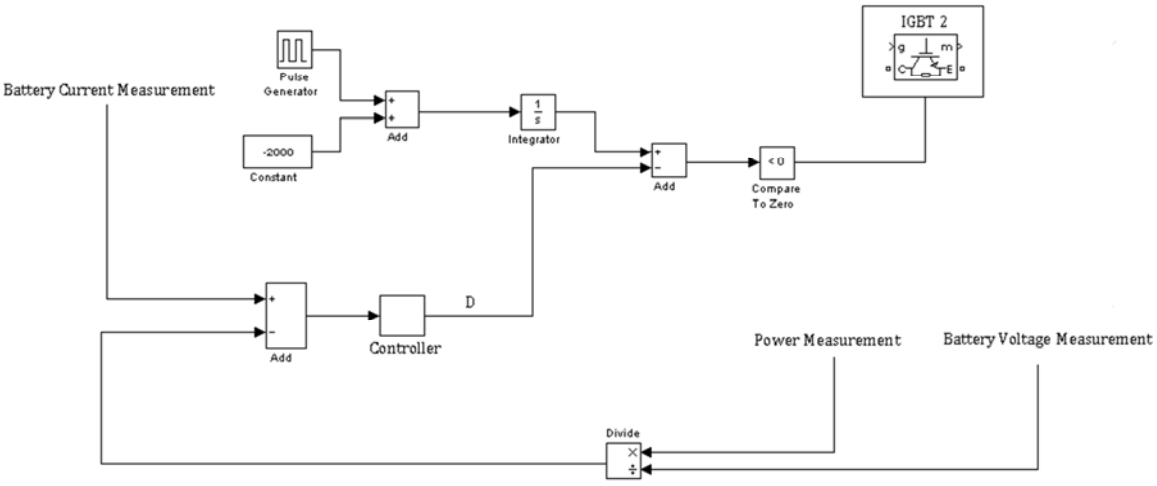

Figure 4.3 – Control strategy for the DC/DC converter

The concept of active and reactive power at the DC side doesn't exist: the power is one and it is only active: the current can always be seen as "phased" or "not phased" with respect to the voltage (so the power can be positive

or negative, but always active). This means that the power which is involved in the charging of the battery consists only on the active power absorbed by the grid, whilst the reactive power doesn't affect the DC side of the AC/DC converter. The active power can be directly measured in correspondence to the AC side of the rectifier, so between the AC/DC converter and the grid, and it is labelled in fig. 4.3 as "Power Measurement" (active power measured and active power required have to be the same, so the power measurement is done also for safety reasons: in this way the control system is sure that the power introduced inside the system is always correct and constant). Since this active power, which is absorbed by the battery charger, has to be the same absorbed by the battery at steady state, also the voltage of the same battery has to be measured. The simple (Eq. 4.2)

$$P = V * I \tag{4.2}$$

presents only one unknown term to calculate, which is the value of the proper current which has to feed the battery verifying the equilibrium between powers. The control system implements exactly this equation in the block scheme, calculating the ratio between the power measured at the AC side and the voltage of the battery. The value found in output is the current reference value, and the idea is that the controller has to change the duty cycle of the DC/DC converter in such a way to produce the real current flowing inside the battery equal to the reference value calculated. For the achievement of this aim, the measurement of the real current is needed. The difference between these two currents (reference and real) will give in output an error, whose sign and magnitude will be the input of the controller.

Before discussing about how the controller is built, it is supposed that the same controller will give as an output a value which is function of the input. If the maximum output value is limited to 1 and the minimum to 0, the same output can be used as the constant signal D, which is compared to the triangular carrier signal, introduced in fig. 4.2. A positive error (input) means that the reference current is higher than the real current, so the duty cycle D (output) has to be increased; a negative error (input) means that the real current is higher than the reference and it has to be decreased, so the duty cycle D (output) produced by the controller will decrease. All these modifications will take place until the steady state, in which the error becomes closer to be nil, is reached. The strategy of the control scheme already done achieves the equilibrium and forces the system to reach the steady state, and the total amount of energy coming from the grid is exactly the one absorbed by the battery (considering an ideal case of negligible leakages).

The DC/DC converter needs more time than the AC/DC converter to reach the steady state condition with nil initial conditions, because of the presence of reactive components as the inductor and the capacitor. As a consequence, during the first instants the active power absorbed from the grid will have already reached its rated value, but the current flowing inside the battery will be still lower than its reference value, because of a slower grow up speed. The battery charger will absorb more energy than the energy absorbed by the battery; this power (energy) difference will be stored in the capacitor, and the voltage through it will increase. In any case, steady state is reached in a fast way and the amount of stored energy won't be relevant.

The small difference between the new voltage through the capacitor and the original rated value voltage, from the active power absorbed point of view, doesn't produce any relevant variation (the magnitude of the variation is of some volts, as will be shown in the following chapters), but the reactive power exchanged could be subjected to deeper fluctuations. The necessity of monitoring the voltage for the achievement of an almost constant voltage through the capacitor, which has also to be close to the rated value, leads to the application of a capacitor control arm, which will be coupled with the original control scheme of fig. 4.3.

One of the two assumptions can be now removed, getting the battery charger model closer to the real situation. In fact, the losses of the two converters can be assumed now not to be negligible. In this case, the model already used has to be supported through the modification of control schemes.

Let's assume to be at steady state: the control scheme already built is based on the fact that there is power equilibrium between input (grid) and output (battery). The presence of losses will impact in a bad way, because whether the same amount of power in input and output is achieved, but the active power which flows through the system is reduced by losses, the same losses amount is forced be furnished by the same capacitor, and this fact will produce the progressive decrement of its voltage. This is not a stable situation because, as demonstrated, this will impact both on active and on reactive power, and the required steady state will not be kept nor even reached. The solution will be found out by compensating losses through the incoming active power. The unwanted but inevitable consequence is the fact that the power absorbed by the battery will decrease, but in this way equilibrium can be reached. This equilibrium will also be reliable because even if variable losses will take place (for example as consequence of aging of the capacitor or other devices) it will be always reached and maintained. The modified scheme that has to be used if the assumption of negligible losses is removed is shown in fig. 4.5, whilst fig. 4.4 shows the sections in which the measures needed for the application of the control will be taken.

In the scheme of fig. 4.4 the power measurement, which is the measure of the active power flowing through the battery charger, is not performed at the AC side of the rectifier (interface between battery charger and grid), but at its DC side; in this way the measurement will furnish a lower power value, dealing with the fact that the AC/DC converter's losses will produce the decrement of the active power flow. In this way, the control scheme will now deal only with the losses produced by the DC/DC converter. The current absorbed by the battery is measured in correspondence of the same battery, whilst current measurements regarding the capacitor are picked in two sections: before the capacitor, so between it and the rectifier, and after it, so between it and the DC/DC converter. If the capacitor is not absorbing or delivering power, it means that the average current through it has to be nil. These two measures are useful for checking this situation, because once it is verified that the difference between the two is nil, the capacitor is not contributing anymore on power flow, and its voltage will be maintained constant.

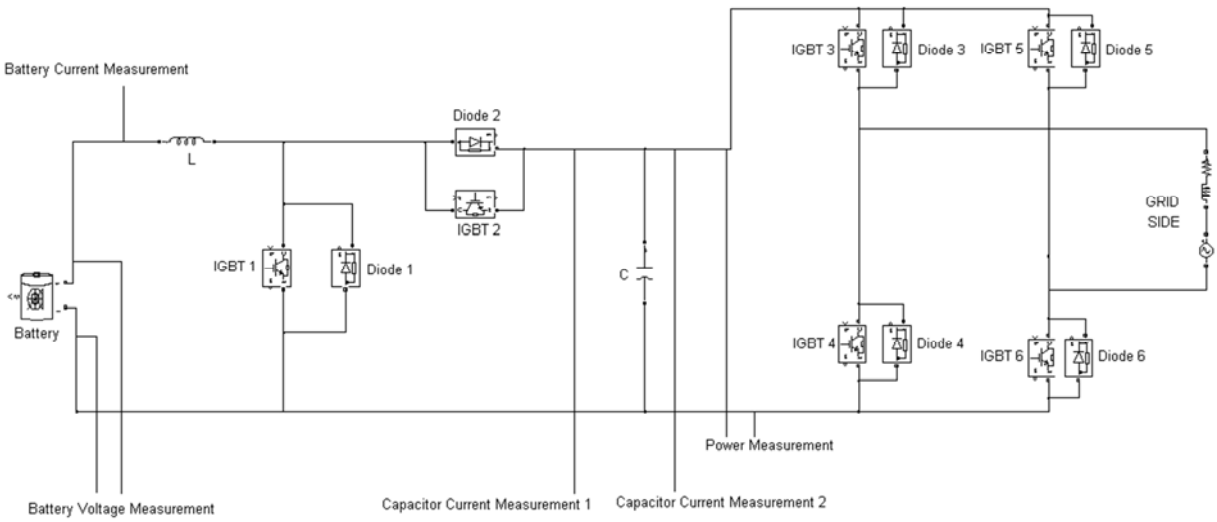

Figure 4.4 – Sections where electrical measurements are taken

Let's now focus on the arm related to the new control strategy (Fig. 4.5): the two current measurements are compared and the error is integrated; the output is multiplied by a constant and then this value is introduced to the sum with reference current and real current. If the error is positive it means that average current is not nil and energy is flowing out of the capacitor, which means discharging. To avoid the discharge, this positive error introduced in the sum, combined with the reference current, reduces the request of real current flowing through

the battery, decreasing the duty cycle of the DC/DC converter's IGBT. In this way, less current will be absorbed by the system composed by the DC/DC converter and the battery, so the energy delivered by the capacitor will be reduced till nil value. The use of the integrator for this scheme is fundamental, and this sentence is demonstrated in the following way.

The assumption for a while is that now the system is working without the integrator block on the capacitor control arm. Initially, the scenario can be that of a difference between the two capacitor currents measured which is equal to zero (so the capacitor is not delivering or absorbing energy). In this theoretical case no error from the capacitor control block would push the current absorbed by the battery closer and closer to the current reference value; again, losses of the bidirectional boost converter will produce a power flow on the capacitor and the error that was nil before now changes and the capacitor turns to be active. This means that a real steady state in equilibrium condition without the integrator block is never verified, and at steady state a non nil input signal coming from the capacitor control arm has to be always present. Thanks to the use of the integrator, when the input (difference between currents of the capacitor) is nil, the output is a fixed value which is constant but not nil.

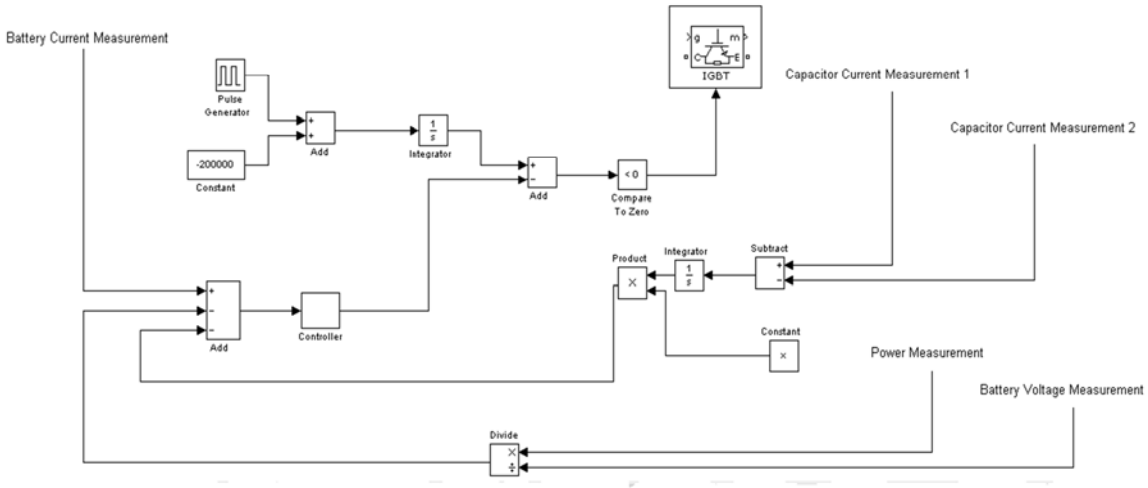

Figure 4.5 – New control scheme with not negligible converters' losses

Some issues regarding the measurements of the magnitudes which will be used as inputs for the control scheme are now considered. The active power which can be measured at the AC side of the rectifier is relatively easy to measure, because voltages and currents are sinusoidal and free of ripples; the situation is different for the power measured at the DC side. In this case the voltage corresponds to the voltage through the capacitor, which is almost constant. The current instead is continue, but not constant. This means that its mean value is positive or negative, but the instantaneous value changes, assuming different values instant by instant. Since the power is V times I and it is constant only when considering the mean value of the current, the signal "power measurement" depicted in fig. 4.5 is find out considering the mean value of the instantaneous current.
Something can be also said about the measurement choice for checking the power absorbed or delivered by the capacitor. There are two equivalent possibilities: the first is to measure the current flowing from the DC side of the AC/DC converter to the capacitor and the current flowing from the capacitor to the DC/DC converter, and then compare them as what has been done before. An alternative which seems to be cheaper is the one of measuring directly the current through the capacitor: dealing with the control strategy, the situation is exactly the same, but in the first option two current transducers are needed, whilst in the second only one is needed. The second option as a consequence seems to be better, but a deeper analysis of the system shows that the power measurement is done at the same point (between AC/DC converter and capacitor), and voltage and current

flowing through that section are needed. This means that one of the two current measurements is already accessible for the control scheme. As a consequence, developing the control through the calculation of the difference between the two signals (the second transducer is put between the DC/DC converter and the capacitor) or analysing just the current through the capacitor (transducer put in series with the capacitor) is theoretically the same regarding the number of devices needed for the achievement of this objective. By the way, if the instruments used for measurements are real and not ideal, it is possible to demonstrate that the difference between two signals that can be quite similar gives a relative error which is very high, so the best solution is the one of handling the current through the same capacitor. Another reason in advantage to this choice is the fact that the "subtract block" is not used. Summarizing the concept, in the ideal Simulink domain the two solutions are exactly the same and the results are coincident in both cases, but for the developing of the real control scheme the second option will be the best. The following figures (Fig 4.6 and 4.7) will show the topology of the control scheme with the improvements brought by this choice.

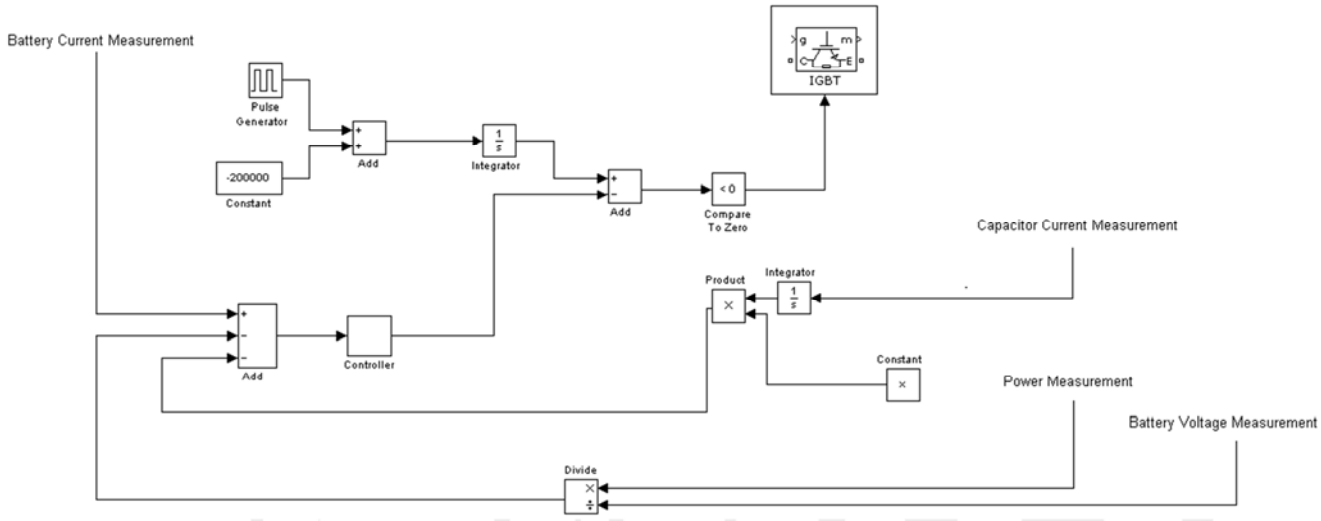

Figure 4.6 – Improved control scheme with non negligible converters' losses

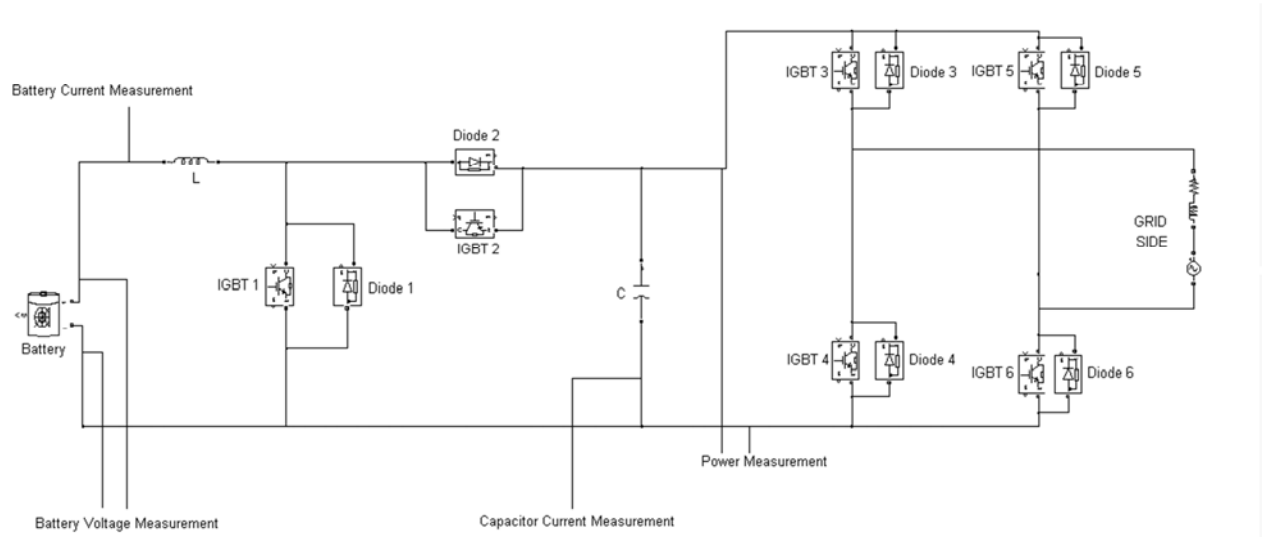

Figure 4.7 – Sections where electrical measurements are taken according to the improved control scheme

4.2 – System Stability: Verification for Charging Mode

Section 4.1 has explained the way in which the controller has to work for piloting the two converters of the battery charger in order to reach the required steady state, analysing all the control issues that can affect the system. The next section has the aim to choose a suitable controller which can lead the system to a stable steady state. This analysis needs the use of the block scheme already built, working on its frequency response using Laplace transformation. It is important to declare that the certainty to dispose of the transformation (with the entire hypothesis that belongs to it) is not present; by the way, the assumption is that there is the possibility to work in this domain.

The **first step** will be that one of modelling the entire system through the Laplace transformation, element by element. The measure instruments are supposed to be linear: this means that if the magnitude subjected to measurement varies making a step, the signal which corresponds to the obtained measure reaches the correct value after some τ, where τ is the time constant of the instrument. In this way a current transducer can be described in Laplace domain, which connects input and output through a transfer function, typing the following law

$$\frac{I_{measured}}{I} = \frac{K_i}{1+s\tau_i} \tag{4.3}$$

Considering this transfer function, there is the possibility to distinguish between K_i which is the static gain and $\frac{1}{1+s\tau_i}$, which is the dynamic gain. The same representation can be applied to the duty cycle of the IGBT of the DC/DC converter. If the constant signal D introduced at the beginning of the chapter, which is compared instant by instant to the triangular carrier signal, varies, the effective variation of the duty cycle of the correspondent IGBT is not immediate, because there is a delay which deals to the fact that the previous switching period needs to finish before the variation takes place. The equation is exactly the same as the one written before, except for the fact that here the time constant τ is the reverse of the working frequency, which is assumed to be 10 kHz: this means that the block which synthesizes the behaviour of the duty cycle variation synthesizes, in time domain, a block which responds in a fast way to input variations. The following (Fig. 4.8) shows the control scheme where Laplace transformation is applied to block measurements, which connects the real physical system to the control scheme.

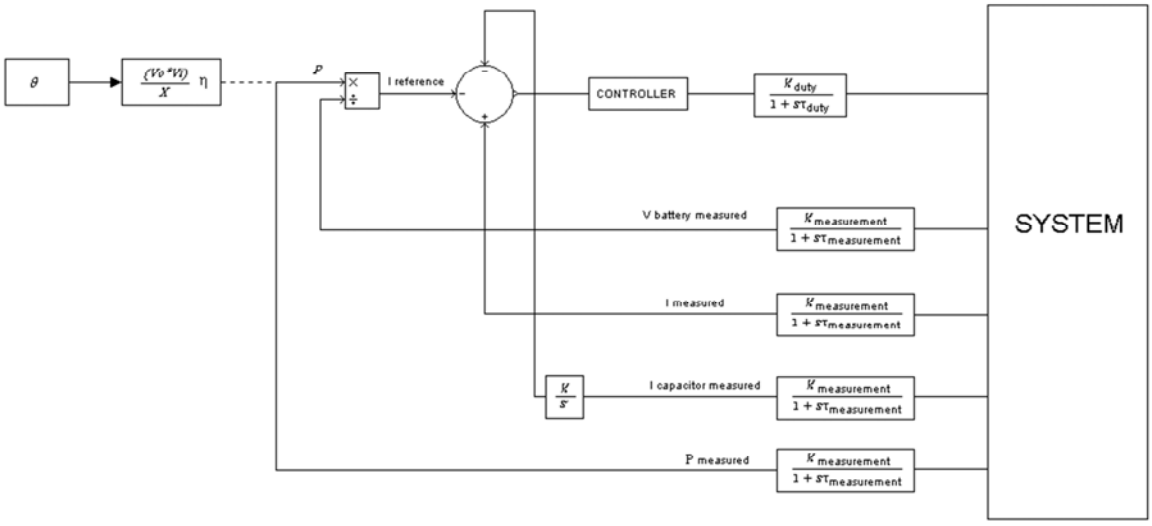

Figure 4.8 – Control scheme according to Laplace transformation

The power value is depicted through the application of (Eq. 4.1), but in the real situation this value is also measured, and the block scheme dealing with this measure is exactly the same as the other measurement block schemes. The two values have to coincide (AC/DC losses have to be considered, so efficiency η of the AC/DC converter has to be applied to the equation of the block of fig. 4.8 for a perfect match between the two power values).

The **second step** is more complicated: the aim is to build a model of the block called "SYSTEM" in fig. 4.8, in order to get a model of the physic of the battery charger. The input of this block is the duty cycle applied to the DC/DC converter, whilst the outputs are the parameters measured. If the system is correctly modelled through block schemes, it can be studied in terms of stability and the proper controller needed can be found out.
It is now considered one switching period in which the IGBT of the DC/DC converter commutes.
Referring to fig. 4.1, the focus stands on the evolution of the system when IGBT2 is closed. In this portion of the switching period the mesh is made by the series of the battery, the inductor and the capacitor, and as can be easily seen, the equation which describes the mesh is the following (Eq. 4.4)

$$L\,\frac{di}{dt} = V_{capacitor} - V_{battery} = \Delta V \tag{4.4}$$

$$i = i_0 + \int \frac{\Delta V}{L}\,dt \tag{4.5}$$

Now, if ΔV is supposed to be constant, the solution of (Eq. 4.4), will lead to (Eq. 4.5), where the current increases linearly with time. Whether the real situation is considered, so the proper control is applied, the current will raise but it will stop increasing after a certain time. In particular, the profile of the current will depends not only on the control strategy but also on the other parameters of the system, like the time constant $\tau = L/R$. The evolution of the circuit with realistic values of ΔV, R and L in case of the application of a unit duty cycle can be transferred in Laplace domain, and the equation which governs this more realistic model is

$$L\,\frac{di}{dt} + Ri = \Delta V \tag{4.6}$$

It is easy to see that the maximum current that can be theoretically reached with unit duty cycle is certainly too much high to be tolerated, in fact at steady state the inductor will be a short circuit and the resistance is not as high to limit the current produced by the difference between the voltage through the capacitor and through the battery. However this is not a problem, since the growth rate of the current, even during the first moments, is not too much high and it can be easily monitored and handled by the control system using a correct controller and appropriate parameters of the devices (for instance high switching frequency of the IGBT). Another factor which brakes the excessive growth of the current is the fact that the inductor used is relatively big, so the current doesn't vary in a too much fast way: the increment is slow and the regulation of the entire system is able to control its profile instant by instant, so even if a duty cycle equal to 1 is applied, the current starts to grow up linearly but with a slope which can be tolerated.

The dynamic of the system during the remaining part of the switching period, so that one in which IGBT2 is open, will be studied. It is easy to see that no current flows from the DC side of the AC/DC converter, but this does not mean that nil current is flowing inside the battery: fig. 4.1 shows that the equation which govern the mesh is

$$V_{battery} = L\,\frac{di}{dt} \tag{4.7}$$

and this time the voltage of the battery induces a decrement in the current which flows through the system.
Even in this case the presence of resistors is not considered in the equation, but they are present and have influence on the dynamic of the system.

Now that the two possible working conditions have been studied, it is easy to understand how the entire model works. The system can be classified as a system in which an input (duty cycle), which is applied starting from nil initial conditions, pilots the IGBT in such a way that the output (current) grows up with a certain profile and reaches a certain steady state value, function of the same input. In this case the output is even proportional to the input; nil duty cycle means nil current flowing, duty cycle close to 100% means current closer to its maximum, but reached with a certain delay. As a consequence, the system could be described with a first order transfer function, and what can be done is the application of a model which is described with the following transfer function

$$I_{system} = \frac{K_{system}}{1+s\tau_{system}} * U_{duty\ cycle} \tag{4.8}$$

Where I_{system} is the real current through the DC side of the battery charger and $U_{duty\ cycle}$ is the input applied. This model is quite similar to the real working condition, in which according to the application of a duty cycle not nil, the current increases almost linearly in the first moments and then after a determined period of time it reaches steady state if no more modifications of the system overcome. The static gain gives the proportion between the duty cycle in input and the real value assumed by the current at steady state in output, whilst τ_{system} is the time constant of the physic system and it is expected to be quite high with respect to the other time constant related to control scheme. The situation is that of a first order system with a relatively high time constant.

Some peculiar characteristics of this block scheme already made have to be pointed out. Three feedbacks (Fig.4.8) are present. One deals with the real current flowing through the circuit, one with the voltage of the battery which is used for calculating the reference current, and one with the current which flows through the capacitor. The step already concluded has pointed out the dynamic of the first feedback, the one which deals with the real current flowing through the system, but there are still two others feedbacks to analyse, and the next step is their modelling. The second one deals with the voltage through the battery. Since the battery shows an internal resistance, this value changes in function of the current flowing through it; but the low value of this resistance and the fact that the voltage variation caused by the charging mode needs long time to become influent make the relation between the first and the second feedback negligible, so these two arms can be considered as decoupled. The third feedback, instead, deals with the current flowing through the capacitor. The following equation shows the dynamic of the situation, where $P_{capacitor}$ depicts the power absorbed or delivered by the capacitor, $V_{capacitor}$ and $I_{capacitor}$ are voltage and current through it, P_{in} is the power coming from the DC side of the AC/DC converter. The subscripts "battery" instead of "capacitor" means the power, the current and the voltage through the battery.

$$P_{capacitor} = V_{capacitor} * I_{capacitor} \tag{4.9}$$

$$P_{capacitor} = P_{in} - P_{battery} \tag{4.10}$$

$$P_{capacitor} = P_{in} - V_{battery} * I_{battery} \tag{4.11}$$

Since the current which flows through the battery coincides with the measured current, so exactly the "$I_{measured}$" of the block scheme of fig. 4.8, it is easy to write the equation which connects it to the current through the capacitor.

$$I_{capacitor} = \frac{P_{in}}{V_{capacitor}} - V_{battery} * \frac{I_{measured}}{V_{capacitor}} \tag{4.12}$$

Thanks to this development, it is possible to redraw the block scheme that was introduced with the previous

(Fig. 4.8), substituting it with the new block scheme shown in fig. 4.9. This will give the possibility to understand the way in which all the blocks will act and combine together. For an easy handling of this system, which is complete but not so comfortable, some assumptions can be made in order to get a simplified scheme.

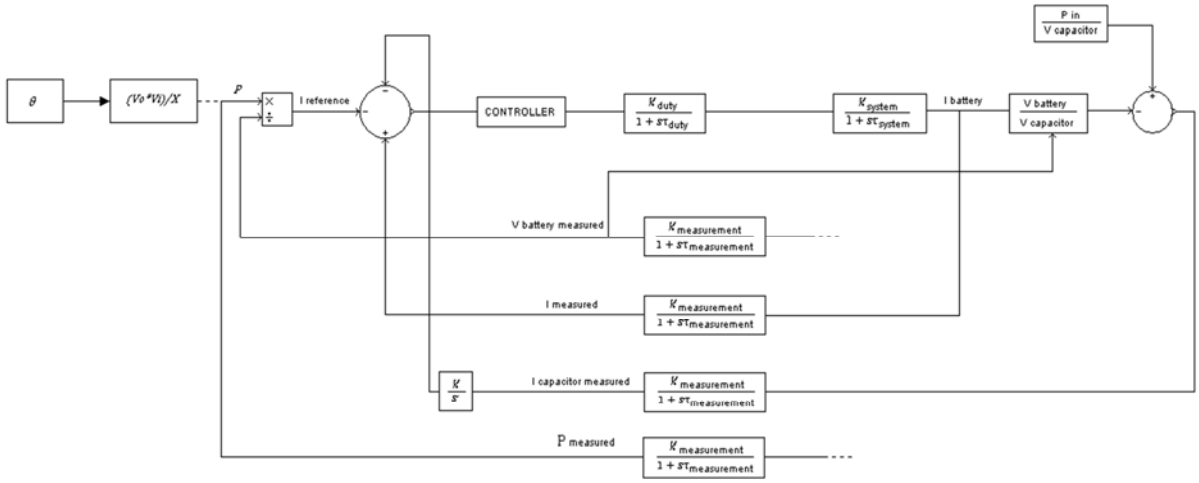

Figure 4.9 – Block scheme of the whole system

The system built in this way reproduces the behaviour of the G2V mode of the battery charger, both from the physical point of view and from the control scheme point of view. Since three feedbacks are present and one of them ($V_{battery}$) even influences one other ($I_{capacitor\ current}$), or it is better to say that they influence each other, a way to improve the scheme for a better comprehension of it has to be done. The behaviour of the voltage of the battery is now studied: this value surely changes because of the increment of the SOC. In any case, the charging process is quite long and takes hours (this is the case of a domestic charging, not a fast charging). This means that the growth rate of the voltage is very low, and can be considered to be negligible if compared to the physic of the system. Indeed, it can be demonstrated that the same system is not influenced by these continuous little increments of the voltage through the battery. This means that this magnitude can be treated as a constant value in the following consideration, and as a consequence the feedbacks from three they become two, simplifying the system.

The dynamic which deals with the capacitor control needs now to be analysed. During the first moments, when the circuit is energized and steady state is not yet reached, an unbalanceness regarding powers is always present. The transient state that regards AC/DC converter ends quickly, and the active power pumped into the system reaches in few moments the rated value. Longer time is needed for the DC/DC converter to reach its steady state: this means that during the first instants the battery absorbs less power than the power incoming, and during these moments the difference between the two power flow is stored inside the capacitor. The issue lies exactly here: whether the gain of the capacitor arm's integrator is set to high values, the error will be amplified and a relatively high signal coming from the capacitor control arm will be introduced: this will contribute to the input signal (error) of the controller from the very first moments, with the consequence of interfere with the first step of the dynamic, in which the real current gets close to the reference value (this first step will be called "primary control"). There is the possibility to read the same situation in a different and simpler way: the control scheme feels that the capacitor is charging, so it reacts increasing the reference current in such a way that the duty cycle will grow more, and the current absorbed by the battery increases in a fast way. This capacitor arm control feedback, although it is necessary for achieving the equilibrium of the system, is not positive during these very first moments, in which the battery charger is still far from its steady state, even if this interference produces good effects. The influence of the capacitor control arm on the primary control, whose aim is to make the real

current close to the reference current, is negative and does not allow to reach properly and in a stable way the steady state condition.
The control strategy should be divided into two steps, the primary and the secondary control. Since for these two controls (the primary control which deals with the increment of the current from nil value to a value close to the reference one, the secondary control which deals with the variation of the current from the reference value to a value which is the one that guarantees powers equilibrium) is better to work in a separate way, the value of the integrator gain will be set in such a way that the signal coming from the capacitor control arm will start to be influent only when the primary control will be reached and the current will be close to its reference value.

These considerations are able to impact on the block scheme, which can be now represented in fig. 4.10, where only one out of the original three feedbacks is presented. It is important to remember that the other two feedbacks are still present, but their characteristics don't produce relevant modifications in the system's dynamic during the first instants.
It can be demonstrated that if the primary regulation is well achieved, the other two feedbacks cannot make the system unstable anymore. Even the blocks regarding the measures can be neglected, since their behaviour doesn't influence the whole system's behaviour, which can be now studied in the following way.

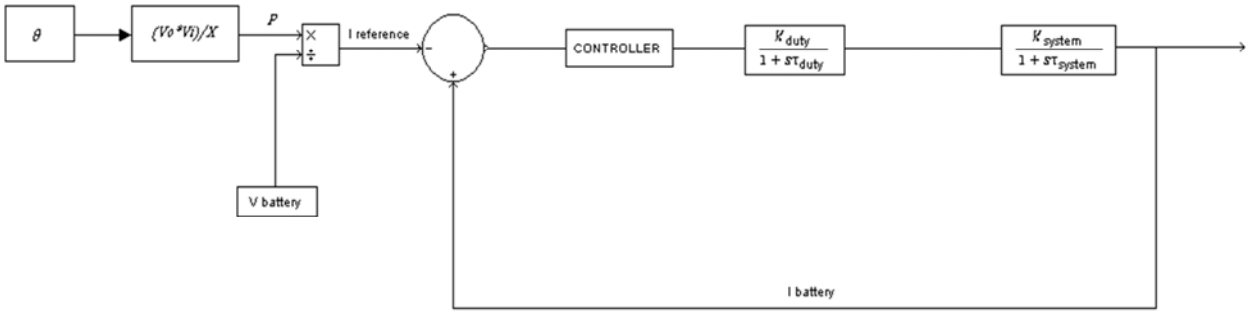

Figure 4.10 – Block scheme studied for the controller design for the primary control

Since the input (θ) and the voltage through the battery are constant, the same reference current ($I_{reference}$) is constant. The **third step** is the analysis of the transfer function of the open loop without the controller. As a simplification, the two static gains present in the block scheme (gain of the system and of the duty cycle control) are incorporated to the static gain that will be assigned to the controller. This fact leads to the writing of the following open loop transfer function without the controller

$$H_R(s) = \frac{1}{(1+s\tau_{system})\,(1+s\tau_{duty})} \tag{4.13}$$

The Bode diagrams will show how the system behaves. Since the frequency of the triangular signal for the control of the DC/DC converter's IGBT is equal to 10 [kHz], this means that $\tau_{duty} = 1/frequency$. The plot of fig. 4.11 describes the magnitude and the phase of the dynamic model frequency response which has been already built. The transfer function $H_R(s)$ is analysed without the presence of the controller, which will be introduced later.

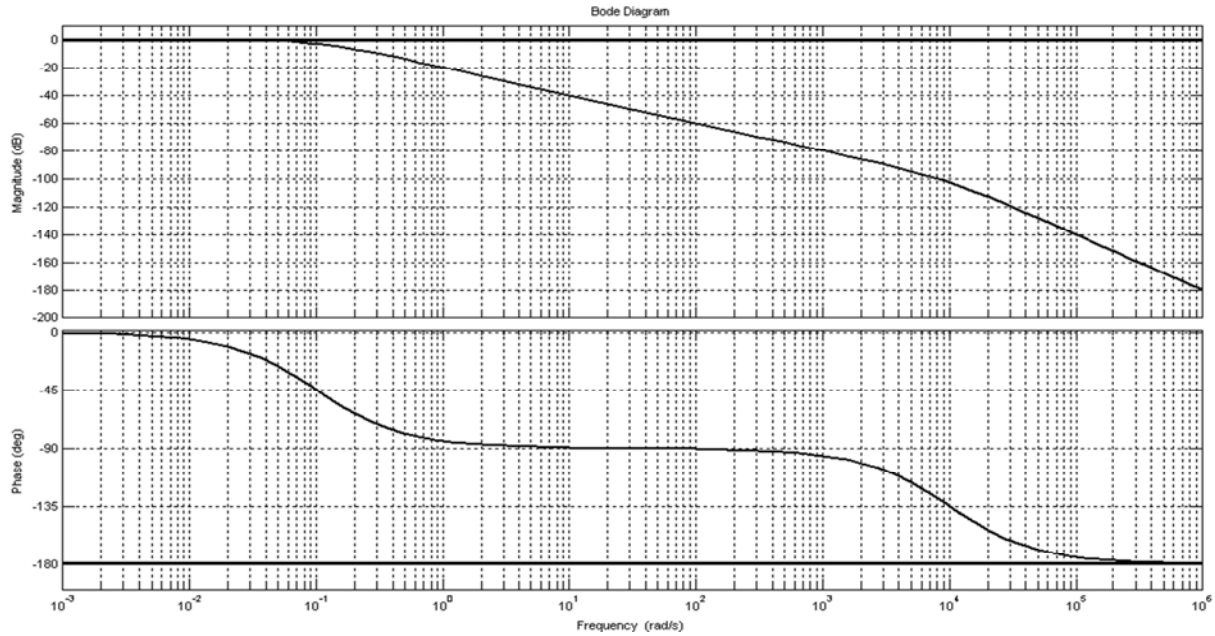

Figure 4.11 – Magnitude and phase of the open loop transfer function without the controller

The **two key parameters** which are involved in the system response are now pointed out, dealing with its stability: they are the **cross frequency** (ω_{cross}) and the **phase margin** (m_{φ}). First of all, let's consider the cross frequency: this value corresponds to the frequency (in rad/sec) in which the magnitude of the transfer function plotted is nil, considering logarithmic scale. The phase corresponding to this pulse is defined as the phase margin of the system. For having a stable system, which can reach a steady state and can be controlled, the value of the phase margin needs to be higher than the fixed value $-\pi$. In the real case, a phase margin value which is higher than $-\pi$ by some degrees (so not so much higher) depicts a stable but dangerous system (even if the phase margin is verified), because a little physical variation of some parameters of the circuit can modify the frequency response and make the system unstable. As a consequence, the system will be considered stable if the phase margin is higher than $-3\pi/4$. The cross frequency determines the bandwidth, which is the highest frequency of a reference signal that the system can follow keeping limited its error under a fixed value. The increment of the bandwidth makes the system to become faster, i.e. the steady state can be reached in less time, and this can be an important advantage; on the other hand, the possibility to produce overshoot while reaching steady state will increase too. Analysing the figure, it is easy to understand that the maximum bandwidth is limited by the switching frequency of the DC/DC converter's IGBT.

Now that these two parameters are introduced, the design of the controller can be faced: the aim of this block is to modify Bode diagrams (Fig. 4.11) in a way that the open loop frequency response can be improved. Two different solutions can be tested; the first option is to implement a P (proportional) controller.

P CONTROLLER

The P controller is just a proportional block which multiplies the input error, and its effect on the transfer function are described by the increase or decrease of the magnitude of the frequency response, whilst the phase diagram won't be modified. This means that the following equation of the open loop transfer function can be written (the subscript "R" is not present because the controller is applied)

$$H(s) = K_p * \frac{1}{(1+s\tau_{system})\,(1+s\tau_{duty})} \tag{4.14}$$

It is important to remember that K_p incorporates all the static gains, the ones of the system and the one of the same controller. This means that this term is not exactly the one which has to be set for the controller, which is defined as $K_{controller}$. This parameter can be set in such a way that the bandwidth will get close to the switching frequency of the IGBT, but this frequency can't be exceeded. The most important disadvantage which comes from the usage of a P controller is that the steady state error will not be nil. In fact, going backward and looking at the block scheme of fig. 4.10, an easy consideration can be made. Since the hypothesis is that steady state is reached, the output is $I_{battery}$, which is constant, and the variable "s" of Laplace transformation is equal to zero. As a consequence, the input of the system will be $I_{battery}/K_{system}$. For the same reason, the input of the duty cycle block will be $I_{battery}/ (K_{system}*K_{duty})$. Finally, the input of the proportional controller, which will be also the error between the reference current and the current flowing through the battery, will be equal to $I_{battery}/ (K_{system}*K_{duty}*K_{controller})$. If a fast response is required, and the bandwidth needs to be consequently increased, the increment of $K_{controller}$ for the achievement of the objective increases also the steady state error, which will be, in any case, not nil for any choices of $K_{controller}$ values. The application of a PI controller will avoid this error.

PI CONTROLLER

The PI controller is composed by a block which multiplies the error and a block which integrates it. In terms of Laplace transformation, the block's equation can be written as

$$R(s) = \left(K_p + \frac{K_i}{s}\right) \tag{4.15}$$

$$R(s) = \frac{Kp*s+Ki}{s} \tag{4.16}$$

$$R(s) = K_i * \frac{1+s\tau_R}{s} \tag{4.17}$$

with $\tau_R = \frac{K_p}{K_i}$. Even in this case the value of the parameter Kp incorporates all the static gains present in the open loop block scheme, whilst $K_{controller}$ is the proportional gain of the only PI controller. The correct choice on the values of the two parameters can produce an improvement on Bode diagrams. This kind of controller presents for high frequency values (high *s* values) the same behaviour as the proportional controller, because the phase is not modified and the magnitude is multiplied by Kp. For low frequency values (*s* close to nil), instead, the situation changes and the controller starts to influence the frequency response of the system. If this controller is applied to the system, the correct values of the two parameters have to be calculated.
The first step for this calculation is the setting of ω_{cross} and phase margin, but independently from the exact value picked up for both, it has to be verified that the phase margin is greater than $\frac{\pi}{4}$ in correspondence of a cross frequency lower than $1/\tau_{duty}$. The full transfer function (with PI controller) of the open loop is the following

$$H(s) = R(s) * \frac{1}{(1+s\tau_{system})\,(1+s\tau_{duty})} \tag{4.18}$$

$$H(s) = K_i * \frac{1+s\tau_R}{s} * \frac{1}{(1+s\tau_{system})(1+s\tau_{duty})} \tag{4.19}$$

Now the phase margin will be imposed and the phase of the transfer function H(s) will be put equal to this fixed value. Since there is only one unknown term, which is τ_R, this value will be calculated. The second step imposes that in correspondence of ω_{cross} the magnitude of the transfer function has to be equal to 1 (in terms of logarithm). This means that the term "$j*\omega_{cross}$" substitutes the term "s" and the following equation is solved

$$H(j\omega_{\text{cross}}) = 1 \tag{4.20}$$

Since the solution of the second step will give as a result the value of K_i, the problem is solved, because with the two results Kp can be calculated and the design of the controller is done. Since the aim is to produce a steady state with no permanent error (because the rated current value absorbed by the battery has to be achieved), the choice of using a PI controller is the best because in this way a nil steady state error is guaranteed. The following fig. 4.12 depicts the frequency response of the system with the application of the PI controller.

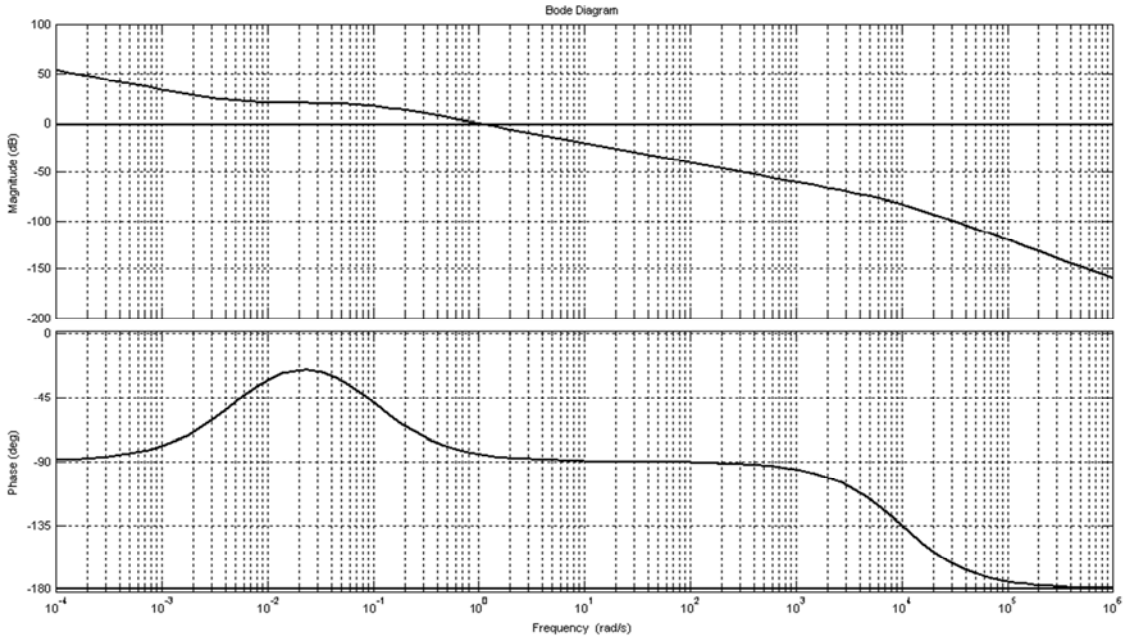

Figure 4.12 – Frequency response of the system with the application of the PI controller

With this tool it is possible to infer whether the system is stable and whether and how much the PI controller proposed can improve stability on the control scheme. The case already applied shows a stable system with a phase margin of +95° and a cross frequency ω_{cross} of 10^0rad/sec. Since the maximum bandwidth still deals with the switching frequency of the duty cycle of DC/DC converter's IGBT, even according to the application of a PI controller there is the same maximum value of the bandwidth that can't be exceeded. The only way to go beyond this limit is the use of a PID controller, but the system analysed shows that this is not necessary so this option won't be considered.
Considering the PI controller, the maximum speed level can be achieved increasing the proportional gain of the controller, in such a way to increase the cross frequency keeping stable the system (because the suitability phase margin is still verified). In any case, if this increment is applied, it is important to remember that even the gain of the controller's integrator has to be increased, because the ratio $\tau_R = K_p/K_i$ has to be kept constant.

The model studied has led to the design of a PI controller which should be able to control the entire system in a proper and stable way under all the introduced simplifications. The assumption made regarding the fact that the voltage of the battery is considered constant, because of the very slow dynamic of the energy storage device if compared to the system, can be easily confirmed in the real case. Instead, with regards to the capacitor control, the static gain of the integrator block of the capacitor control has to be set to the proper value, in such a way that the effect of this feedback takes place after the primary control is almost complete. Paying attention to this last point, the same primary control's stability is not influenced, and the model analysed in this chapter for stability purposes will effectively follow the real system dynamical behaviour.

4.3 Discharging Mode (V2G)

This is the case of the reversed active power flow, which goes from the vehicle to the grid. The physic of this configuration is different from the analysis made for charging mode, and this is mostly due to the presence of the inductor. Although this difference is present, the frequency response of the new discharging mode system without the controller is close to the one studied for charging mode: this means that the same analysis can be made and a new PI controller can be used. The stability of the system is guaranteed even for this case; the analysis won't be repeated.

The achievement of a proper control system for both the two modes allows the run of two different simulations, respectively for charging (G2V) and discharging (V2G) mode, with the aim of analysing the dynamics of the electrical parameters which take place during transient states: in fact the system, which is now demonstrated to be stable, will present particular dynamics of its electrical parameters, which have to be suitable for its application in the real world; the achievement of the steady state is not sufficient.

5 – G2V (Grid-to-Vehicle) Mode: Simulation

Since in chapter 4 the stability of the system has been verified and the system is demonstrated to be stable, the next step will be that of the running of a simulation in which the charging of the battery of an EV plugged to the grid is considered. All the electrical parameters during both transient state and steady state will be analysed, because the profile of the power flow and the evolution of currents and voltages inside the system have to be considered suitable for the actual realization of the device.

The grid is modelled as an ideal sinusoidal voltage source (RMS equal to 230 [V]) connected in series with impedance. The capacitor's initial voltage is set to 650 [V] in such a way that the sine wave produced by the rectifier will have almost the same amplitude of the sine wave of the grid (acting also on the modulation index). The angle phase θ is set to be equal to 13°. The power introduced with this value is high and close to the limit allowed for a domestic plant. The voltage through the battery is equal to 100 [V], but this value can be far from reality, considering the current status of the technology. By the way, the value assumed by this parameter doesn't influence the dynamic of the system, since it will only influence the final amplitude achieved by the current absorbed by the battery. (The choice of a lower voltage through the battery with respect to the state of the art corresponds to an highlighted current profile). The current is expected to start from nil value and grow up till steady state value. Finally, the simulation time is set to 1.5 [s]. Now that all the initial conditions are described, the simulation can be run and the results can be checked.

The **active power** flow at the AC side of the AC/DC converter of the battery charger has to be considered as first: the measures are taken in correspondence of the section where the device is plugged to the grid. The active power flowing, after a short transitory of about 0.05 [s], will settle to a fixed value of 3300 [W]. Figure 5.1 shows this evolution (negative value means that as a convention the power is flowing from the grid to the battery).

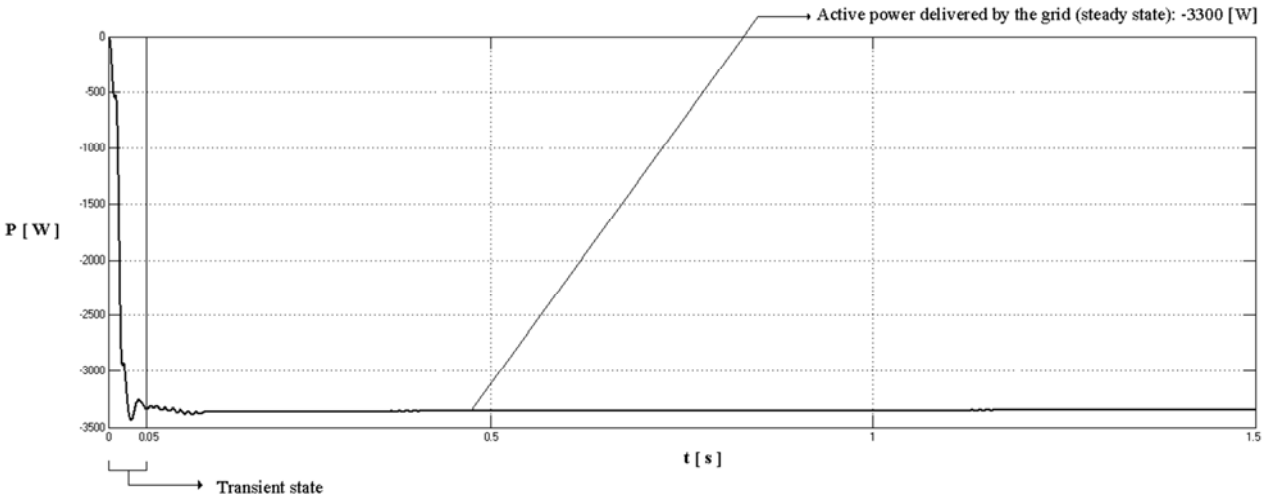

Figure 5.1 – Active power delivered by the grid to charge the battery

In correspondence of the same section, even the measure of the **reactive power** exchange can be achieved. In this case the steady state will be reached in longer time, and the transient state will be consistent, due to the variation of the voltage through the capacitor. Figure 5.2 depicts the evolution of this parameter.

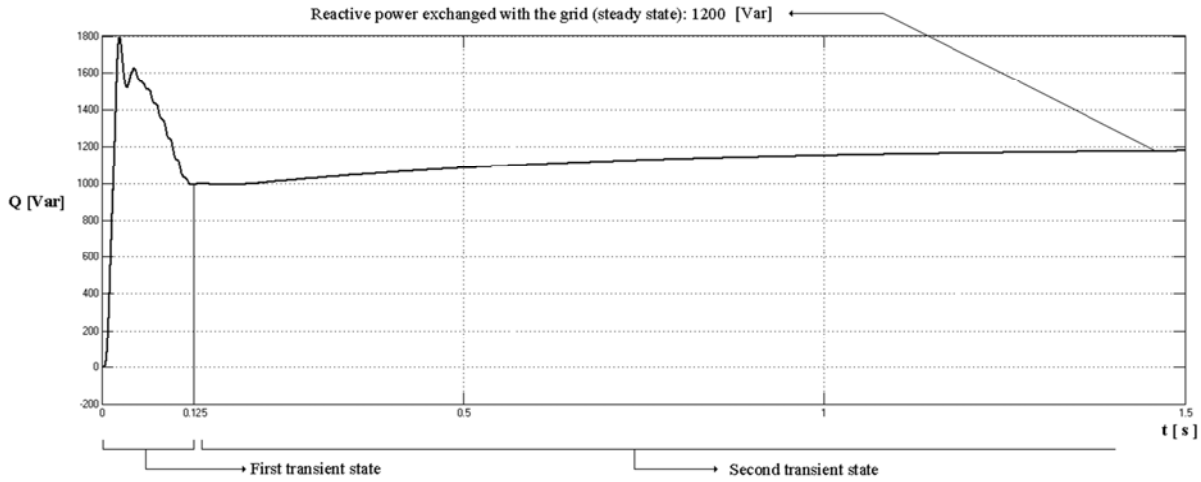

Figure 5.2 – Reactive power flow from the grid to the battery charger

As can be seen, the transient state of reactive power is more prominent, and it is composed by two periods: the first one ends after 0.125 [s] and it is characterised by the achievement of a high peak followed by a sudden decrement of the reactive power exchanged value, whilst the second one is characterised by a smoother and milder profile than the previous, and leads to the effective steady state after few seconds. This dissertation will not focus on the reactive power control, but the possibility to improve the control scheme of the battery charger introducing an arm which can deal with the modulation of the exchange of reactive power is available, and the theory already introduced can demonstrate that two different controls for active and reactive power can be conducted independently.

Since the implemented control scheme doesn't use active power data from the AC side, but from the DC side, fig. 5.3 will show the **active power flow measured at the DC side**, which is used as a reference for the control. It has to be pointed out that the two powers which have been considered till now are not described in the same way. In fact, whilst the active power flow at the AC side is effectively constant, the DC side presents basically a fluctuating value: this happens because the constant voltage value through the capacitor is multiplied by a direct (but not constant) current value. This means that the only multiplying operation is not enough for achieving a proper (constant) control signal: its mean value has to be calculated. In fact, if the instantaneous value is applied to the control scheme, the reference current will be subjected to fluctuations. For this reason fig. 5.3 shows the mean value of the power flow instead of the instantaneous one, which wouldn't be useful. The period of time needed for the achievement of values of the reference current which can be suitable for the control is of 0.25 [s]. Thanks to the control scheme the reference current and consequently the real current which feeds the battery starts to increase in few instants after the starting of the simulation.

Figure 5.4 depicts the profile of the controlled current, according to the convention that negative current means current absorbed (and energy stored) by the battery. As can be seen, the profile of this electrical parameter, which is very important, is free from over shoots and it reaches its rated value after an acceptable transient state, which is 0.20-0.25 [s] long, and is characterised by a linear growth of the current. This profile is suitable for the

charging of the battery, since nor during transient state neither during steady state electrical stresses are present in it.

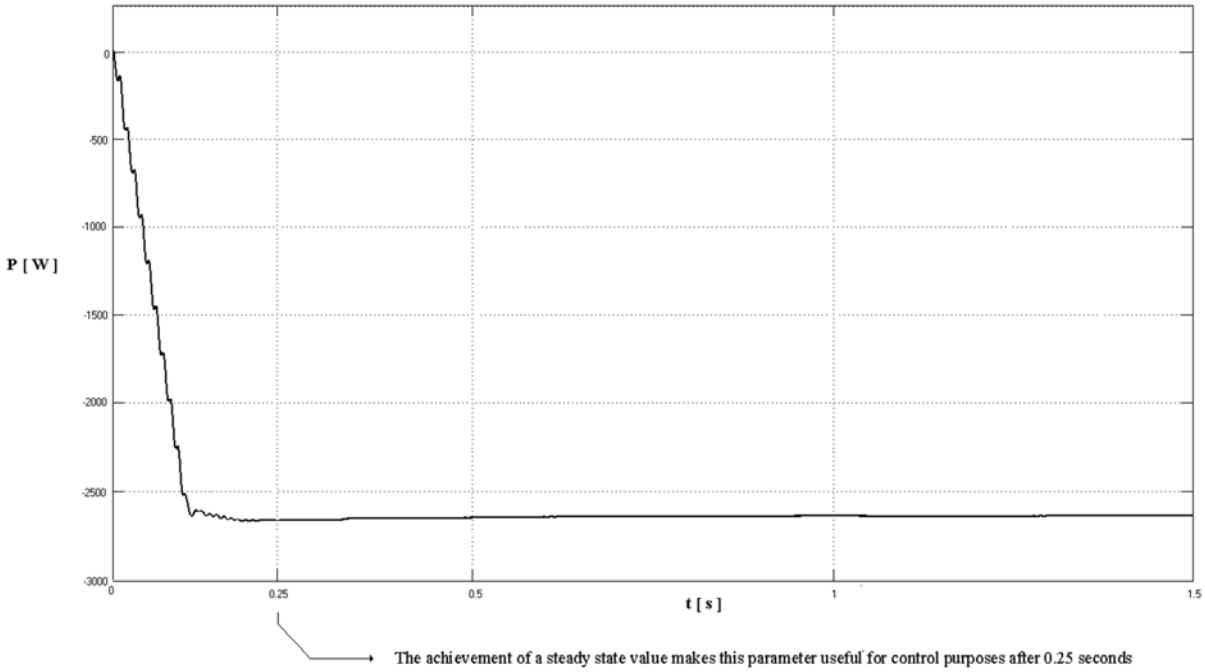

Figure 5.3 – Power absorbed by the DC/DC converter (used as the input for the calculation of the reference current)

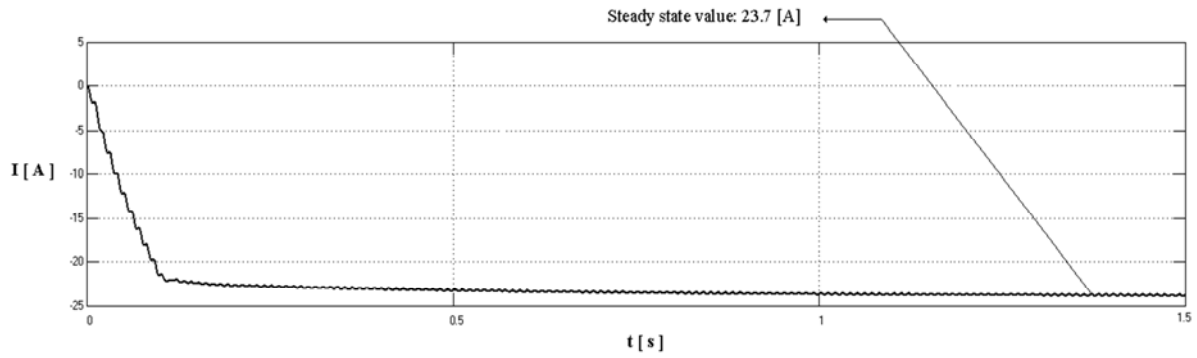

Figure 5.4 – Current absorbed by the battery

The initial current profile growth is almost linear and fast, because the difference between the reference current and the real current flowing, which generates the error, is relevant. As a consequence, the PI controller makes the IGBT of DC/DC converter to work with high values of the duty cycle, which are close to unit. After 0.20 [s] from the starting of the system, the primary control is already ended and the current has almost reached its rated value, really close to the reference value of the current. This is the moment in which the capacitor control arm starts to be influent, and the following time period brings the system to its steady state condition, where a current of 23.7 [A] is absorbed by the battery.

The transient states of the inductor and the capacitor needs now to be analysed. The first device that will be considered is the **inductor**. The analysis of the circuitry of the battery charger shows that the current absorbed by the battery is the same which passes through the same inductor. This current, already studied (Fig. 5.4), depicts that once reached its constant value's steady state, the voltage through the inductor will be nil and no net power

will be stored or delivered by this device. However, this does not mean that the inductor won't exchange power at all, because the current through it is not really completely smooth and constant: little variations of the current, which can be easily noticed on its profile (ripples), induce a not nil voltage through the inductor; as a consequence, this element can't be considered as a real non active element during steady state. In fact, when the current increases during a ripple there will be the induction of a positive voltage through the inductor; this means that in that period the inductor is storing energy. On the other hand, the following decrement of the current produces a voltage with opposite sign through the inductor, and the energy which was stored before now will be delivered. Considering the mean value of the power flow, this value at steady state is nil.
If the focus is put on its transient state, always keeping as a reference the current profile already examined (Fig. 5.4), it can be seen that during these first instants there is an initial amount of energy which is absorbed by the inductor, since the current is quickly increasing. Figure 5.5 provides the mean power value which interests the inductor, and the integral of the curve is the energy stored in the device. Another thing to notice is that the maximum power peak absorbed by the inductor, which takes place in the middle of the transient state, is equal to 1300 [W].

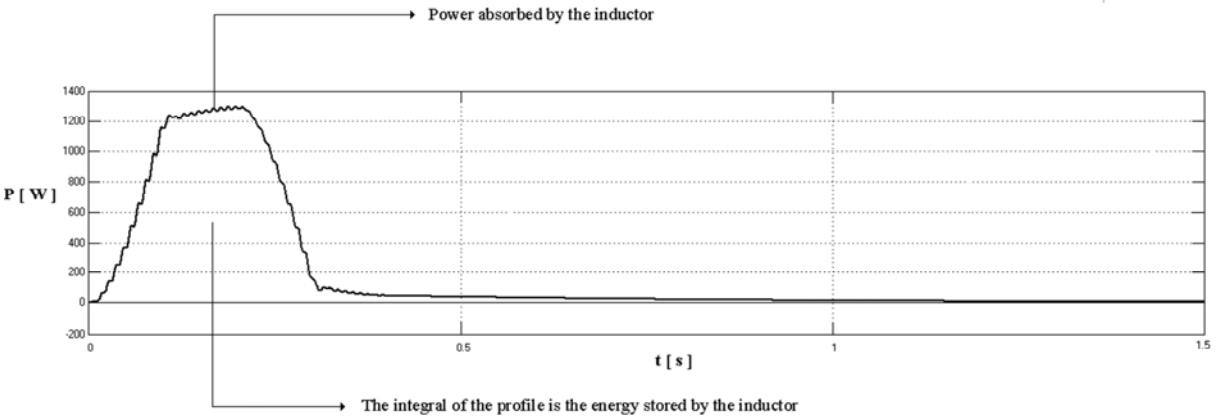

Figure 5.5 – Power exchanged by the inductor

Since the transient state ends in 0.3 [s] and the power peak is not that high, the energy stored by the inductor is not so relevant and it doesn't influence so much the dynamic of the system. It can be demonstrated that a larger inductance is able to furnish a better reduction of current ripples, but at the same time it will influence in a more heavily way the transient state of the system: this issue will be analysed in chapter 7. The fact that nil net power at steady state means that a stable steady state is effectively reached at the battery side.

From the **capacitor** point of view two parameters are controlled. The control system monitors the capacitor current flowing, for the control of its power flow, with the final aim to preserve the voltage through its clamps. Since the current flowing through the capacitor is used just for control purposes, its profile will not be introduced. By the way, the evidence that the control scheme for the capacitor works in the proper way comes from the fact that no energy will be absorbed or delivered by the capacitor at steady state, and as a consequence its voltage will remain constant, and these are the two parameters analysed.

Figure 5.6 shows the profile of the capacitor voltage (instantaneous value) and the simulation starts with the initial voltage through it which is equal to 650 [V]. During the first moments the voltage is subjected to an increment, and this is due to the fact that the transient state which interests the AC/DC converter ends in less time than the transient state of the DC/DC converter. As a consequence, the amount of power absorbed by the

battery charger in that period of time is bigger than the power absorbed by the only battery: this non equilibrated situation produces the absorption of the difference between the two powers by the capacitor.

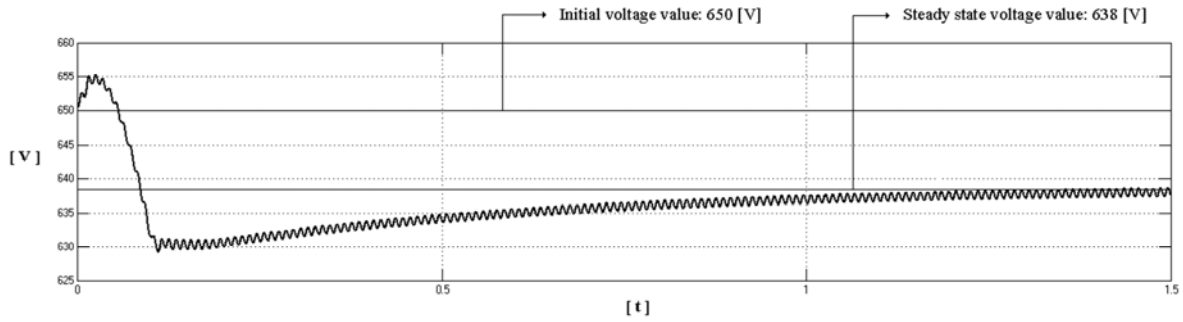

Figure 5.6 – Voltage through the capacitor

During the following instants the current absorbed by the battery increases and its value starts to be close to the reference value, thanks to the action of the main control of the system: the power absorbed by the capacitor will now decrease, and the voltage through it will decrease too. However, since losses in correspondence of the DC/DC converter are not nil and the capacitor arm control is not already active, the same losses are supplied by the energy of the capacitor, whose voltage starts to decrease (because it is delivering energy).

This decrement takes place until the capacitor control system starts to be influent; the consequences of the control can be noticed on the fact that the voltage through the capacitor will stop decreasing and steady state with a constant voltage value is reached after 1.5 [s]. The steady state value of the voltage through the capacitor does not coincide with the initial value of 650 [V] (the final value is 638 [V]) means that the transient state induces a non negligible absorption of power (energy) from the capacitor, which is not balanced by the control system. This does not represent a problem since this voltage variation doesn't affect the active power flow, but only the reactive power flow. As a consequence, if reactive power control is implemented, the voltage through the capacitor will be subjected to additional variations.

Figure 5.7 describes the same capacitor situation already explained in terms of power instead of in terms of voltage. The variation of the power, stored inside the capacitor during time, is analysed considering its mean value. The way in which the measurement devices is applied brings to the situation in which positive power means delivered power, negative power means absorbed power. The connection between voltage and power can be here appreciated: the voltage increment from the initial value can be noticed on the first negative variation from nil power; the decrement of voltage deals with positive power (from absorption of energy to its delivery), whilst at steady state no net power flow is involved, and this can be read as the confirm that the voltage through the capacitor reaches constant value. If the focus is put on the energy flow, it is easy to notice that the energy delivered by the capacitor is higher than the energy absorbed by it: this matches with the previous consideration about the voltage, because if the energy delivered is higher than the energy absorbed, the voltage through the capacitor at steady state has to be lower than the initial value, and this is exactly the case.

The final consideration dealing with the capacitor is the same which was made for the inductor: relevant sizes of the capacitor means that the variation of the voltage from its initial value and the voltage ripples will be reduced. At the same time, costs and weight of the system will be increased. When the design of an EV is made, these parameters have to be studied together and the optimal solution has to be found in function of them. By the way, the capacitor size will have also impact on the capacitor arm control: this is why the idea is to work at the modification of the inductor size in order to get a lighter transient state without the necessity to modify the control parameters.

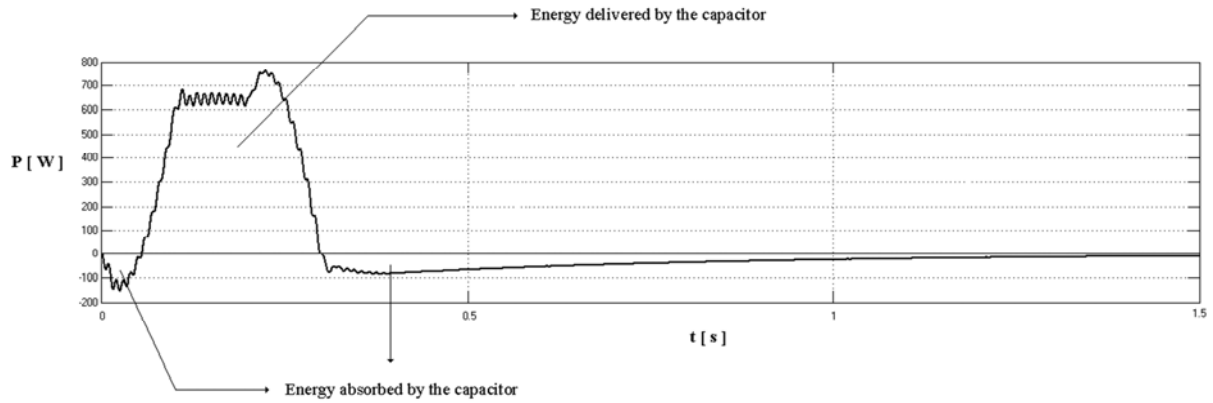

Figure 5.7 – Power exchanged by the capacitor

The last step is to analyse the **power at the battery side**. Looking at the active power absorbed from the grid, which is constant, it is expected to find a constant value even at this side, which can be read as a constant amount of energy stored during time by the device. The profile of the power absorbed by the battery is shown in fig. 5.8.

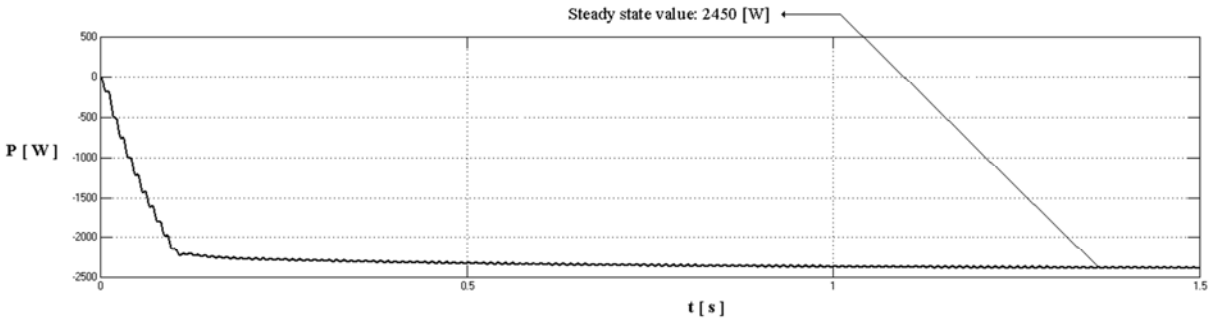

Figure 5.8 – Power absorbed by the battery

The power which deals with the battery at steady state is expected to be lower than the power introduced at the AC side because there will be system losses, which can be quantified. With all the parameters' profiles analysed in this chapter, it is possible to calculate that the power lost during the AC/DC transformation is quantified as equal to 650 [W], with an efficiency of the rectifier of 80.3% (this low efficiency derives from a high switching frequency of the switching devices). On the other hand, DC/DC converter's losses are calculated thanks to the comparison with fig. 5.3, and at steady state (so the inductor and the capacitor are not influent) the profiles of the power respectively at the DC side of the AC/DC converter and in correspondence of the battery are compared. The difference between these two values can be quantified in 200 [W], which means that the efficiency of the bidirectional boost converter is 92%. The total efficiency of the system is calculated and it corresponds to 73.88%, but almost the 80% of the total losses comes from the transformation of the power from AC side to DC side.

The final picture (Fig. 5.9) represents the profile of the battery, inductor and capacitor power flow. The capacitor and inductor power profiles reach nil value at steady state, but the integral of the profiles, which is the energy flow, shows that there is a net flow of energy out of the capacitor (whose voltage decreases) and a net flow of

energy which is stored by the inductor (that means that the inductor stores energy and is charged). This last simulation ends in 2,5 seconds to demonstrate how effectively the two active devices don't affect the steady state of the system once it is reached.

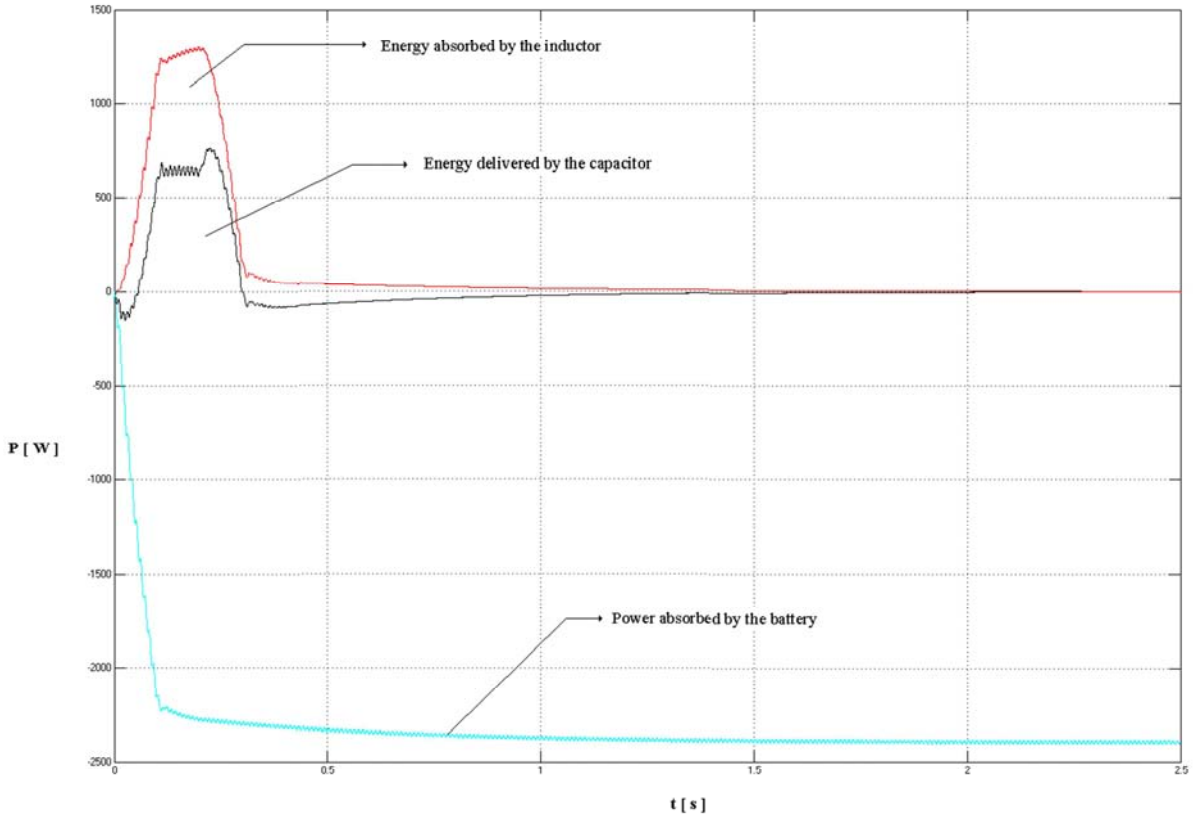

Figure 5.9 – Power flow profiles of battery (blue), capacitor (black), and inductor (red)

6 – V2G (Vehicle-to-Grid) Mode: Simulation

V2G (Vehicle-to-Grid) mode deals with the discharge of the battery, and this delivered energy is then absorbed by the grid. This mode doesn't induce benefits to the battery or, in general, to the vehicle, but it is rather useful for the grid since, according to this, principle ancillary services can take place. If the vehicle is plugged to the domestic electric plant and the grid needs power for any reason (most of the times the need to face peaks of the daily load profile), the same grid is allowed, using this configuration, to absorb a defined amount of energy stored in the battery and use it for these purposes. Before running the simulation, some clarifications have to be made regarding the system, which is now different: the whole topology is still the same, but the way in which it works is different.

The **AC/DC converter** is still working in the same way. A sine wave leading the grid sine wave instead of lagging it will be produced; as a consequence, a reversed active power flow will take place, now from the battery to the grid.

The **DC/DC converter** will run in a different way in this new simulation instead. Figure 2.7 is recalled. During V2G mode the commuting IGBT is IGBT1, whilst IGBT2 is always open. In this way, according to the duty cycle, the power flow will be modulated with proper commutations of the switching device. When IGBT1 is closed, the mesh will include only the battery and the inductor. The current flow charges the inductor, which will store energy. When the same IGBT1 gets open, Diode1 is reverse biased and the new mesh involves the battery, the inductor and the capacitor. The voltage through the capacitor is normally higher than the voltage through the battery, but the voltage through the battery and the inductor becomes higher than the voltage through the capacitor and the current flows through Diode2 charging the capacitor.

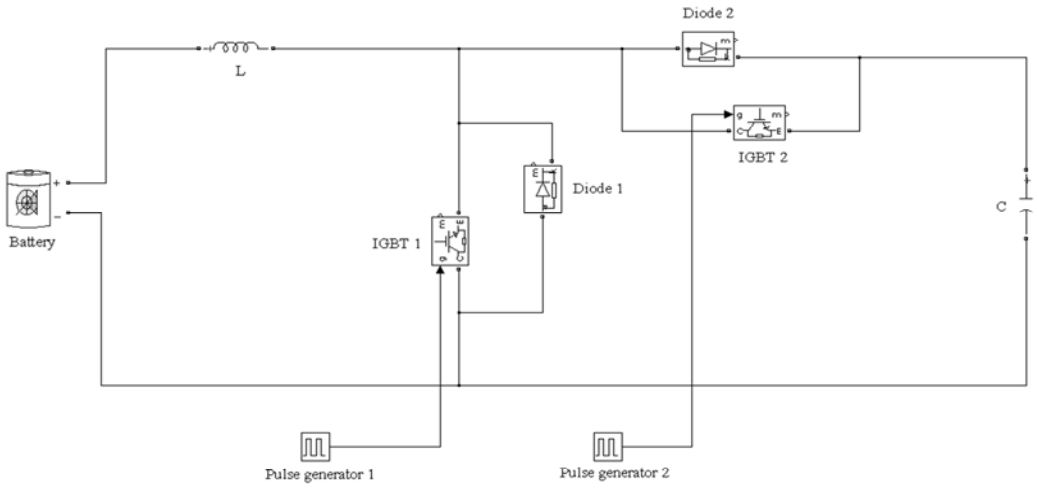

Figure 2.7 – DC/DC bidirectional boost converter

If high values of duty cycle are applied, this means that for the most part of the switching period IGBT1 is closed and energy is stored by the inductor. This energy then will be quickly transferred when the switching device opens. On the other hand, low values of duty cycle mean that just a small fraction of the switching period will

deal with the charging of the inductor, and as a consequence during the complementary fraction the power flow won't be so high: after this transfer is realised, Diode2 is reversed biased and there will be isolation between inductor and battery at one side, and the capacitor on the other side. As what was introduced for G2V mode, even according to this configuration the idea of varying the duty cycle for getting more or less power transfer can be applied, and this means that the control scheme used before is still valid. Some modifications will take place on the setting of the control scheme parameters: since the physic of the system is different, even the block scheme dealing with its description present some differences from the model proposed for charging mode.

The last thing to consider is that from the results of the simulation which will be analysed later in this chapter, it will be noticed that here **higher peaks of power absorption** are involved with the inductor and the capacitor during the first instants; this means that these devices will influence the transient state in a more relevant way than what happened for G2V mode. For this reason, the simulation needs more time for the achievement of the steady state: simulation time is set to 2.5 [s] instead of 1.5 [s]. As a consequence of a longer transient state, the modification introduced in the capacitor control arm will be the setting of the gain of the integrator block to a lower value, because as demonstrated before the two regulation systems (current from nil value to reference value and from reference value to the value which guarantee power equilibrium) don't have to influence each other.

The only external input parameter which is different from the previous simulation is the phase angle θ, which is now set to be equal to -10°. Since the physic of the system is not changed, all the other physical parameters, like the switching frequency and the size of the inductor and the capacitor, are fixed and they are the same as chapter 5. Now that all the differences from G2V simulation have been faced, the simulation is ready to be run.

The first parameter to evaluate is the total **active power flow** at the AC side of the AC/DC converter, which is absorbed by the grid. Figure 6.1 shows the profile of this parameter. As can be seen, this profile is completely different from the active power delivered by the grid for V2G mode from the profile point of view. Here the period of time needed for the achievement of the steady state is over 2 [s], where the amount of active power reaches at steady state 2450 [W]. Even the **reactive power** exchanged profile is different, and it is shown in fig. 6.2.

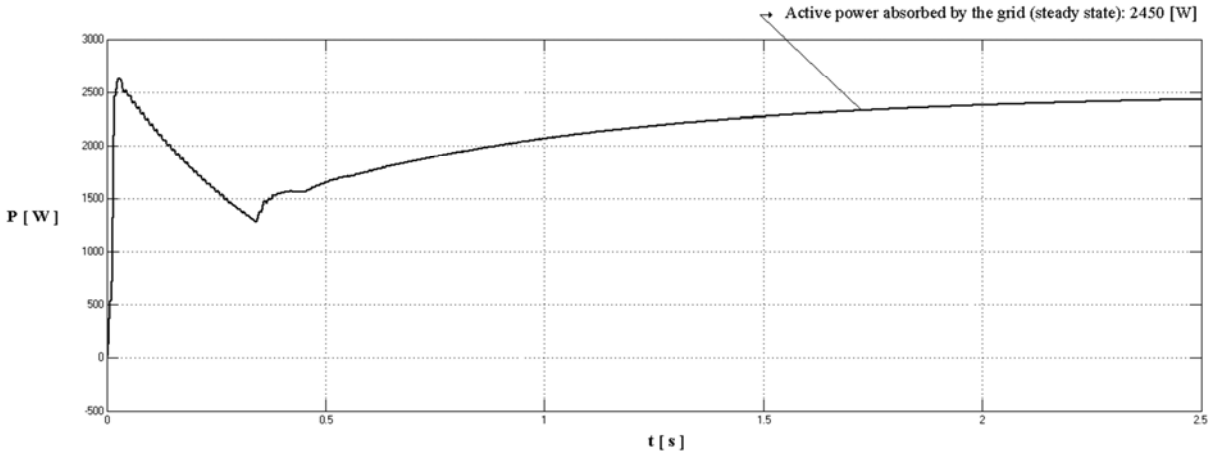

Figure 6.1 – Active power absorbed by the grid

These strong fluctuations of active and reactive powers during transient state deal with the variation of the voltage through the capacitor, which induces a variation on the amplitude of the sine wave produced by the AC/DC converter. Since this variation is quite important, the first instants will be characterized by deep

fluctuations of active power too, although the same active power is expected to be mostly determined by the phase angle.
The strong variation of the voltage through the capacitor takes place because there is no equilibrium between the two sides, the battery and grid. Since the AC/DC converter usually needs just few instants [ms] to reach its active power rated value (it is possible to see that the active power reaches quickly the proper steady state, increasing in a linear way from the very first instants), the problem deals with the DC/DC converter. Indeed the bidirectional boost converter's steady state is not reached as fast as the AC/DC converter's steady state because of the inductor, as it will be shown later, and this will influence the battery charger's work. The simulation will be entirely analysed, the transient state is relevant and it produces deep fluctuations on the electrical parameters before steady state is reached. Chapter 7 discusses the possibility to modify some parameters of the system in order to reduce the impact of the transient state in V2G mode, but at the same time the transient state of G2V mode, which is suitable for the connection to the grid, has not to get worse.

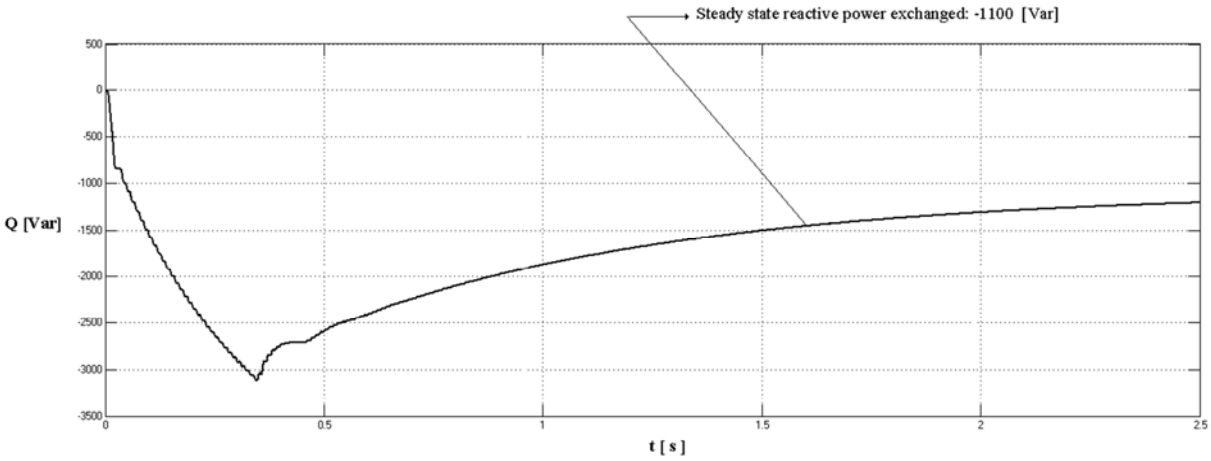

Figure 6.2 – Reactive power absorbed by the grid

The following step will consist on the analysis of the **voltage through the capacitor**. Considering the power flows already studied, an important variation of its profile is expected. In fact, fig. 6.3 shows that the initial voltage value through it is of about 650 [V], and it decreases almost linearly to 507 [V] in 0.4 [s]; the comparison with fig. 6.1 and fig. 6.2 shows that this decrement effectively deals with the fluctuations of active and reactive powers. During the following instants the capacitor control arm starts to be influent and the voltage through the capacitor is pushed to higher and more suitable values: as a consequence of this kind of control, at the end of the transient state the voltage through the capacitor will be constant and no more power will be delivered by the capacitor. This situation makes the same system suitable for the connection to the grid, because although the transient state produces very deep variations on active and reactive powers, when the transient state comes to an end, the required electrical values are reached. This happens in spite of a heavy transient state, because the voltage through the capacitor, after the low peak is passed, reaches the value of 625 [V], and the difference from the initial value of 650 [V] is not so relevant to modify active and reactive powers from the original expected values.

The profile depicted in fig. 6.4 shows the amount of power absorbed or delivered by the capacitor. During the transient state's first moments a 3000 [W] **power peak delivered by the capacitor** is reached, and the integral of this profile is the amount of energy furnished to the grid, since the rated amount of energy which should be delivered by the battery system is not yet achieved. Such a high power involved makes the capacitor voltage to decrease in a deep way and this will generate a relevant reaction on the capacitor control feedback, and the

capacitor control arm will heavily influence the input of the PI controller producing an increment of the duty cycle applied to the DC/DC converter's IGBT.

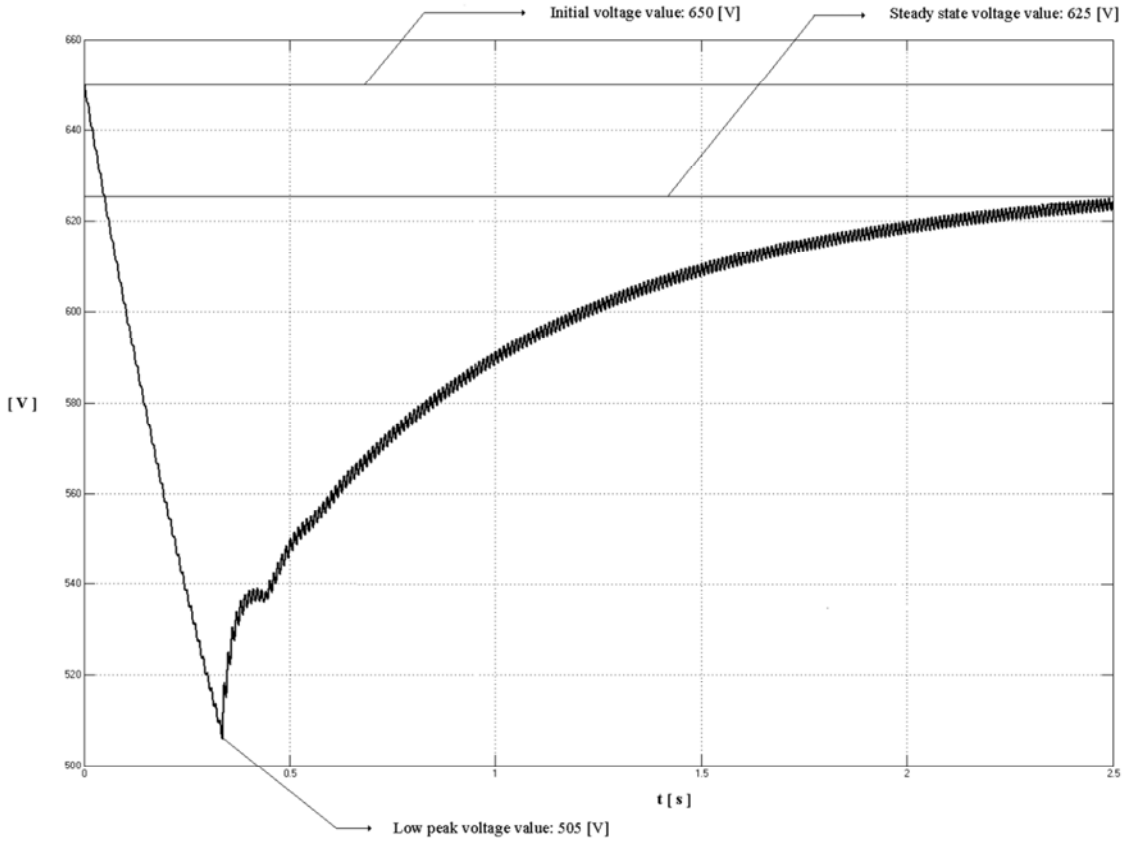

Figure 6.3 – Voltage through the capacitor

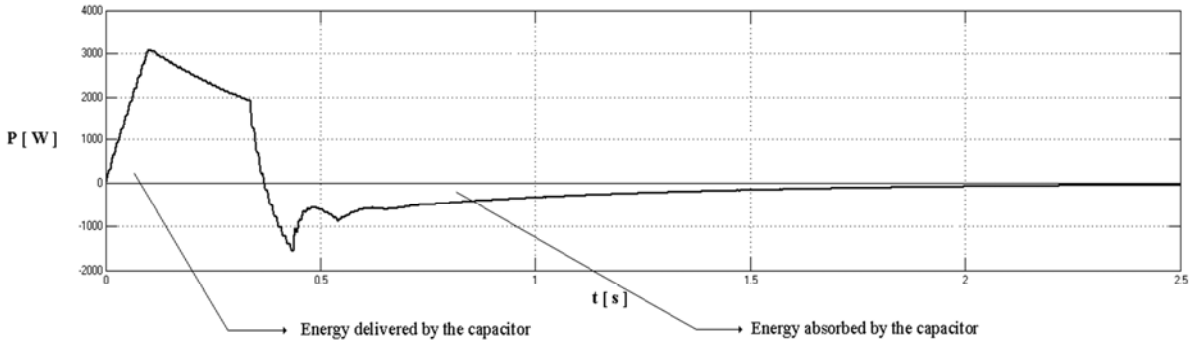

Figure 6.4 – Power exchanged by the capacitor

As a consequence of the capacitor control arm action, the capacitor's power flow is reversed: the device is forced to absorb a fraction of the energy which was delivered during the first transient state, in such a way to increase the voltage through it.

This fact is relevant and fundamental for the achievement, once reached the steady state, of active and reactive power values which are close to their rated values (the truth is that only active power, whose dependence on the voltage of the capacitor is not so strict, reaches almost its rated value after the transient state. The fact that the voltage variation, once reached the steady state, is not negligible (25 [V]), means that the rated reactive power value is not reached. The transient state, as can be seen, doesn't end quickly, but after 0.5 [s] from the simulation's start all the parameters have already passed their deep variation phase and they only vary in a mild way, reaching with an almost exponential profile their steady state values.

The issue dealing with this mode is simply the fact that the DC side of the battery charger is not physically able to deliver the power asked by the grid in the first instants. The reason of this deals with the presence of the **inductor**, which needs to be charged. During these first instants, instead of releasing power to the AC side, the inductor stores energy. The evidence of this can be noticed from fig. 6.5, in which, as can be seen, (using the mean value to draw the profile) energy starts to be stored in the inductor unless a power peak of 2800 [W] is reached; a comparison of this profile with the profile of fig. 6.4 shows how, since this energy is stored and not delivered, the capacitor has to compensate and deliver energy by itself, with the consequent reduction of the voltage through its clamps. By the way, when steady state is reached, the inductor doesn't store any more energy, and powers delivered by the battery and absorbed by the grid assume the same value (losses have to be considered for the balance). The profile of the power and the current delivered by the battery are shown in fig. 6.6 and fig. 6.7; since the voltage through the battery can be assumed to be constant, the two profiles are very similar.

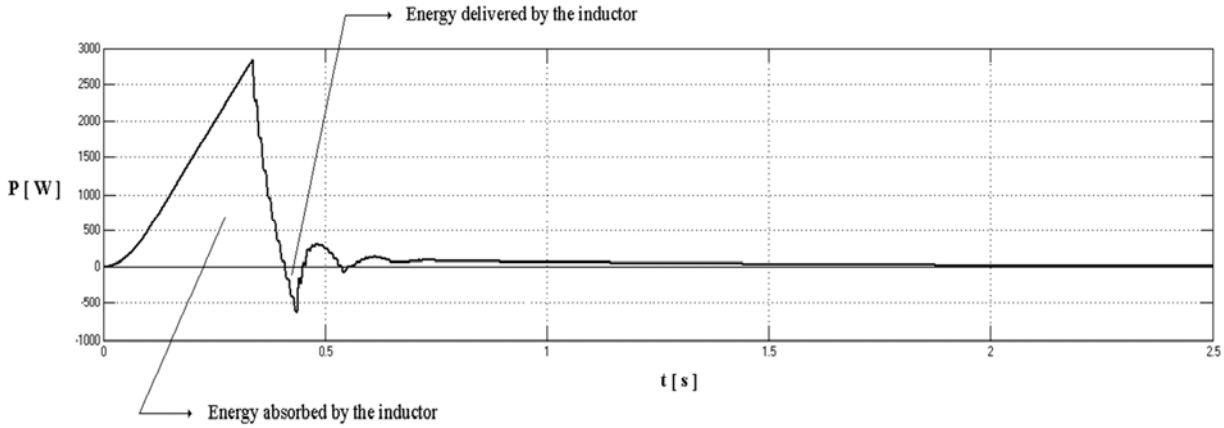

Figure 6.5 – Power exchanged by the inductor

Figure 6.6 shows the profile of the power delivered by the battery; the comparison with fig. 6.5 highlights the fact that from 0 seconds to 0.35 seconds, almost all the amount of the power delivered is absorbed by the inductor. Also fig. 6.7, which describes the current through the battery, helps to understand this fact.

The first instants of the simulation are characterised by a high error between real current and reference current. As a consequence, the current delivered by the battery is increased, and this corresponds to the increment of the power delivered by the DC side. By the way, the current through the battery is also the current through the inductor, and its linear increment induces voltage through it: this is the reason why all the power delivered by the battery reaches the AC side with a certain delay: the inductor acts as a sort of brake for the power flow. The situation described has no alternatives which can act improving the profile of the analysed parameters: the current has to increase, but the presence of the inductor impacts on this dynamic, dynamic that was not so annoying for G2V mode. In that case indeed the fact that the inductor was storing energy was not influencing the

power absorbed by the battery, and at the same time the power peaks of capacitor and inductor were lower, so a lower impact on the transient state was guaranteed.

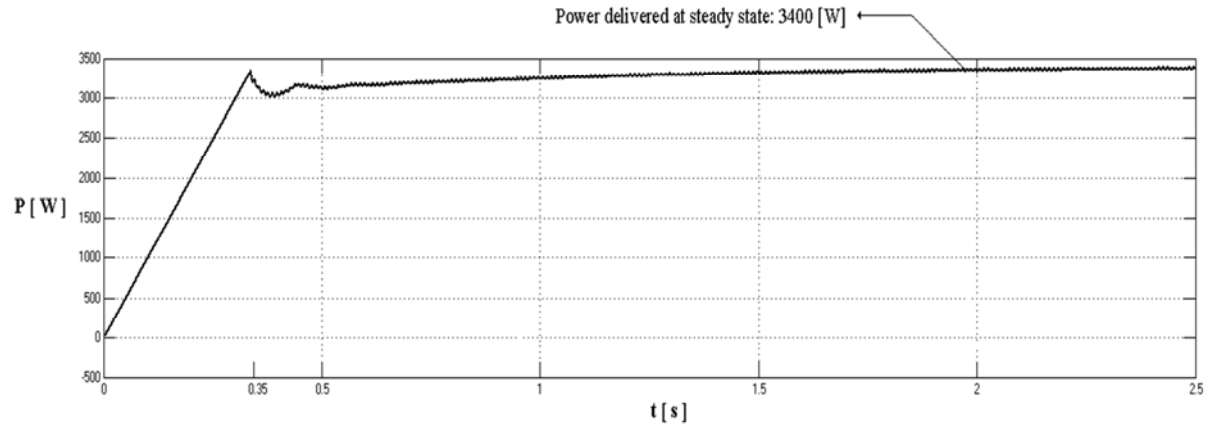

Figure 6.6 – Power delivered by the battery

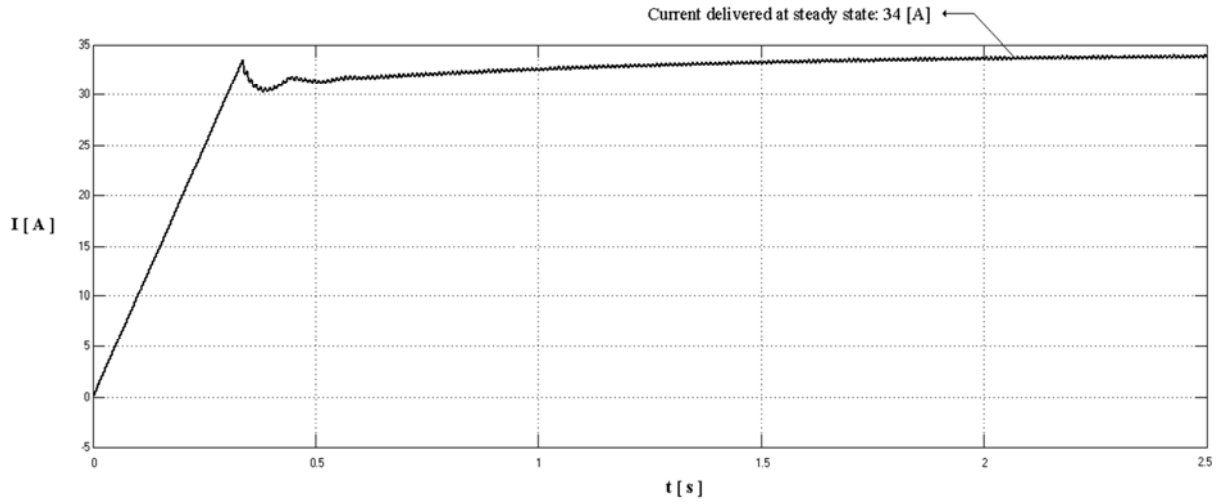

Figure 6.7 – Current delivered by the battery

Figure 6.8 shows the profiles of the power flow at the DC side of the battery charger, so battery, inductor and capacitor powers' parameters are considered. Once steady state is reached, nil net power flow interests the inductor and the capacitor, whilst the power delivered by the battery becomes constant. During the transient state the powers which interest respectively the inductor and the capacitor are relevant, and their profiles' peaks are almost close to the power delivered at steady state by the battery. Although the steady state is reached without any problem with regards to the profiles of the electrical parameters, both at grid side and at battery side, some modification can take place so to improve the physic of the system especially according to V2G mode, in order to make the transient state lighter. This will be the aim of the next chapter.

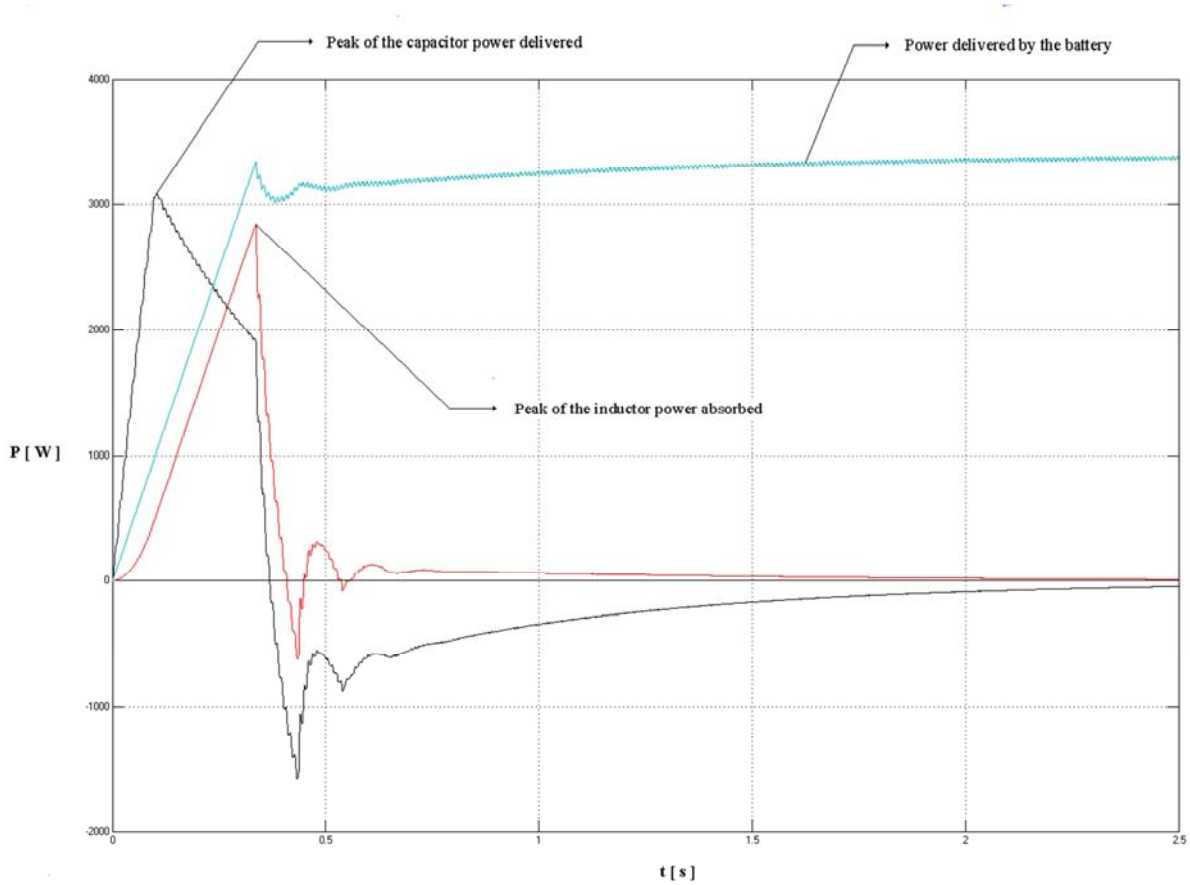

Figure 6.8 – Power flow profiles of battery (blue), capacitor (black), and inductor (red)

7 – Improving the System: the Variation of the Inductor Size

Two devices composing the battery charger can be modified in order to get an improvement of its dynamic: the inductor and the capacitor. Since the capacitor's electrical parameters (voltage and current) are important both considering the control strategy and the achievement of the steady state, it is better not to modify its size, acting rather on the inductor size, which is instead the most influent device regarding transient states.

The inductor size can influence both transient state and current ripples (as can be seen by the profiles already analysed, current ripples affect only the DC side), but the former is the most relevant way in which the modification of the inductor size impacts on the system. Since progressive increments or decrements of the inductor size won't produce an improvement of all the electrical parameters of the transient state, a deeper analysis is required, in order to find the most suitable inductor size for both charging and discharging purposes considering each different aspect.

The reduction of the inductor size from the original one, used in the previous simulations, leads to a possible improvement of both current and power transient state profiles. Unfortunately this will impact also on the power quality, because the ripple amplitudes could be subjected to increments. Besides the analysis of the new transient states, the analysis of the electrical power quality will be carried on for these current ripples, in order to ensure that the achievement of a lighter transient state will not produce a too much low power quality, which will be able to degrade the battery. An example can be now conducted running two simulations with a reduced inductor size. How much will be this reduction? The original size used till now was of 1 [H]; the following simulation instead will run with 500 [mH] and 100[mH].

7.1 – First Simulation: G2V Mode

The simulation is now run for G2V mode and the three different DC current profiles which describe the charging of the battery (coming from the three different inductor sizes applied to the system), are analysed. As can be seen from fig. 7.1, the current profile already analysed in chapter 5 is depicted with the two new profiles, generated by the application of the new inductor sizes. Basically, these inductor size variations don't influence the electrical parameters at the AC side, regarding active and reactive power, when the steady state is reached. It can be demonstrated also that active and reactive powers reach their steady state values through a transient state which is comparable to the one already analysed with the original size of the inductor (always considering G2V mode, chapter 5). At the DC side, the electrical parameter which is influenced by this inductor size variation is effectively the DC current which is absorbed by the battery.

Fig. 7.1 is analysed in order to study the profile of the current in correspondence of the battery. The comparison between the three profiles shows that all the three transient states lead to the same steady state, and this is obvious because the inductor becomes a non-active element (and its size is no more influent) after the current becomes constant. As can be seen, the first reduction of the size of the inductor brings to the reduction of the transient state's duration of the system, thanks to a quicker variation of the current profile. The profile dealing with the second modification, when the size of the inductor is fixed to 100 [mH], instead of reducing the duration of the transient state, produces an overshoot which increases it in correspondence of the DC side.

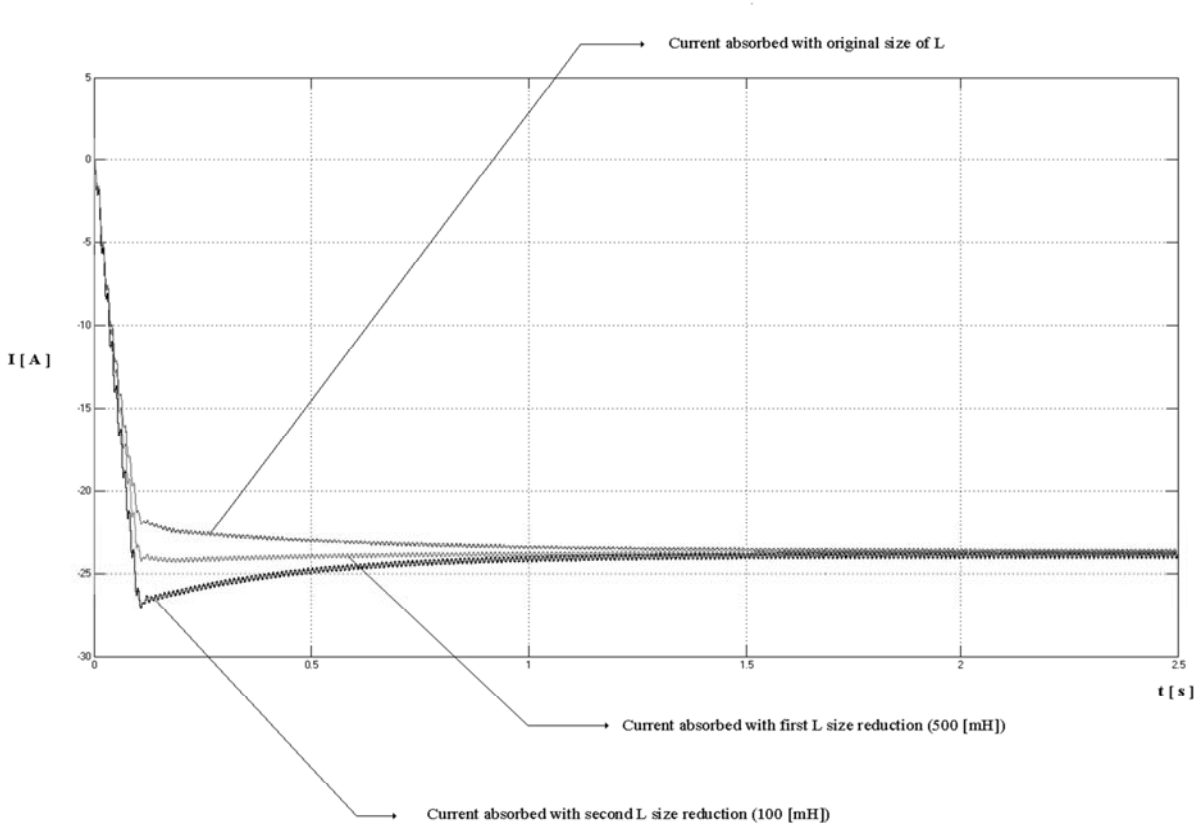

Figure 7.1 – Comparison between currents absorbed by the battery with different values of L (1 [H], 0.5 [H], 0.1 [H])

From the curves' profiles, it can be concluded that the three of them are suitable for the battery charger's work both for AC side and the DC side: this means that a size reduction can be effectively done. At this point some other factors can play, for example the cost of the inductor and its weight.

The focus can be now moved to the amplitude of current ripples, which is the second current parameter that needs to be checked. The impact of the variation of the size of the inductor can be measured by the evaluation of the amplitude of the current ripple generated; the results of the measurement shows a peak-to-peak ripple amplitude of 0.25 [A] for 500 [mH] and 0.46 [A] for 100 [mH]. These values are effectively higher than the current ripple which can be measured applying the original size of the inductor, which was equal to 0.18 [A]. However, these increments are still so small that they can be considered negligible and still suitable for the battery. As a consequence, the reduction of the size of the inductor can take place, and this improvement has the purpose of generating a better response of the system regarding the DC side transient state, lighter weight and less costs.

Since the size of the inductor is fixed and it is the same for both V2G and G2V mode, a compromise is needed and the value which will be chosen has to satisfy in the best way possible both charging and discharging mode. As a consequence, before taking the choice of the optimal inductor size to apply on the battery charger, the analysis regarding V2G mode has to be lead. Finally, the only data to register is that the 500 [mH] option is the most suitable for this configuration.

7.2 – Second Simulation: V2G Mode

A different situation is faced if the inductor size is modified and V2G mode simulation is run. In this case the original size of the inductor is particularly influent during the dynamic state of the system; in fact, with regards to the study of the transient state, in chapter 6 deep fluctuations of all of the electrical parameters were found, also regarding the active power absorbed by the grid. The sensibility that V2G system presents regarding the variation of the size of the inductor brings more complexity to the same battery charger design, whose work in V2G mode seems not to be as flexible as the work in G2V mode. This means that the choice of the best size of the inductor will be necessary more heavily influenced by V2G mode than by G2V mode.

The modification of this parameter produces variations of the transient state which are not comparable to the ones of G2V mode; they are indeed deeper variations. If simulations are run for this mode according with a reduced size of the inductor, the results according to the hypothesis are described by the following figures. The comparison between active and reactive power flow profiles achieved with the modification of the inductor size or with the original inductor size has to be conducted, since these are the output which are required to present the lighter transient state possible, for a fast steady state's achievement.

The **first step** deals with the analysis of the **first size reduction**, from 1 [H] to 500 [mH].

Figure 7.2 shows the impact of the reduced size of the inductor on the active power absorbed by the grid; when the simulation was run with the original size of the inductor there was an active power lower peak of 1300 [W], whilst during the steady state the power absorbed was of 2500 [W], but now according with a lower size of the inductor the power absorbed in correspondence of the lower peak is increased to 2400 [W] and the steady state power absorbed doesn't change, since the steady state still present an active power absorption of 2500 [W]. In other words, the lower peak reached during the transient state passes from 48% to 4% of the steady state active power absorbed value, and this is a very important result from the point of view of the response of the system. With regards to the figure, the two profiles identify the active power absorbed by the grid with reduced size of the inductor (black line) and with the original size of the inductor (grey line), which is reported from chapter 6.

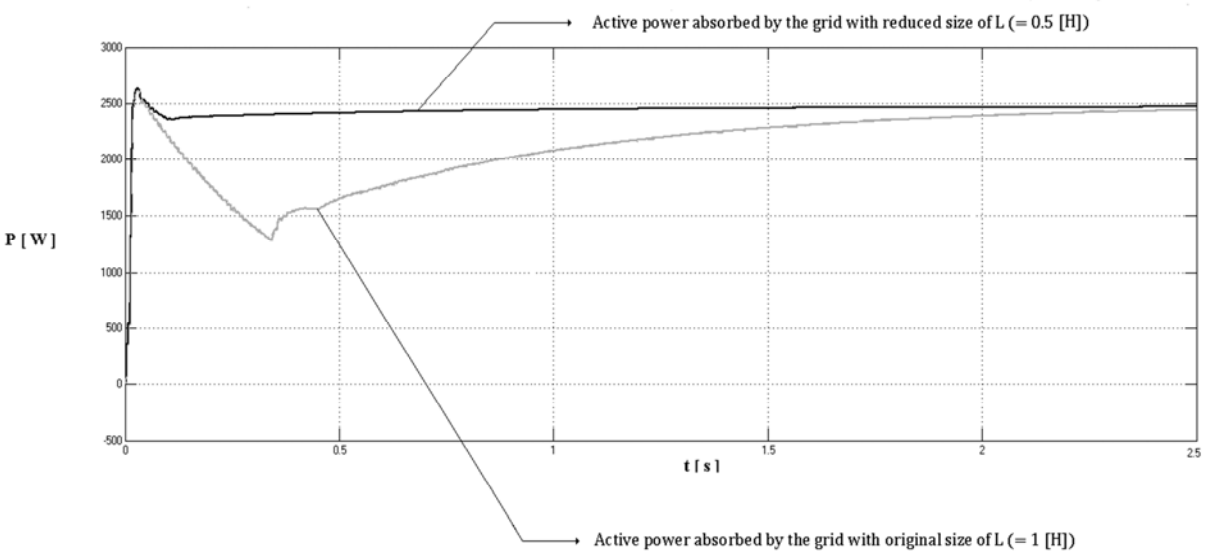

Figure 7.2 – Active power absorbed by the grid with original (1 [H]) and reduced (0.5 [H]) size of L

The profile of the reactive power exchanged will be also subjected to smaller fluctuations of exchanged reactive power during transient state, as can be seen in fig. 7.3: in this case, with the reduction of the inductor size to 500 [mH], the lower peak sets to 1320 [Var], whilst the previous V2G simulation run in chapter 6, which is depicted in grey in the figure, was showing a 3100 [Var] lower peak.

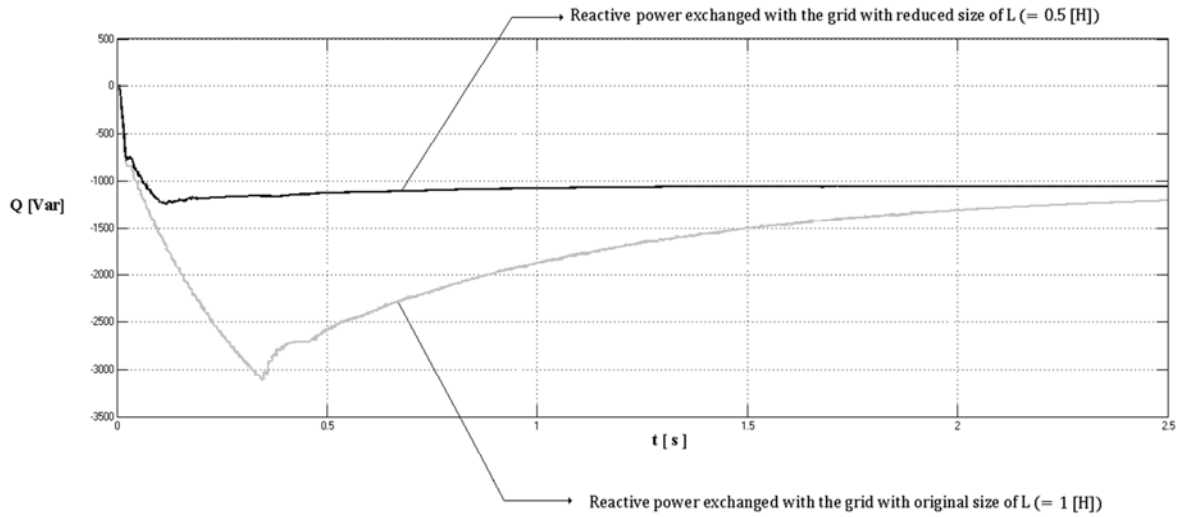

Figure 7.3 – Reactive power exchanged by the grid with original (1 [H]) and reduced (0.5 [H]) size of L

What can be infer by the comparison regarding active and reactive power exchange is that the influence of the size of the inductor basically stands on the fact that in this way the capacitor is not so much stressed as before: in fact the reactive power exchanged, which mostly depends on the voltage through the capacitor instant by instant, shows a profile which reaches steady state after a relatively quick transient state. What is expected with regards to the capacitor's dynamic is a lower voltage drop, because less power will be delivered, and the evidence which proves this theory is shown in fig. 7.4. The lower voltage peak reached with this configuration is 568 [V], whilst in the previous case the voltage was decreasing till 507 [V] (from the initial state in which the capacitor was holding a voltage equal to 650 [V]).

Since the two dynamics are different, the total amount of power released by the capacitor in these two situations will not be the same, and this will produce a little difference on the voltages through it. By the way, what can be infer is that the difference between the two power flows which interests the capacitor with the two different configurations is not so deep and can be easily considered negligible, because the system response is fast and avoids critical variations. Regardless the inductor, the highest will be the capacity of the capacitor, the lowest will be its voltage drop. If the control system wasn't fast enough to face the voltage variation in a very small period of time, one of the solutions possible would have been the one of the use of a capacitor with higher capacity.

The **second step** for the achievement of stronger improvements at the AC side of the battery charger by the modification of the size of the inductor can be now made, working the same V2G simulation with the **second decrement of the size of the inductor**, which this time is set to 0.1 [H]. The results of this further decrement will highlight the influence of this device in the dynamic of the battery charger for V2G.

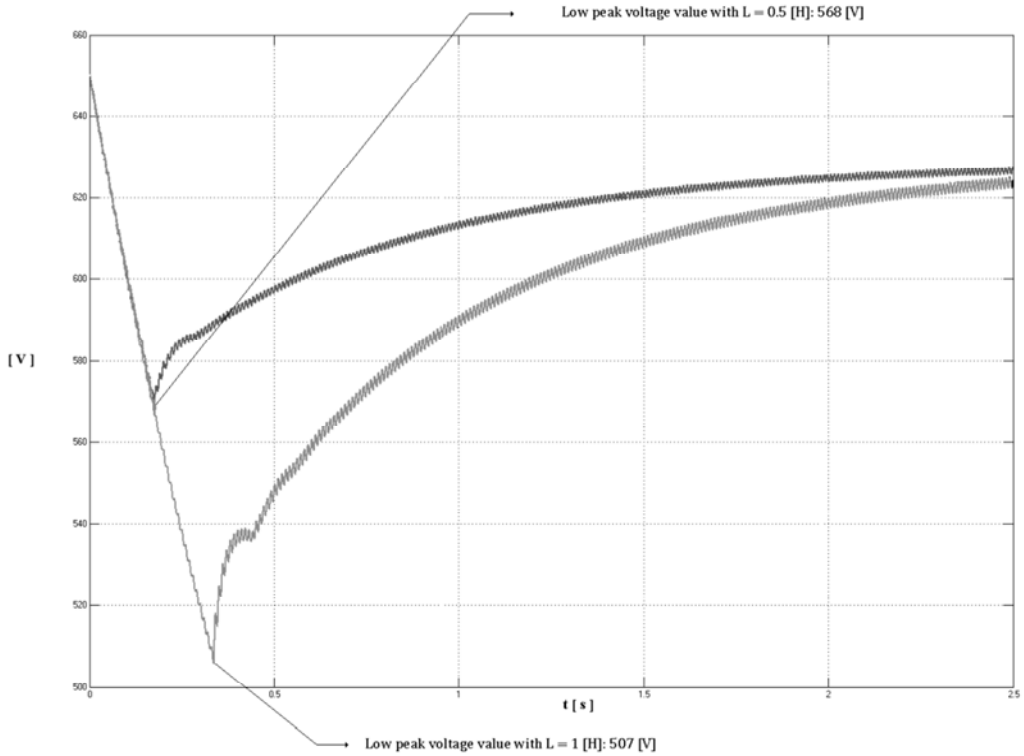

Figure 7.4 – Voltage through the capacitor with reduced and rated value of L

The following figures (Fig 7.5 and Fig. 7.6) show the active and reactive power flow.
The active power absorbed by the grid (Fig. 7.5) is almost the same as the active power absorbed according to the first reduction, when the inductor was set to 0.5 [H]. This means that the variations coming from the modification of the size will be visible at the AC side only having a look to the reactive power exchanged, whilst in correspondence of the DC side modifications can be seen on the voltage through the capacitor and the profile of the current delivered by the battery.

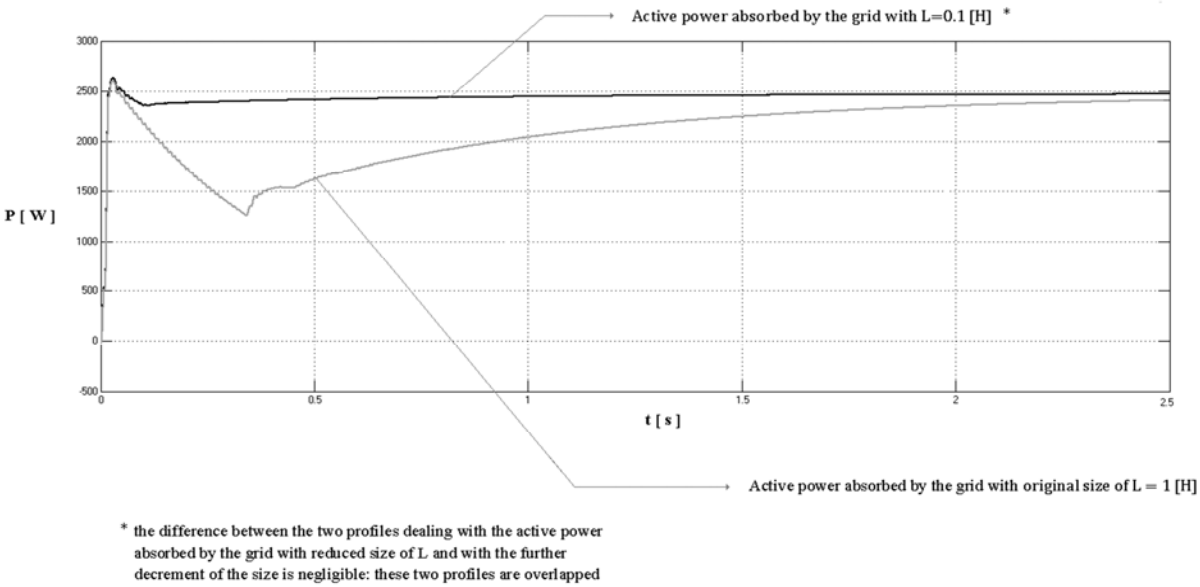

Figure 7.5 – Active power absorbed by the grid with a stronger reduction of the size of L

The reactive power exchanged profile depicted in fig. 7.6 shows that the size reduction doesn't influence so much the profile of the curve: the variation is barely noticeable between the reactive power exchanged applying 0.5 [H] or 0.1 [H]. As a consequence, it can be infer that additional reduction of the size of the inductor will not bring any more advantages from the AC side transient state point of view.

The active and reactive transient states, which were particularly deep and difficult to manage before, with their deep variations of active and reactive power, in this case can almost be considered negligible: the time needed for the achievement of the steady state is relevantly reduced, profiles are milder and transient state's higher and lower peaks are almost not present anymore.

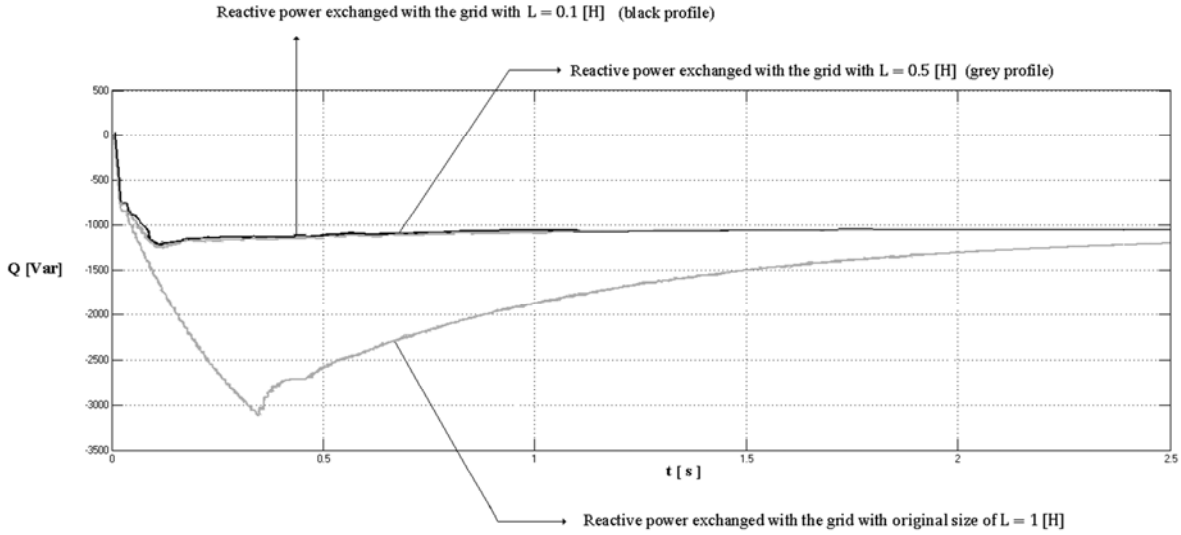

Figure 7.6 – Reactive power exchanged by the grid with stronger reduction of L

An important conclusion can be achieved looking at fig. 7.7, which shows the voltage through the capacitor according to the second reduction compared to the previous two cases. As can be seen, this second low peak reduction is relevant, since the lower value reached is 627 [V] instead of 568 [V], but this decrement of the fluctuation of the voltage through the capacitor doesn't influence too much the transient state of active and reactive power. This situation is peculiar, because the low peak is strongly reduced by the application of 0.1 [H] size, but almost no impact is visible at the AC side of the system.

The last step for being sure that these reductions are both well accepted by the entire system is the verification of the electrical parameters in correspondence of the DC side.
Figure 7.8 shows the three current profiles which interests the battery in correspondence of the three different inductor sizes applied. As what was done for G2V, the first step consists in the analysis of the shape of these currents to understand whether they are all suitable. All the three profiles are shown in the same graph, so it is easy to notice how fluctuations of the current through the battery during the transient state are reduced by the reduction of the same inductor size: the three possible size are effectively suitable.
The analysis of the profile of the DC current and the analysis of the transient state of active and reactive power leads to the result that the best inductor size for this second simulation is 0.1 [H], because at both sides the transient state is very light and free from fluctuation. The last verification which is asked as a confirmation of the size suitability consists on the evaluation of current ripples.

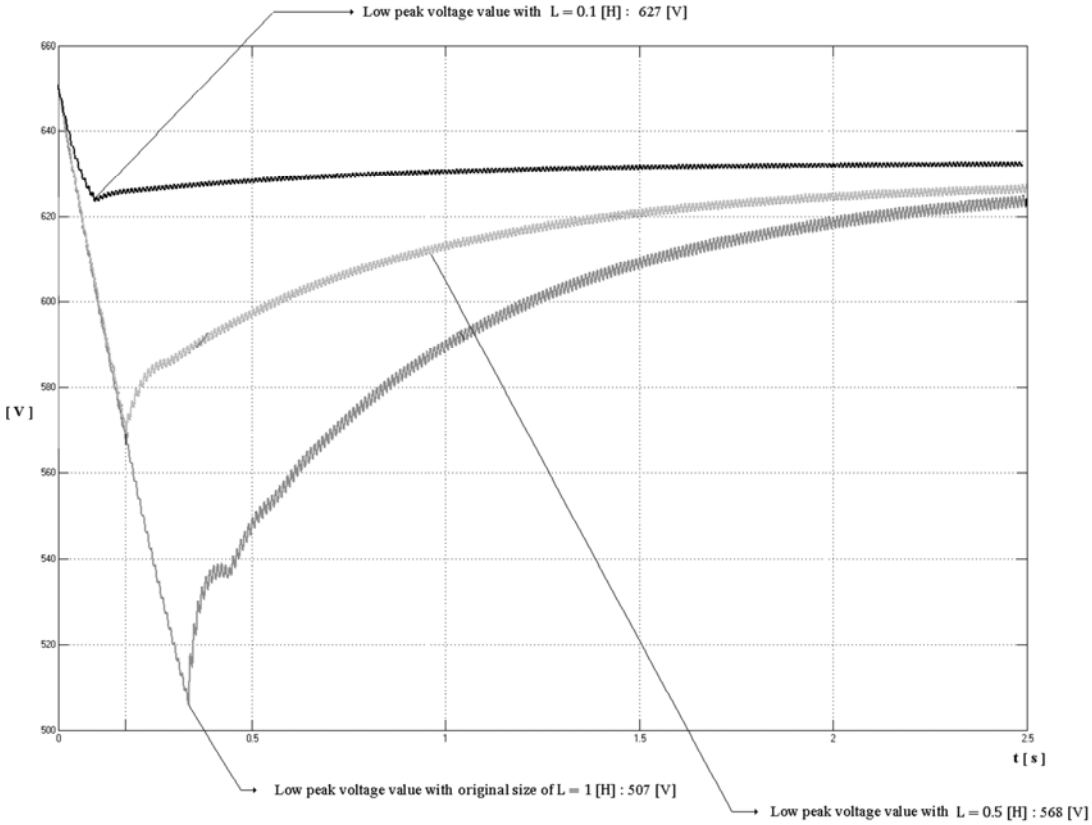

Figure 7.7 – Voltage through the capacitor with stronger reduction of L

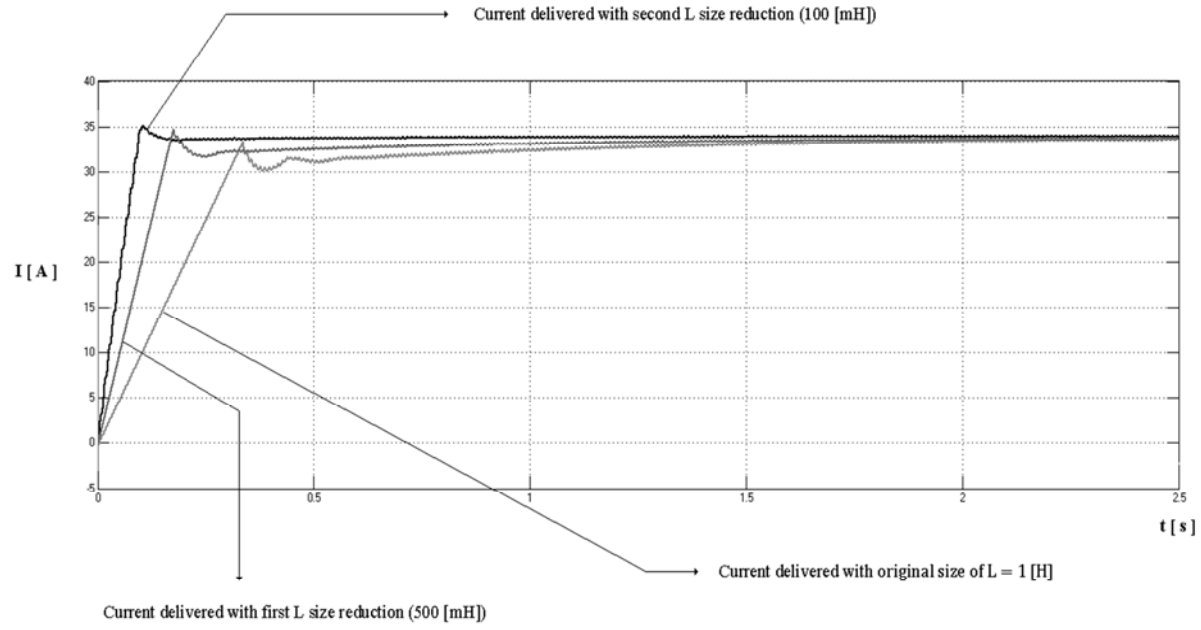

Figure 7.8 – Comparison between currents delivered by the battery with different values of L

Before analysing the dynamic of the battery charger according to the best size of the inductor, the parameters which influence the current ripples have to be pointed out.
First of all, there is dependence from the switching frequency of the DC/DC converter, which is 10 [kHz]. Since this frequency is quite high, the analysis of the current spectrum demonstrates that no 10 [kHz] frequency current component are present in the current which flows through the battery. This happens because although the switching of the IGBT induces two different voltage values through the inductor during the switching period, the current won't be affected by these quick switches, thanks to the natural action of the inductor.

The amplitude of current ripples depends also on the size of the inductor, and it is demonstrated that the size already used is suitable for the achievement of a smooth current (peak-to-peak ripple amplitude of 0.18 [A], which doesn't generate battery's degradation). It is easy to infer that, from the ripple point of view, the most the inductor size is big, the most reduced will be the ripple amplitude.

There is a third parameter which influences the amplitude of the current ripple, which is related to the voltages applied to the mesh during the switching period. The most the voltage difference (difference between capacitor/battery and inductor voltages) is small, the most the ripple amplitude will be reduced. The equation which synthesizes all these considerations and describes the peak to peak inductor ripple current (which is the same ripple which affects the battery) is the following

$$\Delta I = f\left(\frac{V*f}{L}\right) \tag{7.1}$$

where f is the switching frequency of the DC/DC converter and V is the voltage variation which is applied when the IGBT switches its state. Working on the parameter L means working for the reduction of the ripple without forcing the voltages and the switching period.

The advantage of working with a current which is almost free from ripples brings to the disadvantage of a system which needs big inductor sizes, but this can affect both AC and DC transient state: since this target is more important, the idea is to privilege it in spite of the DC quality, even because the battery's requirements are not so strict. Every choice taken regarding the modification of the inductor size can be made, being aware of the consequences that are produced inside the system, from the output active and reactive power, to the DC current ripple and the evolution of the transient state point of view. Since the current ripples which affect the three current profiles of fig. 7.8 are all suitable for the battery, which can tolerate them without degrading, the best solution can be the one of a lighter size of the inductor which ensures a better transient state, as well as lower weight, costs and space occupied: this means that **the inductor size will be fixed to 0.1 [H] value** for next chapters.

8 – Dynamics of the Battery Charger

The two different simulations have been run into two separate frameworks, each one with its own control, with the aim of analysing transient states and powers, voltage and current profiles of each mode. However, even if the physic of the system is the same for both the two modes (since the battery charger's physical parameters are the same for V2G or G2V modes), the controller parameters are not the same for both the modes, because the dynamic of the system, considering charging and discharging mode, is different. As a consequence, the **primary aim** of this chapter will be that one of creating a single control scheme, with which it is possible to work the battery charger both for charging and for discharging the battery, and switch from one mode to the other in a proper way as well. Since during the real working situation of the battery charger there is usually an alternation of charging, standstill, and discharging modes, the necessity of testing the evolution of the system with some input variations (so variation of amplitude and sign of θ, which means variation of amplitude and direction of power) has to be considered. This will be faced in the **second part** of the chapter, in which the quality of the switch will be analysed and, if necessary, improved.

Before creating the control scheme, it can be interesting to analyse also the reasons which can lead to the need of switching the working mode of the device from one mode to the other (or to standstill mode), and all these reasons come from the scenario in which the electrical vehicle is considered. The hypothesis, which is true for almost all of the vehicles, is that the EV is always plugged to the domestic electrical plant if the vehicle is parked at home, so this means that the vehicle will be plugged for all night and a portion of the day. Since this "plugging time" is greater than the time needed for the charging of the battery, V2G and G2V modes can both be applied, so the grid operator has the possibility to apply the "smart charging": thanks to this, the vehicle will be charged in the cheapest way possible for both the grid and the EV owner. This means that the battery won't start charging immediately when the vehicle is plugged, but there will be the possibility for the grid to defer the energy that has to be transferred to the battery during all the time the vehicle will stand connected. This situation deals with one or more switches from standstill mode (the vehicle is plugged without exchanging energy with the grid) to charging mode (G2V).

If an emergency situation instead occurs, or simply the grid has to face a peak power required from the loads, charging mode (if the battery is being charged) or standstill mode can be quickly replaced by discharging mode (V2G), where the same battery delivers power to the grid, supporting its work. Basically, two boundaries are defined regarding this working method: first of all, when a fixed amount of time (for instance all the night) lasts, the SOC of the battery has to be at 100%, because it shouldn't be forgotten that the primary aim of the plugging of the vehicle to the electric plant from the vehicle's owner is to charge the battery. On the other hand, during all the period of time in which the vehicle is plugged, the SOC has to be always greater than a fixed threshold, because if the EV's owner has to disconnect and use the vehicle for any reason, there has to be enough energy stored in it.

According to this scenario, it is easy to infer that many possible switching combinations can take place. The consequences of these requests are that the electrical parameters (controlled by the same charger) have to evolve in the fastest and most suitable way possible to reach the new equilibrium. This is directly connected to the second issue that is solved in this chapter: the design of the single control scheme for piloting both the two modes is not realised only for guarantee the achievement of a global control of the device, but also to realise fast and suitable switches between modes.

8.1 – The Whole Circuit

The first step of the chapter is now faced; the aim is to design a single controller which is able to pilot the battery charger and achieve V2G, G2V and standstill mode.

This target is achieved by linking the two different circuits used for the two different simulations in one single circuit, which can handle the working of the battery charger in both the two modes. From the physical point of view the circuit is always the same; the difference comes from the fact that now the control scheme has to work in two different ways in function of the power flow. The modified scheme which allows both V2G and G2V modes is realised according to (Fig. 8.1). As what was assumed in previous chapters, the controller is a PI controller, composed by a proportional gain and an integrator. In addition to this, there is an arm of the control scheme which controls the capacitor and works with an integrator and a proportional gain. The values of two proportional (static) gains, the one of the PI controller (P) and the one applied to the capacitor's integrator, are different for the two modes, since the dynamic of the system is different too. As a consequence of this, the PI controller has to be realised as the parallel of a proportional gain (P), and the series of an integrator and its proportional gain (I) in such a way that modification dealing only with the proportional arm (P) can take place.

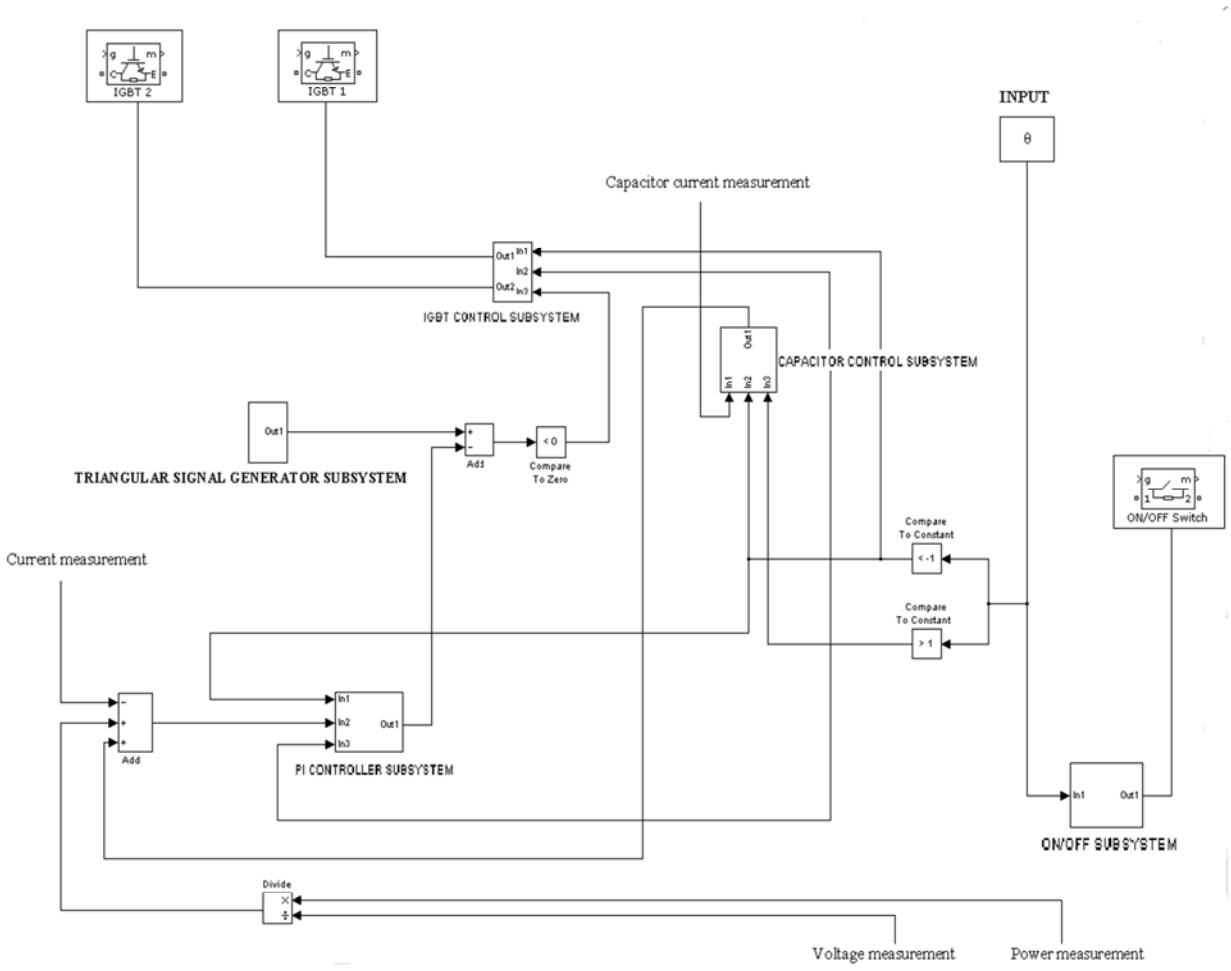

Figure 8.1 – Modified control scheme for both V2G and G2V mode

The differences from the block scheme realised in fig. 4.6 (Chapter 4) have to be pointed out. Figure 8.1 is composed by five different subsystems that have to be analysed, each one with its own function. Only the subsystem called “Triangular Signal Generator Subsystem” is exactly the one used for the previous control scheme, but the other four are subjected to modifications.

The information about the angle phase θ, which determines the working mode of the battery charger, has a primary importance. This term is used as a variable input and the dynamic of the system will be studied in function of this real time variable. If the phase angle θ is greater than zero, this means that the battery will be charged, since the power flows from the grid to the same battery; the opposite situation will take place for negative values of it. The idea is that the block scheme will be designed in such a way that if the output of the block which compares to zero the term θ is equal to 1 (which means that the same θ is positive) the control scheme parameters will be set to G2V mode, thanks to the static gains applied. If the output will be zero, no action will be produced by the control strategy introduced, and the control scheme will work with its default parameters, which are the ones of V2G mode.
An important clarification is pointed out: a better working situation can be reached by modifying the two comparative blocks: the input phase angle can be compared to a value which is not zero (and this is the case shown in fig. 8.1, with angle phase θ = 1°), because this will allow the fixing of a minimum input threshold for having the working of a mode, so that of a minimum power threshold which will flow through the system. As a consequence, thanks to this variation, next simulations will be run giving in input just the value of the angle phase, and the control scheme will act in the proper way setting automatically the proper parameters.

What can be started now is the study of the four subsystems used in the control scheme, and then the analysis of the dynamic of the circuit with angle phase variations.

8.1.1 - ON/OFF SUBSYSTEM

This subsystem presents in input the phase angle value θ, and in output a signal which is able to open or close two relays. These relays are installed between the capacitor and the AC/DC converter and between the AC/DC converter and the grid, and they are used to open the circuit when the value of the phase angle is not suitable for V2G or G2V mode. This comes because if the same phase angle value becomes too small or too high for V2G or G2V mode as consequence of malfunctions, or simply the active power value exchanged is too much high for the battery, the battery charger needs to disconnect from the grid for saving its devices and the same battery as well, producing a galvanic isolation. The discriminating value used in the simulation is 1° phase angle, but different angles can be set. This configuration is activated only with phase angle values which are smaller than the fixed limit, since greater values are usually blocked previously by other protection systems of the battery charger or by the same domestic plant, which won’t support high power flow.

This subsystem cooperates with another subsystem, the IGBT control subsystem, which opens both the IGBT of the DC/DC converter when this situation takes place, in order to ensure galvanic isolation between the circuitry and the battery.

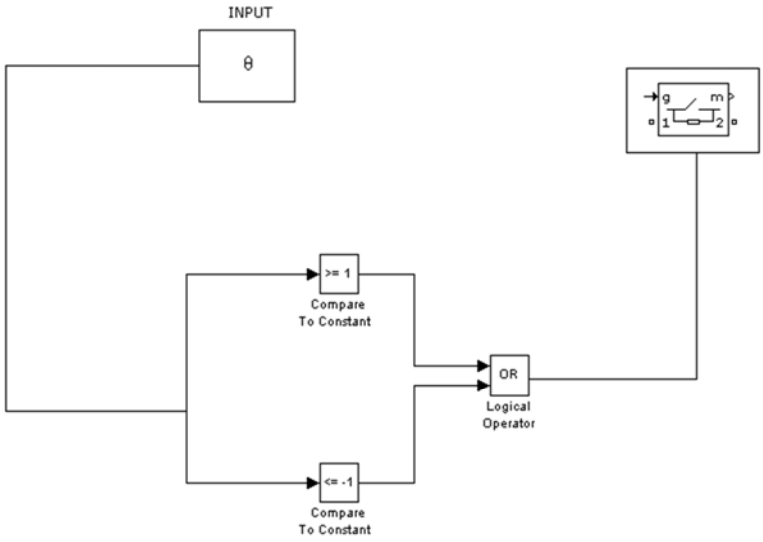

Figure 8.2 – Control scheme of the ON/OFF subsystem

8.1.2 - CAPACITOR CONTROL SUBSYSTEM

The subsystem shown in fig. 8.3 works with the measured capacitor current and the signals related to the comparison between θ and the constants; these are the two inputs, whilst in output there will be the error signal dealing with the capacitor, which will be used for the control strategy, because it will be added to the real current and the rated current (calculated dividing power by the voltage of the battery) signals. The addition of these three addends gives the total error necessary for the PI controller to achieve the control.

If θ is positive and greater than 1°, this means that the power will be absorbed from the grid to charge the battery. As a consequence, the control parameters have to be the one of **G2V** mode, and for this reason the static gain of the integrator of the capacitor control arm has to be modified from its initial value, set for V2G mode. The output of the comparative block " >1 " is equal to 1, whilst the output of the other block is nil. As can be seen in fig. 8.3, the addition (considering also the gain equal to 2) gives as a result the value 2, which is then multiplied by the initial parameter of the static gain of the integrator. In this way, the previous parameter is replaced by the new value of the proportional gain, which is exactly the term used for G2V mode.

Now the suitability of the control scheme for **V2G** mode has to be demonstrated. In this case the angle phase value is negative and, for instance, it can be set to -10°. The outputs of the two comparative blocks are opposite with respect to the previous case. The output of the " > 1 '' block is nil, and as a consequence it is nil also the addend which will be added to the other arm's result. In turn, " < -1'' block will give in output the unit value. This means that the result of the addition will be unit, and since this value is multiplied by the initial parameter, which was the one of V2G mode, it is easy to infer that if this situation takes place, the control scheme works properly with the V2G parameters required.

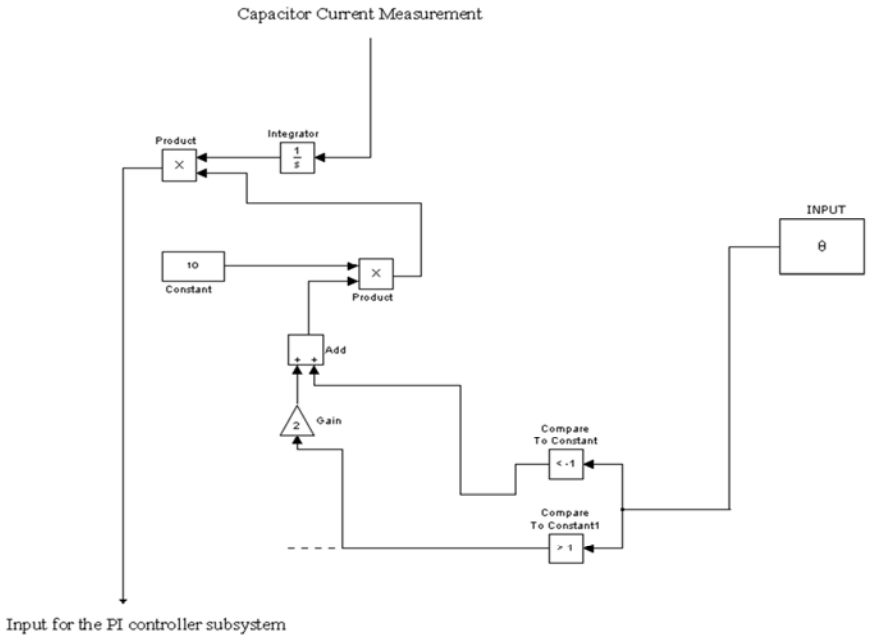

Figure 8.3 – Control scheme of the capacitor arm subsystem

8.1.3 - PI CONTROLLER SUBSYSTEM

This subsystem coincides with the model of the PI controller.
The variation of the parameters (which takes place when switching from V2G to G2V and vice versa) interests only the proportional gains of the controller, so the same controller has to be represented in its complete topology, made by a parallel of a proportional gain and an integrator (with its own proportional gain). The inputs of the subsystem are the total error (proper addition of real current measured in the circuit, rated current calculated, integral of the current flowing through the capacitor) and also the output of the two comparative blocks, which are needed for modifying the control parameters for V2G or G2V mode. The following fig. 8.4 shows the topology of this subsystem.

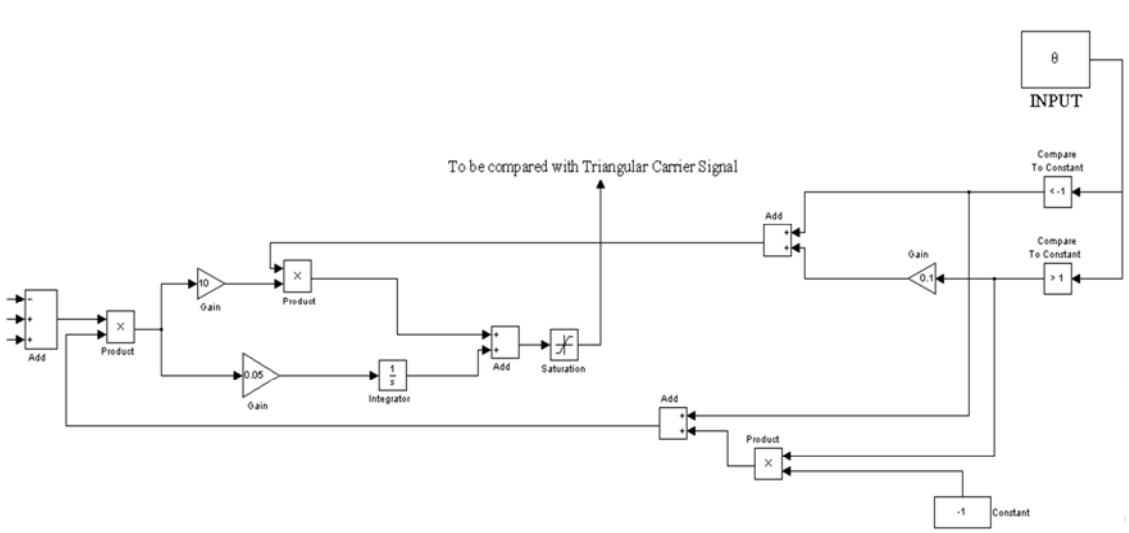

Figure 8.4 – Control scheme of the PI controller subsystem

For a better comprehension of the two working modes of this scheme, let's make now the hypothesis that the angle phase θ is positive. This means that PI controller's parameters have to be suitable for G2V mode. Since the default condition is that both of the arms of the controller are set with V2G parameters, the scheme has to be able to vary the gain of the proportional arm of the PI controller. From the fact that the angle phase is positive, the output of one of the two comparative blocks is nil; as a consequence, the output of the other one is positive and equal to one. The modification of the hypothesis brings to the opposite situation, and in both cases the two comparative blocks are able to impact on the PI controller's features.

Two arms connect the comparative blocks to the PI controller. The first arm brings a gain which will be multiplied by the proportional parameter set on the proportional arm of the PI controller (P). From the hypothesis of G2V mode, the value of the gain which will be multiplied by P is equal to 0.1, but if the hypothesis would have dealt with negative values of θ (discharging mode), the gain would have been unit and it wouldn't have influenced the default parameter, so to implement properly V2G mode.

The second arm influences the sign of the input error: this comes because reference current and measured current can be negative or positive in function of the mode, so at the same time the error can changes its sign. Since this sign-switch is not good for the control scheme used, the idea is just to multiply it with +1 if the sign of the error is correct for the mode, or to change its sign multiplying it with -1. The saturation block used after the sum of the two PI controller's arms is a block which avoids the output to overcome the upper limit of unit and the lower limit of nil. This is done because the triangular carrier signal has unit amplitude, with lower value of zero and upper value equal to one, so the duty cycle in this way will always assume a value between 0% and 100%.

8.1.4 - IGBT CONTROL SUBSYSTEM

This last subsystem takes as inputs the outputs of the two comparative blocks and the result of the comparison between the PI controller subsystem output and the output of the triangular carrier signal subsystem (this comparison creates basically the proper duty cycle to be applied), for the achievement of the piloting of one of the two DC/DC converter's IGBT.
The aims of the subsystem are to pilot in the proper way the right switching device during V2G or G2V mode using its output, which is exactly the duty cycle value to be applied, but also to keep both of them switched off whether the angle phase is not suitable for one of the two working mode, or the grid ask for the battery charger to switch to standstill mode. The following fig. 8.5 shows the topology of this subsystem.

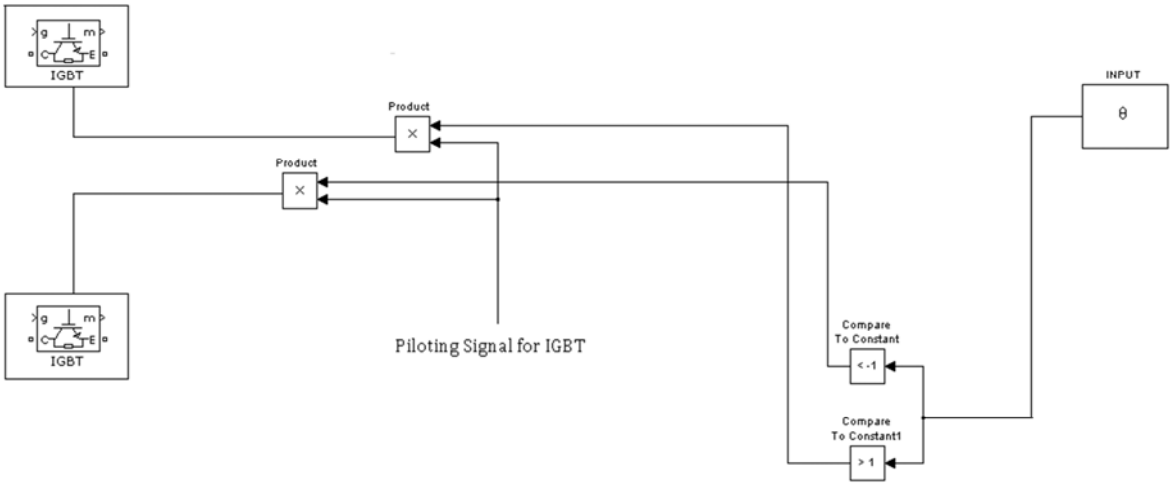

Figure 8.5 – Control scheme of the IGBT control subsystem

As can be seen, if the phase angle θ is included between plus one and minus one, both the outputs of the comparative blocks are nil and no IGBTs are fired. This means that in this case no power can flow through the DC/DC converter and the current through the battery is nil. If a different situation is present and the phase angle is positive or negative with a suitable value, the study of the topology introduced here shows how one of the two arms will be multiplied by zero, so the corresponding IGBT will be kept open, whilst the other one will be properly piloted.

8.2 - From G2V to Standstill or V2G

The first dynamic studied is the one in which the battery charger is asked to change its state from charging mode. Before checking the profile of powers, currents and voltages it can be useful to study in a more detailed way why this mode switching is needed.

During charging mode the battery is seen as a load from the grid's point of view and active power flows from the grid to the battery. While this operation takes place, the request of energy from other loads can increase according to the daily load profile. If the increment of the power required is relevant, the grid has to start to produce active power using its peak power plants, which are more expensive. As a consequence of this, the cost of electrical energy bought by customers increases, and at the same time more losses afflict the same grid, because more power, both active and reactive, needs to be transferred. The conclusion is that both the grid manager and the customers find disadvantages when the grid is overloaded. The solution that can be introduced to relieve these disadvantages is simply to pilot the charging mode of the battery. This means that, during peak hours, the grid will not charge the batteries of the EVs unless it is necessary, whilst this will be done massively when the daily load profile presents its lower peak. In fact, when the active power lower peak is present, the grid should be forced to switch off some of its basic plants, and this will produce money losses; this is why the grid uses this energy for charging the batteries.

Other situations which can force this model to be applied (switching from charging mode to standstill) can be, for instance, the necessity of the EV's owner to use the vehicle although the battery is not fully charged, or some problems dealing with the grid, which can be for instance a failure on the transmission network, or the same battery, like the achievement of a too much high temperature. Another important application can be found on the support of EVs to renewable energy plants. For instance, if the energy produced by one of these plants present a decrement of the produced power, the charging of the EVs fleet which supports the same plant can be stopped. As a consequence of the realization of all these situations, the control scheme can ask the battery charger to stop the charging of the battery or to reverse the power flow, and the following analysis has the aim to study the profiles of the electrical parameters which this mode switch is able to generate through a dynamic analysis.

The first simulation studied is the one in which the **switch from charging mode to standstill mode** takes place. From the start of the simulation till 1.2 [s] the battery charger works following the usual G2V mode and the battery starts to be charged. At time 1.2, the battery charger is forced to stop absorbing energy from the grid. As a consequence of this, the battery charger is disconnected from the grid since no more active power has to flow.

The transient state at the AC side of the system, which brings to the new steady state, is fast and it evolves without any overshoot, as can be seen analysing the active power flow (Fig. 8.2.1) absorbed by the battery charger. The profile shown is effectively suitable for the grid's point of view, since when the input is sent to the same battery charger to stop absorbing power from the grid, its acquisition is followed by a quick and stable action. The action takes place in less than 0.02 [s].
From the reactive power exchanged point of view the dynamic is the same: the system's topology provides a total disconnection between the grid and the AC/DC converter. This means that galvanic isolation is produced and the following profile is the one which can be found (Fig. 8.2.2).

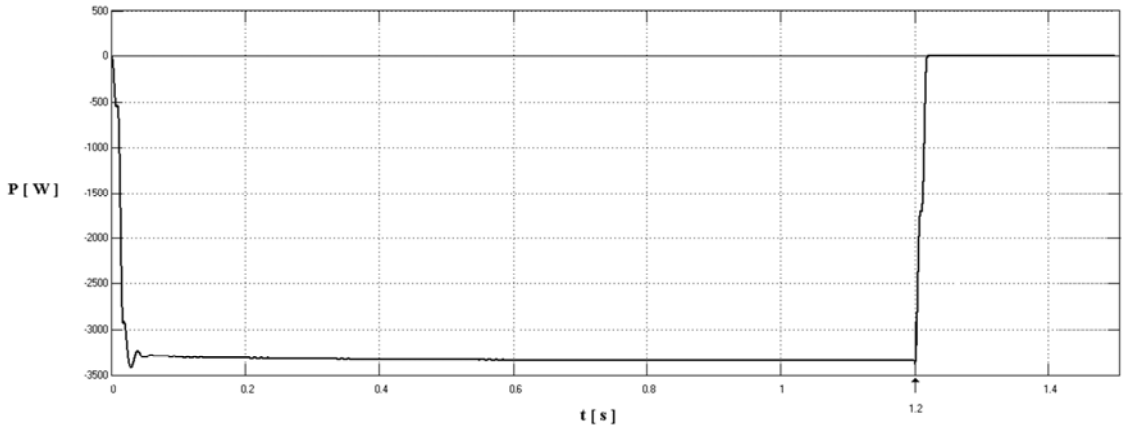

Figure 8.2.1 – Active power delivered by the grid

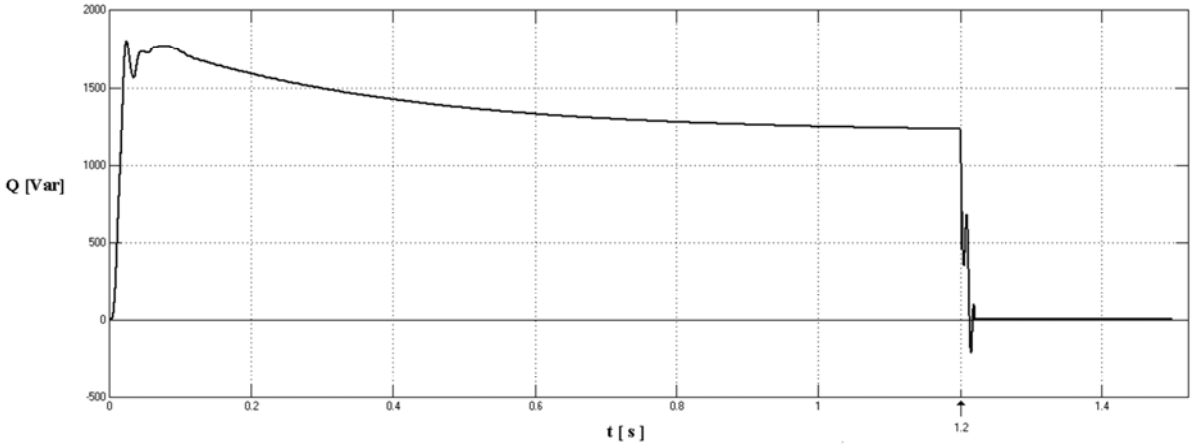

Figure 8.2.2 – Reactive power exchanged by the grid

The time needed for the achievement of the new reactive power's steady state is a little bit longer (0.03 [s]) and some ripples are present. This is due to the presence of reactive elements which influence the voltage through the two clamps of the grid. These fluctuations are small and, as a consequence, the grid side won't have problem dealing with them. Whether reactive power exchanged control is introduced, there is the possibility to set the exchange of reactive power between grid and battery charger (the capacitor of the battery charger) to a fixed value established by the grid, even if the active power flow is nil. With the implementation of reactive power control, the IGBTs of the AC/DC converter will be able to modulate the required value of reactive power in function of the voltage through the capacitor, and this case galvanic isolation cannot be achieved because reactive power flow will be exchanged between the AC/DC converter and the grid.

At the DC side there will be the decrement of the current absorbed by the battery until nil value is reached. At the same time, during the first moments, as a consequence of the variation of this DC current, the inductor will turn active, delivering the energy that was absorbed and stored during the increment of the current through the battery in the previous moments of the simulation.

The mesh regarding the capacitor and the two diodes of the DC/DC converter, considering a system without reactive power control, are now analysed. If no actions are done, the capacitor will maintain its own charge, and its discharge will be caused only by the reverse current flowing through the two diodes. If the capacitor has to be

discharged for any reason when the standstill mode is required, there will be the possibility to add a resistor in parallel to the same capacitor. The control scheme will be able to connect the resistance to the same capacitor when the standstill mode will take place. By the way, if this resistive arm is not installed, the profile of the voltage through the capacitor would be the one depicted in fig. 8.2.3.

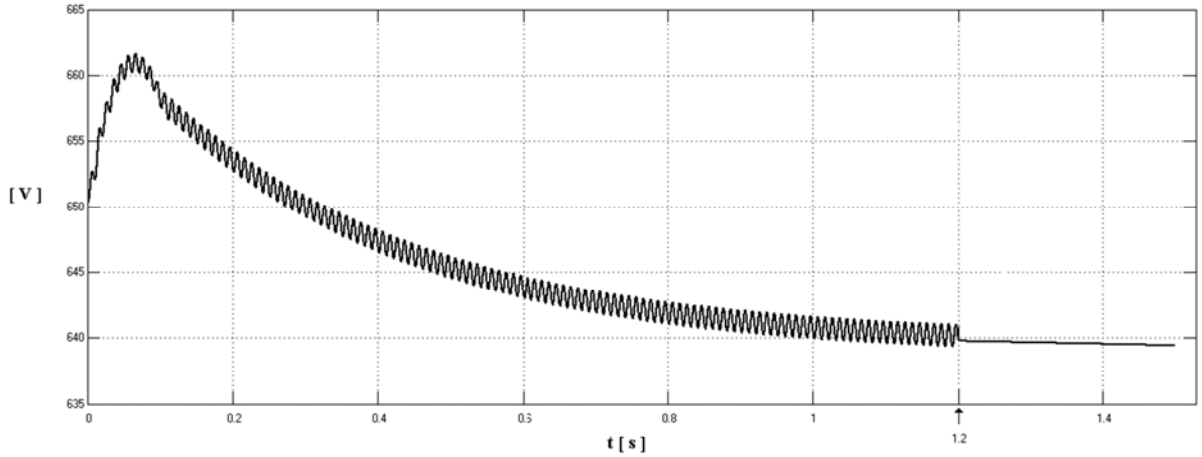

Figure 8.2.3 – Voltage through the capacitor

The next step will be the analysis of the power exchanged by the inductor and the capacitor during all the simulation time, since these two elements are always involved when the modification of the steady state takes place. The first one to be analysed will be the inductor: fig. 8.2.4 shows its power profile. As was noticed before, the two variations (from initial standstill condition to G2V and vice versa) have opposite sign because the first one deals with energy storage, the second one with deliver of energy into the system. It is important to remember that these two figures don't show the instantaneous value of the parameters, but their mean values calculated on an average period of 0.1 [s], in such a way to highlight the energy flow: the real situation deals with deeper peaks. Since the current through the inductor is monitored and checked, the device won't suffer from any damage supporting these variations.

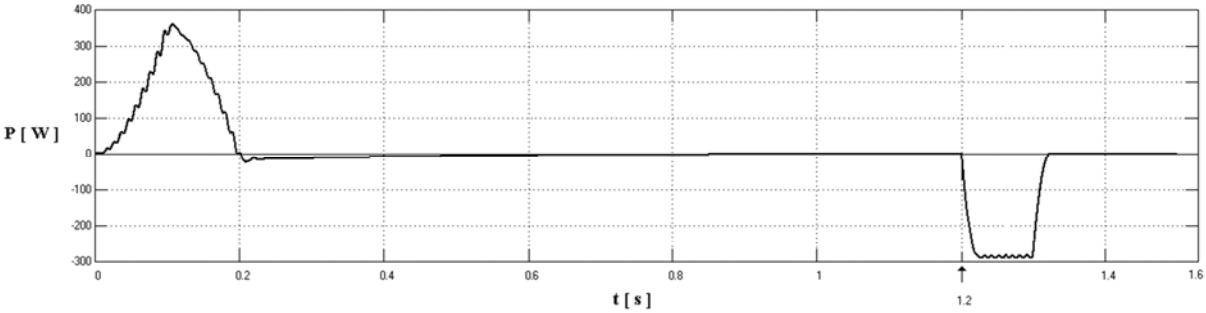

Figure 8.2.4 – Power exchanged by the inductor

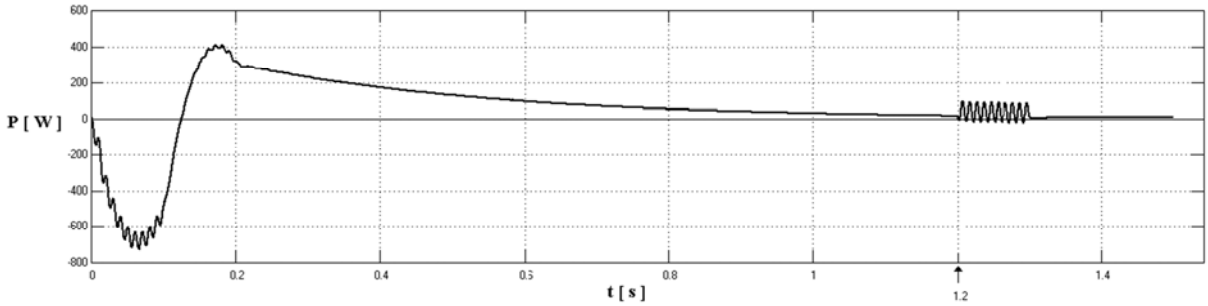

Figure 8.2.5 – Power exchanged by the capacitor

The second figure (Fig. 8.2.5) shows instead the profile of the mean power flow which characterizes the capacitor. As can be seen, the instant in which there is the switch from G2V to standstill (t=1,2 seconds) some ripples take place, but this doesn't influence so much the voltage through the capacitor. If the isolation of the capacitor is realised at 1.2 [s], how it is possible to have a variation of its power? The reason stands on the fact that the connection through the diode is already present and part of the energy stored in the inductor can flow through it, but the transient state considered is very light and no relevant variations of the electrical parameters are found.

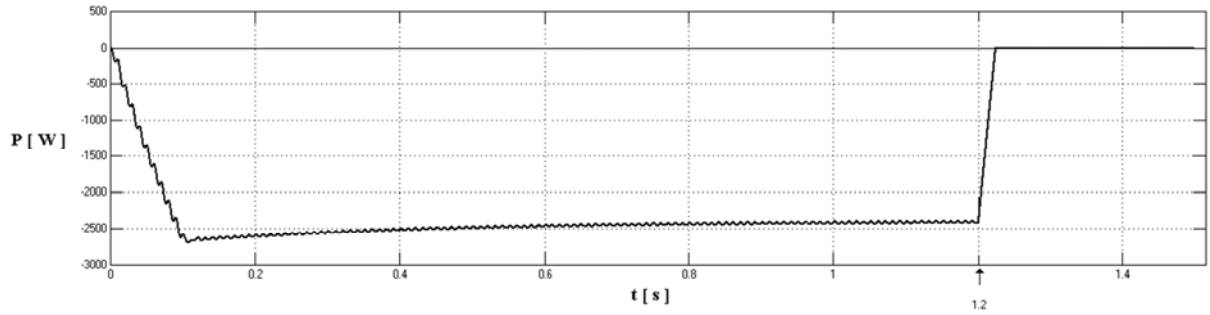

Figure 8.2.6 – Power absorbed by the battery

The profile shown in fig. 8.2.6 is the one of the power absorbed by the battery. Here the modification of the power absorbed takes place in 0.03 [s], and the profile of the current through the battery is expected to follow the same profile, so to be free from any overshoot and varying in a linear way.

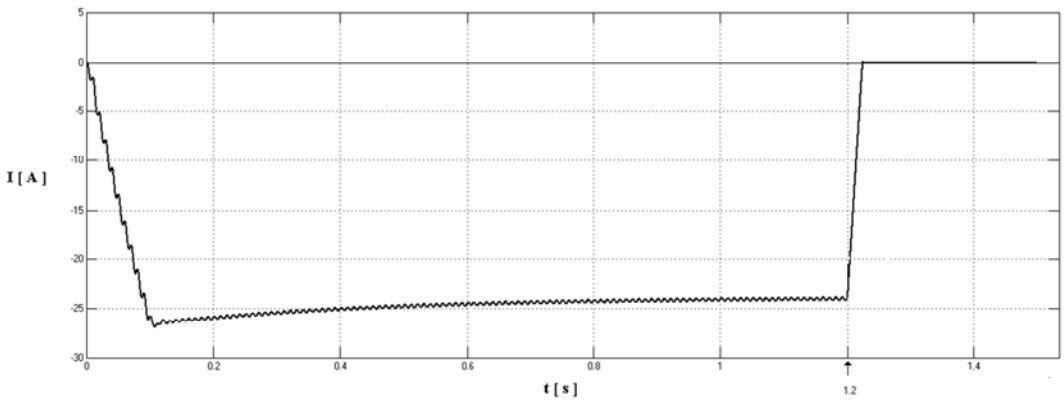

Figure 8.2.7 – Current absorbed by the battery

The results achieved are relevant since they demonstrate that the electrical parameters profiles at AC side are suitable for the grid, but now also the profiles of the electrical parameters at the DC side have been checked and they can be considered acceptable. The current through the battery is checked through fig. 8.2.7: as can be seen its evolution is linear and the ripples in that period of time can be considered negligible. Actually, once reached the new steady state, no more current flows through the battery, and this means that the system becomes standstill, since no power comes inside the system from the grid and no power is absorbed by the battery.

The second part of the simulation deals with the **switch from G2V mode to V2G mode**. Before studying this new dynamic, some differences between this switching mode and the one already completed can be pointed out. The switching from G2V mode to standstill means that the battery charger (and the battery) is treated as a load which can be turned off in some particular occasions. As a consequence, the battery is always seen as a load by the grid, but its characteristics made it better than just a load. The simulation which will be now faced allows the switching from the charging mode to the discharging mode. This means that the battery is not still seen as a "smart load'' by the grid, but as a real active element which can contribute to optimize the entire system absorbing or delivering energy. This is a further step with respect to the previous one, which can relevantly increase the potentiality of the same grid.

When can this switching state take place? As for the first simulation of this chapter, the initial situation can be that one of a sudden increase of the slope of the daily load profile, which can induce the grid manager to switch off the charging of EV's batteries which have reached an adequate SOC. If this variation leads to a state in which generating new energy for the grid (which now has to feed the entire loads except for the disconnected EVs) becomes expensive because peak plants have inevitably to start producing energy, it can be cheaper for the grid to absorb the energy already stored in the batteries of the EVs which are already charged, in spite of producing energy using these plants. This solution has to match an important requirement: only a fixed amount of the total energy stored can be absorbed, depending on the SOC of the batteries.
Vehicle's owner will be refunded for this: there has to be economical convenience for the realization of G2V mode from both grid and customers' side. At the same time, the same EV's owner has to be available, being aware that this means that the battery can suffer from further degradation due to more frequent charging/discharging cycle. By the way, if all these problems are overcome and V2G can be applied, the switch from G2V to V2G is required, and the following figures show the results of the simulation.
With regards to the AC side, figure 8.2.8 shows the profile of the active power modification at time 1.2 [s].

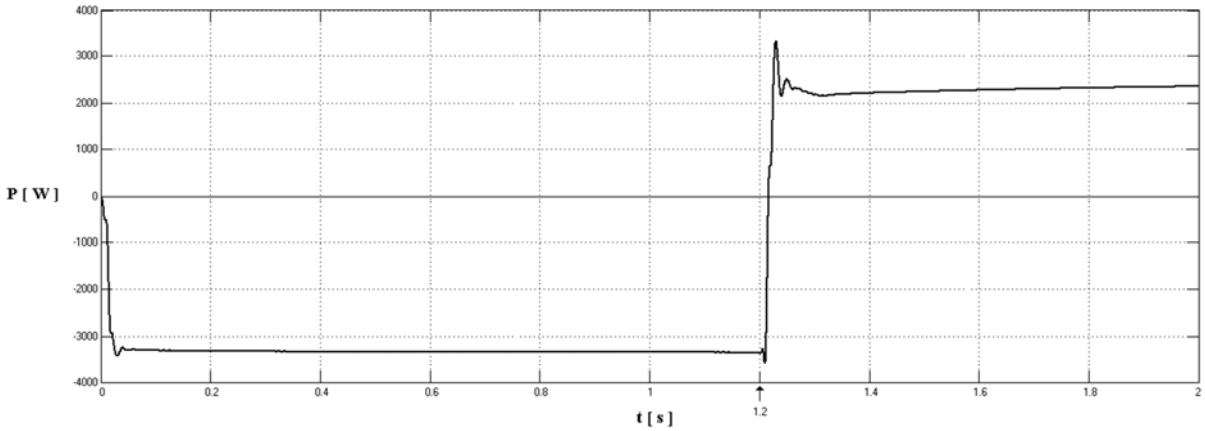

Figure 8.2.8 – Active power exchanged by the grid

As can be seen the transition between G2V and V2G is as fast as in the previous case, but it can be noticed how in this case two overshoots are present, one at the beginning of the transient state and one at its end.
Even if they are present, they can absolutely be considered as negligible, both with regards to the battery and the grid. Different is the case of the reactive power profile, examined through fig. 8.2.9.

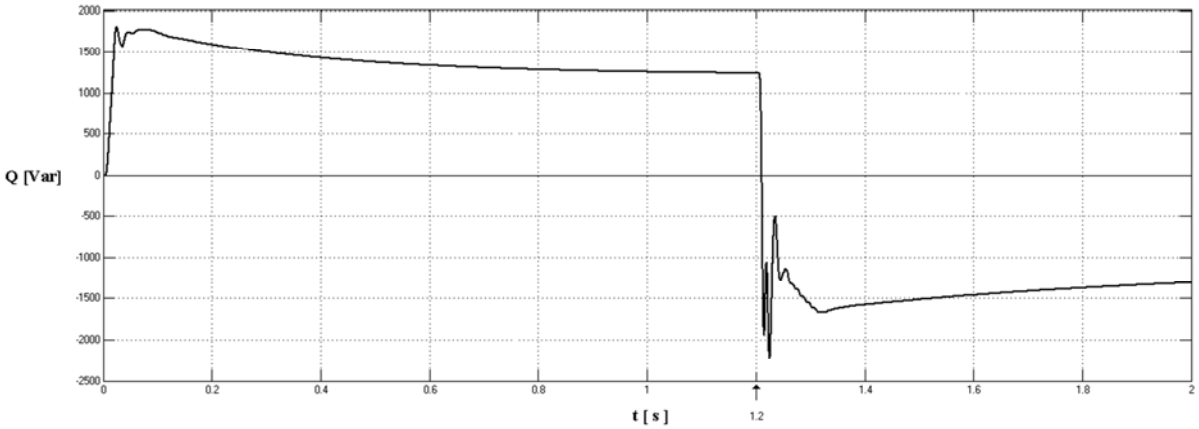

Figure 8.2.9 – Reactive power exchanged by the grid

The transient state of the reactive power exchanged is disrupted and it presents some peaks that are not negligible for the first 0.5 [s]. When this time is passed, the profile gets milder and reaches its new steady state without any other relevant fluctuations. This behaviour deals with the fact that the two different steady states are very different from a physical point of view, with respect to the first simulation. In fact, in that case the power flow was just arrested, but here it is reversed. As a consequence of a deeper variation of reactive power, there will be a deeper variation of the voltage through the capacitor. Figure 8.2.10 allows the analysis of the voltage and it is easy to see that whilst in the previous simulation at time 1.2 [s] the voltage was 640 [V], and it was not going to evolve anymore, in this case the voltage value decreases of 40 [V], and after that it starts increasing with a lower slope till the value of 623 [V]. This fast and relatively deep transient state influences the dynamic of the reactive power profile shown in the figure examined before.

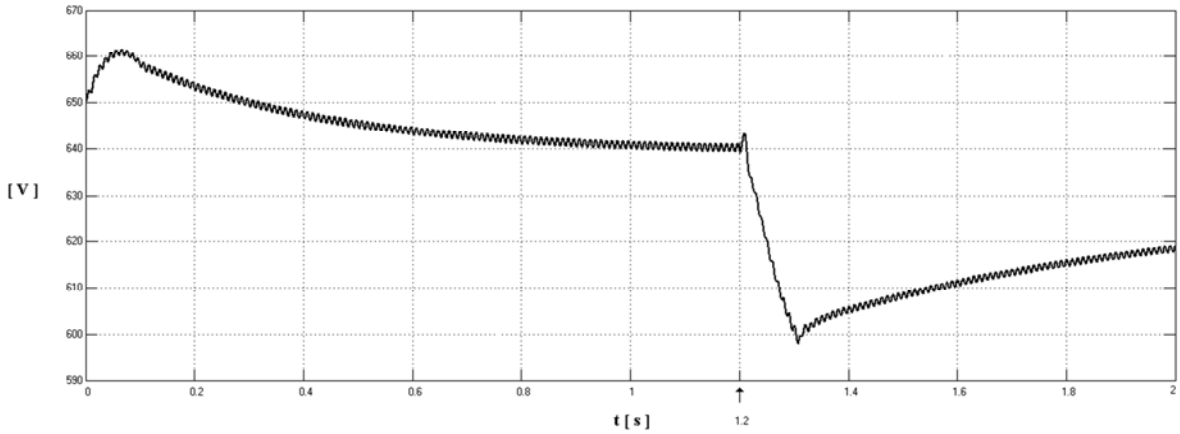

Figure 8.2.10 – Voltage through the capacitor

The variation of another electrical parameter is expected to be relevant, as a consequence of this voltage profile: this parameter is the power absorbed or delivered by the capacitor. As can be seen, what is expected is an initial absorption of power in the starting transient state (already investigated during the previous simulations); this is followed by a slow deliver of power which decreases till the capacitor is considered no more active from net power flow. At 1.2 [s], instead, the switching from G2V to V2G produces a new heavier transfer of electric power, because the system at DC side is slower than the system at the AC side. Thanks to the capacitor control, this delivery of power is followed by a new absorption which increases the voltage through the same capacitor and the new steady state is reached. This explanation, which is pointed out with reference to the voltage profile depicted in fig. 8.2.10, can be easily confirmed by fig. 8.2.11, where the absorption is evaluated as negative and the deliver is positive for the convention used.

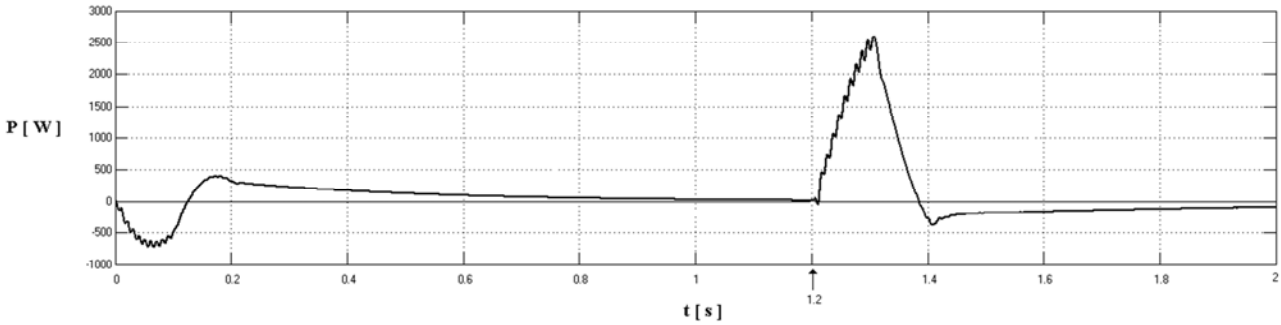

Figure 8.2.11 – Power exchanged by the capacitor

At this point some considerations about the inductor can be pointed out. The first part of the simulation, so the way in which the inductor is charged, is the same as before; but when the switch between modes takes place, the energy stored inside the inductor becomes nil during the first instants, but then will start increasing again, since the new mode will produce a growth of the current with an opposite sign and newly the charging of the device. Figure 8.2.12 shows the profile of the power which interests the inductor.

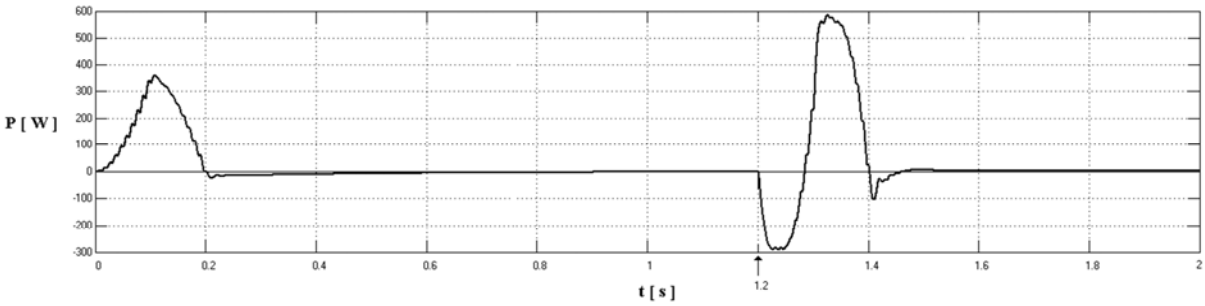

Figure 8.2.12 – Power exchanged by the inductor

As can be seen, the first moments after 1.2 [s] deal with a relevant amount of energy which is delivered by the inductor, which discharges completely. In that moment the transient is not finished, since the inductor starts storing energy for the second time. The following instants describe the achievement of the steady state, in which the inductor has stored a fixed amount of energy, but the current flow now is reversed and V2G mode is applied.
A better analysis of the dynamics of the inductor can be brought by the study of the current profile of the system sampled for all the simulation time, and represented in fig. 8.2.13. The equation which describes the voltage through the inductor (and its power flow) depends on the slope of the profile of the current: as a consequence, it is easy to see that there is a first absorption of energy, due to the fact that the inductor is charging from standstill,

which is followed by a small deliver due to the fact that the current is characterised by an overshoot. When the current reaches its G2V steady state, no more power is absorbed by this device. The switch between states creates as first a strong decrement of the current, which reaches nil value. After the achievement of this value, the current will grow up with opposite sign. From figure 8.2.12, it is possible to see that this new increment of current produces a new power absorption.

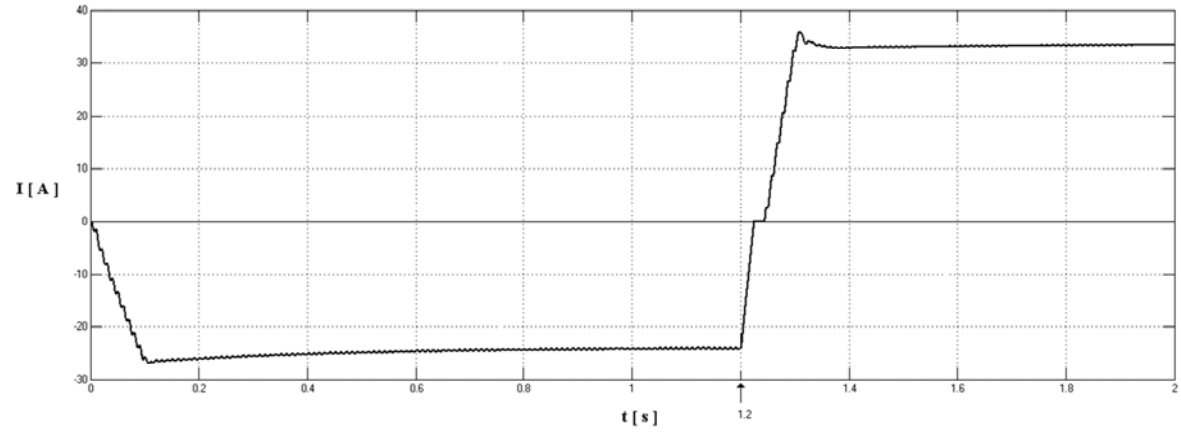

Figure 8.2.13 – Current flowing through the battery

Another current profile can be now evaluated. In the switching case considered, in fact, there is the variation from G2V (+13°) to V2G (-10°) and this means that the AC current will be subjected to both an amplitude and a phase variation. Figure 8.2.14 depicts the variation which takes place at 1.2 [s]. From the safety's point of view this amplitude variation phenomenon doesn't produce any issue to battery charger's devices or to the grid, but it can be limited if necessary, for instance to avoid protection intervention. Since the distortion ends in one period, which is a short period of time in this case, the switch between modes can take place when the instantaneous current is close to be nil, in such a way to avoid any amplitude excesses.

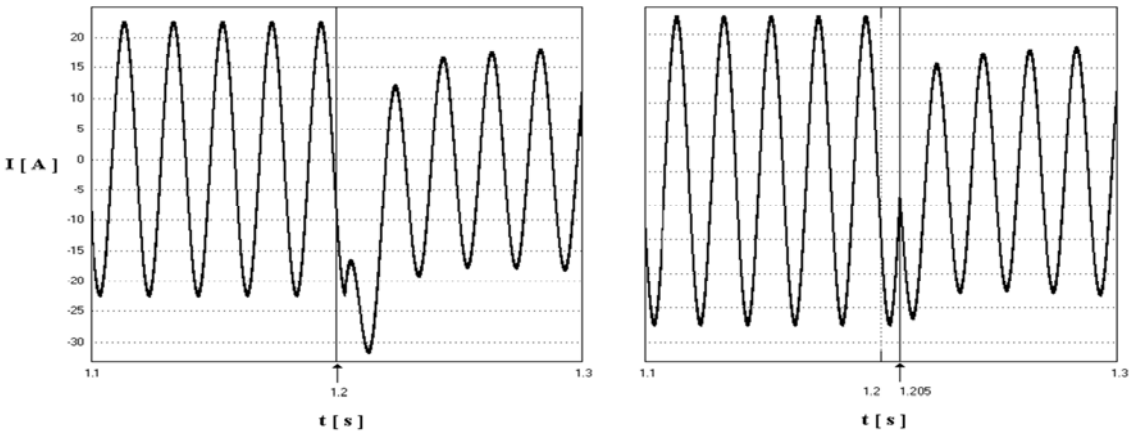

Figure 8.2.14 – Instantaneous AC current values with switching mode at 1.2 [s] and 1.205 [s]

8.3 – From V2G to Standstill or G2V

Here two other simulations are run, and their aim is to analyse the profiles of the electrical parameters which are involved when the battery charger needs to switch its working mode from V2G, demonstrating that all the profiles are suitable for the battery charger. Before analysing the results of the simulations, the reasons of the switch from V2G mode have to be exposed. Basically, more than the analysis of the reasons for this switch, it can be interesting to see why the system is working in V2G mode: this is the mode in which active power flows from the vehicle to the grid. The basic reason for V2G working mode application deals with the fact that, for the grid, buying energy from EV's owners in some periods of the day can be cheaper than producing power from its electrical power plants. Other reasons can be that of an emergency, in which the grid needs, for instance for frequency regulation purposes, a fixed amount of active power to be absorbed, or that of a renewable energy plant support. The simulation **from V2G mode to standstill mode** is needed because sooner or later the discharge of the battery has to stop, and electrical parameters have to reach a new steady state in a safe and reliable way. What can be expected from this analysis? The scenario expected is similar to the one found for the switch from G2V, with some variation due to the different physical characteristics of the circuit before and after the switch.

First of all the most important parameters, so the ones dealing with the active power flow, have to be checked. Grid's requirements are always the same: the mode switch has to lead to the new steady state through a transient state which has to be as fast and light as possible and it doesn't have to produce relevant fluctuations with regards to currents and voltages. In correspondence of the DC side, even the battery requires a transient state which is free from deep overshoots or fluctuations, to avoid any degrading phenomena or stresses regarding the same battery. Figure 8.3.1 shows the active power profile at the AC side.

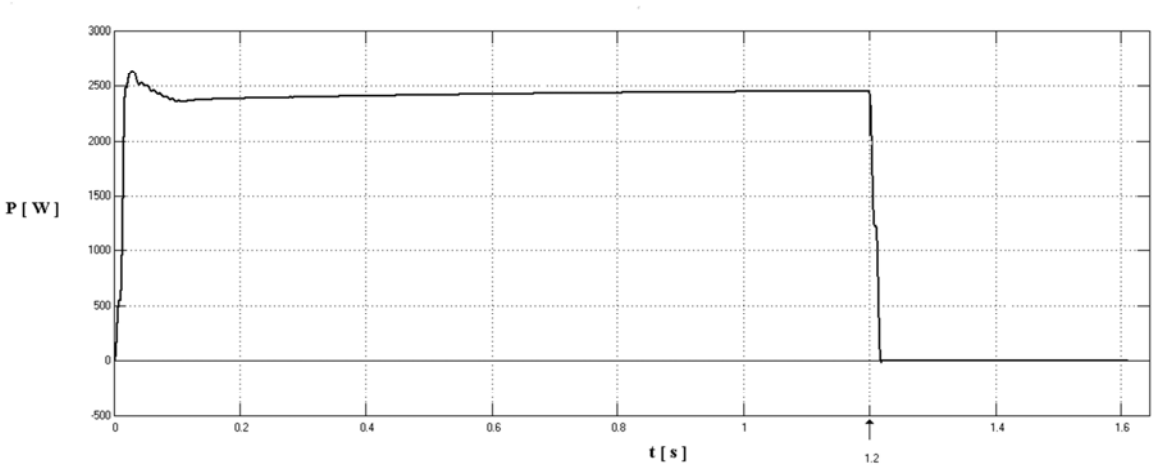

Figure 8.3.1 – Active power absorbed by the grid

As can be noticed, the time needed for reaching nil power flow is exactly the same as was calculated for the previous simulation from G2V to standstill and it is the time for achieving the opening of the switches of the AC/DC converter. From the reactive power exchange point of view, in the following figure (Fig. 8.3.2) the profile is depicted. Even in this case the comparison made between these results and the G2V-to-standstill ones furnish some similarities: the profile reaches the new steady state with some fast fluctuations and it presents an overshoot (which by the way is not so high) both in the start and at the end of the transient state.

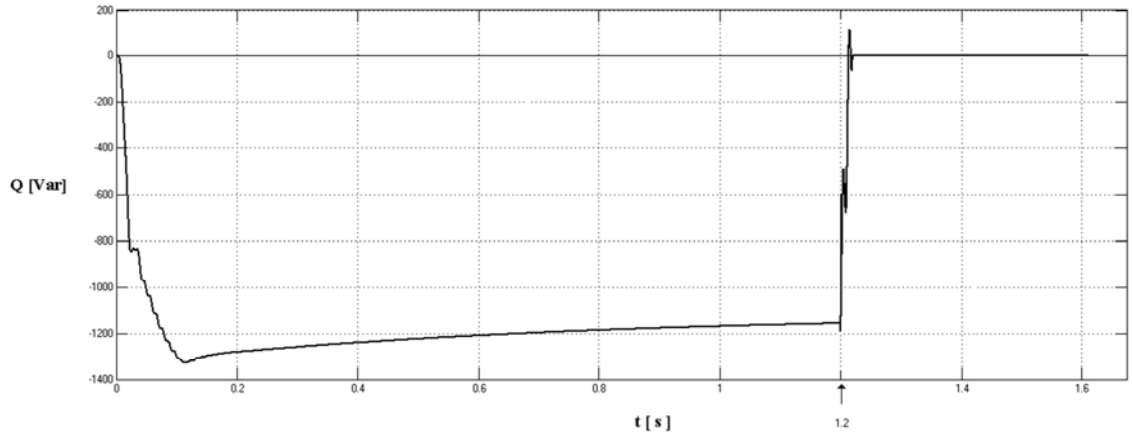

Figure 8.3.2 – Reactive power exchanged with the grid

Since the profile of the reactive power is connected to the profile of the voltage through the capacitor, even its profile is analysed, and it is checked how its variations are effectively suitable for the normal operating mode of the battery charger. Even before the analysis it is easy to see that the reactive power exchanged profile evolves without strong variations: the voltage through the capacitor won't suffer from deep fluctuations as well.

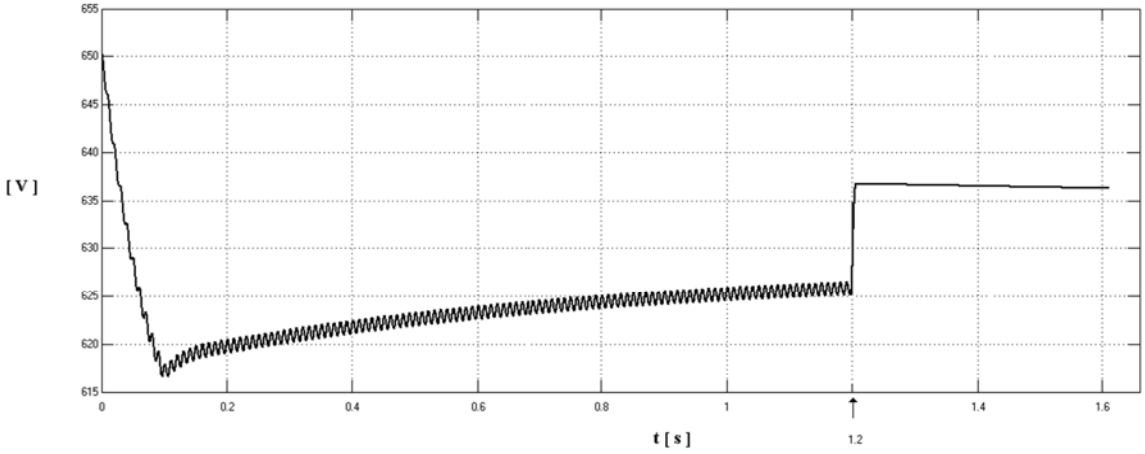

Figure 8.3.3 – Voltage through the capacitor

A peculiar thing can be noticed: that is the discontinuity that can be appreciated in correspondence of the switch between modes: there is an increment of 13 [V] which takes place in a very short period of time, the time needed to bring the reactive power to its nil value. After that, the profile is no more subjected to ripples, because no switching devices are commuting. The slow decrement of its voltage comes from the circuit losses, but for safety reasons there can be the possibility to dissipate the energy stored through a resistance. This voltage step was not present in the previous case, but all depends on the different dynamic of the system: from G2V to standstill (paragraph 8.2), the openings of the switching devices produced the isolation of the two systems, so reactive power exchange was going to become nil and the voltage through the capacitor was not affected by any discontinuity. In this case instead V2G mode is operating, so the openings of the switching devices generate nil reactive power exchange but at the same time the DC side is not already at its steady state. This is the reason

which produces this small voltage increment. The instantaneous power flow which interests the inductor and the capacitor can be analysed thanks to the following figures.

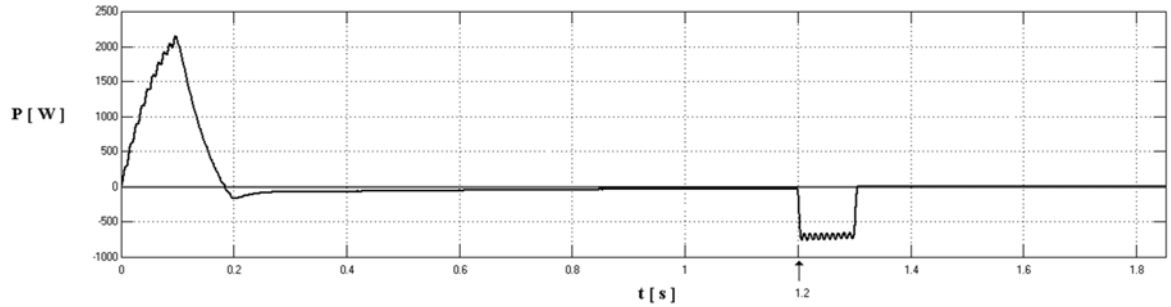

Figure 8.3.4 – Power exchanged by the capacitor

Figure 8.3.4 represents the profile of the power flow dealing with the capacitor. The correspondence with the profile of the voltage through the device can be easily found, and the sudden increase of the voltage, which was pointed out before, can be read as a sudden but temporary increment of the power (and energy) absorbed. This capacitor transient state ends very quickly. The power represented through the figure is the mean power flow, evaluated with an average period of 0.1 [s]. As a consequence of this choice, the profile loses its connection with the real situation when very fast fluctuations take place, like in this case; the figure depicts that the power is absorbed for 0.1 [s], but the real case is that of a faster absorption which ends in some [ms]. At this point, some doubts about the fact that a fast power absorption can deal with some problems which can afflict the device can rise: this is not the case, since the voltage through the capacitor is sampled in its instantaneous value (Fig. 8.3.3), and it shows that the voltage step produced by this sudden absorption of power is not so high and can be tolerated by the capacitor; at the same time, also the total amount of energy exchanged, which is the integral of the power, can be considered a low value (also the current through it cannot be too much high).

The other battery charger's active device profiles can be investigated in order to check whether its electrical profiles are suitable for the switch to standstill. Figure 8.3.5 shows the profile of the power exchanged by the inductor.

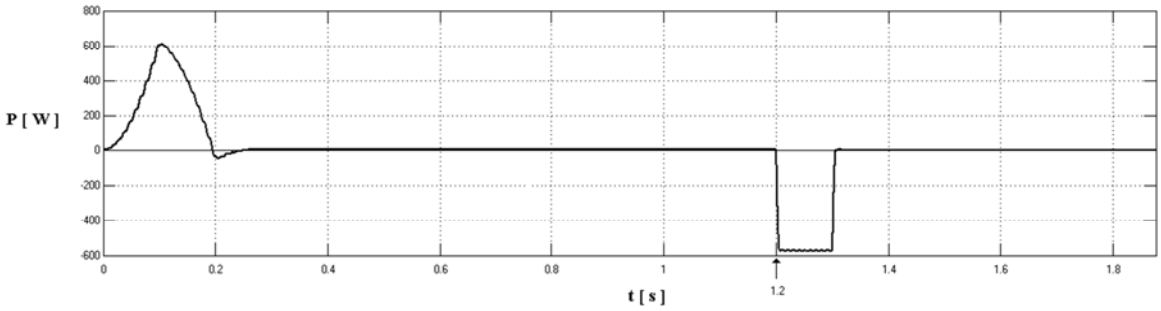

Figure 8.3.5 – Power exchanged by the inductor

This profile is evaluated applying the mean value function too (where the time window is set to 0.1 [s]). The way in which the inductor absorbs and delivers energy is depicted through the starting transient state and the transient state which deals to the switch into standstill state. The difference between these two transient states stands on the speed in which the two different steady states are achieved, and this can be easily infer even looking at the profile of the current through the battery. Figure 8.3.6 shows how the current increases till almost its rated value

in 0.12 [s], but also how quickly then it turns to nil value. As a consequence, even the time needed for discharging the inductor will be less than the time needed for its charging. Figure 8.3.7 shows the power delivered by the battery (which can be added to the power delivered by the same inductor); it can be seen that its profile won't reach the nil value immediately, and as a consequence the capacitor will be subjected to the voltage step already analysed.

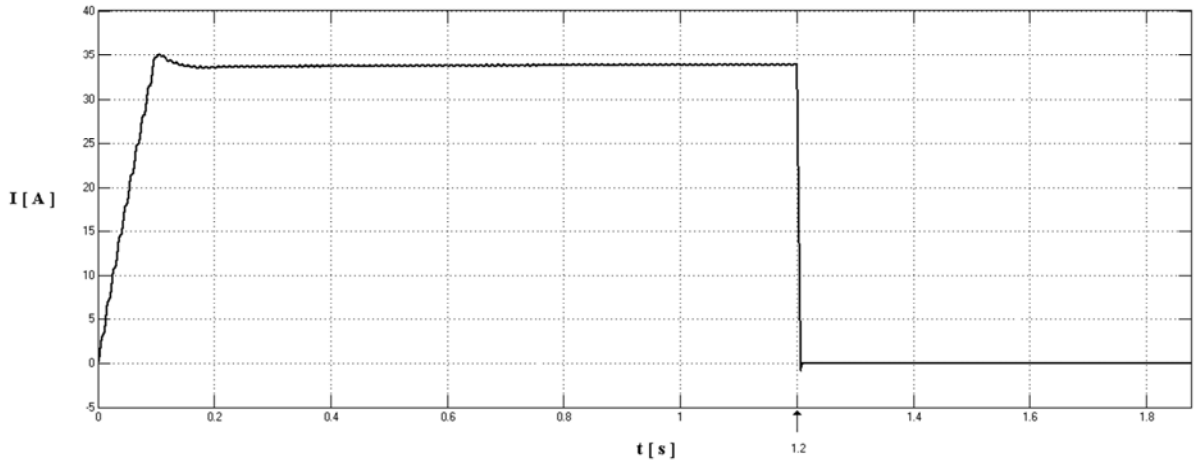

Figure 8.3.6 – Current delivered by the battery

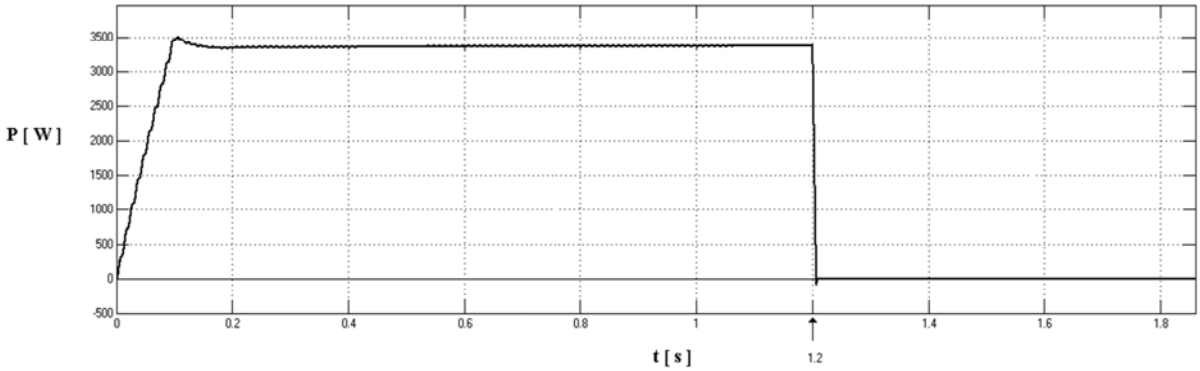

Figure 8.3.7 – Power delivered by the battery

It can be seen from the figures that ripples are negligible and the same power delivered decreases to nil value after a period of time which can be evaluated in milliseconds. The system, from this point of view, is really fast and the battery is able to stop delivering power with no delays. This is a safe situation because a fast response without overshoot is the best scenario that can be produced, so the first part dealing with the simulation from V2G to standstill can be considered suitable for the working of the battery charger in the real world.

The second simulation deals with the **switch from V2G mode to G2V mode**. This switch doesn't represent a very common situation, but some examples of why it takes place can be briefly pointed out. The first and most important one deals with the fact that an emergency or an important power flow variation (for example disconnection of heavy load or of an entire grid portion during peak hours) happens inside the grid. The same grid, which was absorbing energy (V2G) from the battery since the power required from the other loads was high, sudden receive the information that the power required is decreasing. The first step which can be done for

facing this situation can be the one of switching to standstill mode the battery chargers of the EVs, but if this is not sufficient, for instance because a portion of the same grid is disconnected for an electric failure (and the loads connected to it can't be feed anymore), there can be the necessity to store the exceeding active power produced and not consumed. This can be made turning the battery chargers to G2V mode and making the batteries to store this energy.

The configuration of the system in this situation is different from the switch from (and to) standstill. The reversal of the power flow produces fluctuations that are more relevant and which need to be carefully studied. The analysis of this new transient state starts with the evaluation of the active power flow, which has always to be as fast as possible and free from overshoot or fluctuations both during transient state and during steady state (Fig. 8.3.8). Together with the evaluation of the active power there will be also the evaluation of the reactive power exchanged by the system (Fig. 8.3.9), which is always dealing with the voltage through the capacitor. Even this profile has to be well controlled. The aim of this analysis, which is lead here, will be that of being sure of the evolution of a fast and free from deep variations transient state, which brings the system to a new steady state in a safe and suitable way.

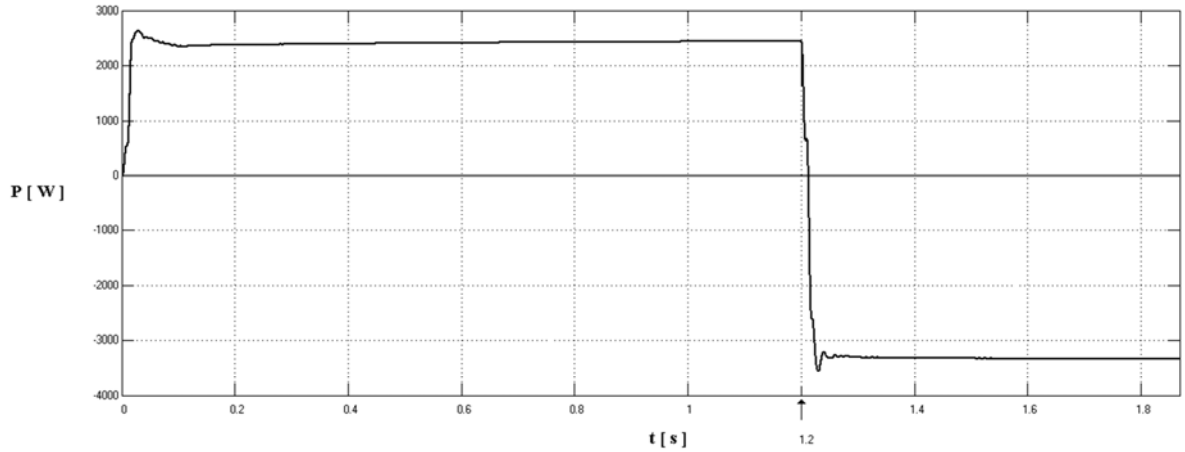

Figure 8.3.8 – Active power exchanged with the grid

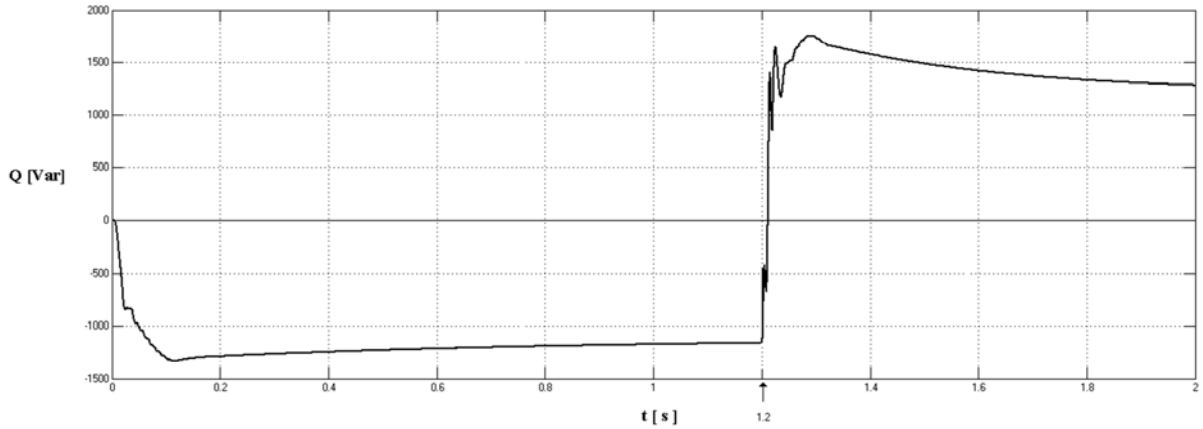

Figure 8.3.9 – Reactive power exchanged with the grid

Both the transient states regarding the reactive power, the one from nil initial state to V2G and the one from V2G to G2V, can be considered as quite long states, since around 1 [s] is the period of time needed for them to be completed. It can be seen that when the switch between the modes takes place, at time 1.2 [s], the former steady

state is not completely reached yet, and at the end of the simulation neither the second steady state is reached, although the available period of time for the achievement of the steady state is respectively of 1.2 [s] and 0.8 [s]. By the way, it can be seen that although the second transient state takes a relatively long time, the variation from the steady state value can be considered negligible (Fig. 8.3.9) since after the first 0.2 [s] the value of the reactive power calculated is already close to the steady state value. From fig. 8.3.10 it can be seen that even the voltage through the capacitor shows a profile which doesn't reach its steady state in the period of time considered, but whose slope tends to become close to be nil, symptom that steady state is not so far. The first transient state (achievement of V2G) produces a decrement of the voltage through the capacitor, since as told before the AC side is faster than the DC side and reaches the full absorption of power in less time. This means that some energy stored in the capacitor is delivered to the grid.

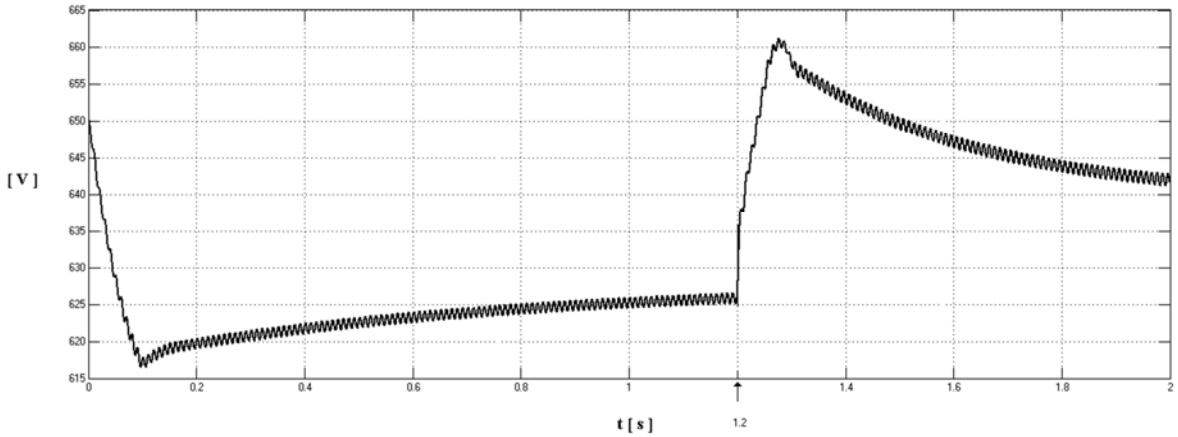

Figure 8.3.10 – Voltage through the capacitor

During both the transient states studied, the capacitor control limits the total amount of energy that the capacitor delivers or absorbs, forcing the DC side to absorb or deliver more energy, in such a way to preserve the power equilibrium. As a demonstration that the second transient state is actually evolving to a steady state which is the one that can be expected, it will be enough to watch the profile of the voltage, since it is going to reduce its slope until nil slope is reached.

A further demonstration can be sorted out from the profile of the mean power exchanged by the capacitor, which can be analysed through fig. 8.3.11. The first positive peak which can be noticed in its profile deals with energy delivery, and corresponds to the decrement of the voltage through it. The capacitor control operation leads to a following power absorption (depicted as negative profile) which decreases to nil value in a period of time which goes from 0.1 to 1.2 [s]. This means that the capacitor increases its voltage in this time window, and it is going to reach its steady state.
The fact that at 1.2 [s] the net power flow is not nil, so the voltage through the capacitor has not yet reached its rated steady state value, is not a problem, since the transient state can be considered already completed.
Focusing on the second transient state, it is easy to see that almost the same evolution but with opposite sign is repeated. In fact, there is at first a negative power peak which indicates the absorption of energy from the capacitor and the increment of its voltage, which then becomes positive thanks to the control action.

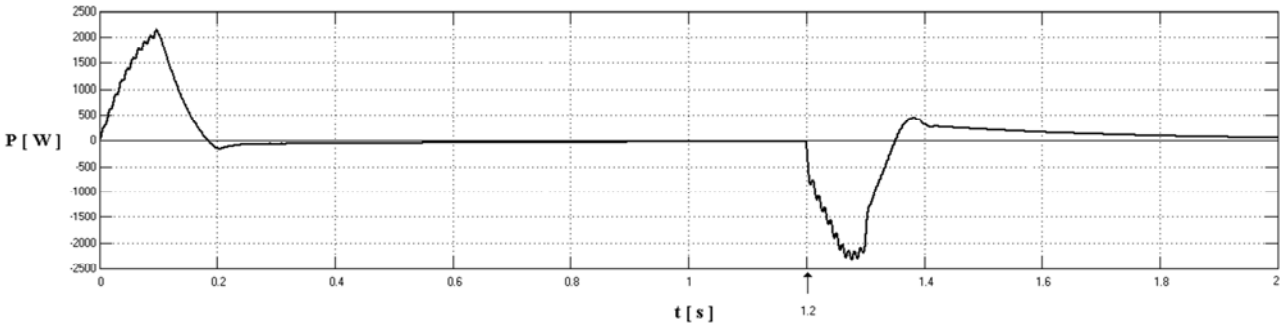

Figure 8.3.11 – Power exchanged by the capacitor

The different parameter set for the static gain of the integrator, when the switch between modes takes place, and the different physical system which is created, produce a reaction which is stronger than the first transient state. This can be seen in a wider area below the power profile, which means that more energy is involved and delivered by the capacitor. This avoids the voltage to change too much from its initial value, but the profile of figure 8.3.10 demonstrates effectively the reason why the profile of the second transient state presents a slope which is higher than the first. By the way, the power profile tends to achieve nil value with exponential mode, and this confirms that even the voltage profile is going to reach its steady state voltage with nil slope.
The following figure depicts the current profile (Fig. 8.3.12).

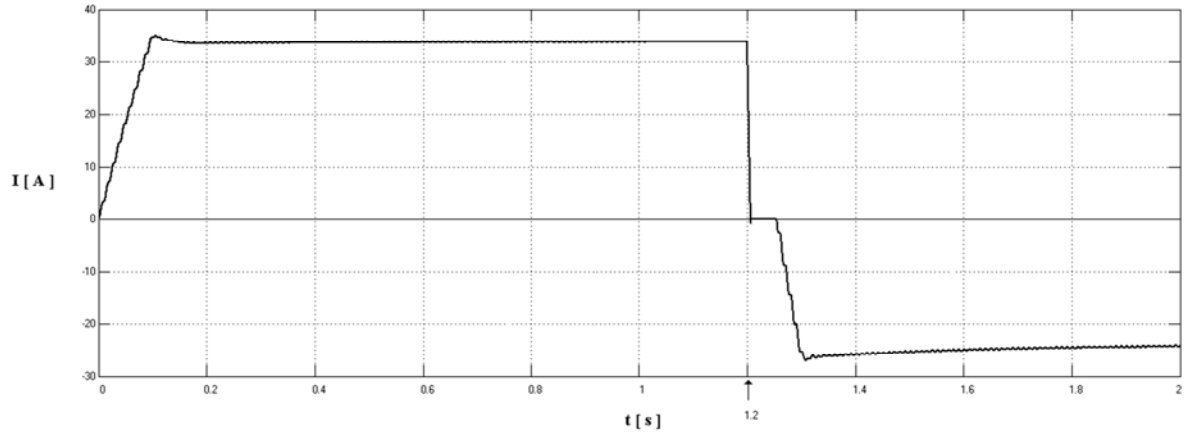

Figure 8.3.12 – Current flowing through the battery

From the choice of the 0.1 [H] inductor made in chapter 7, little overshoots in both the transient states which lead steady states are present. The amplitudes of these overshoots are really limited and they don't produce any bad effect on the battery. An important characteristic can be noticed: the transient state regarding the capacitor doesn't influence at all the current delivered or absorbed by the battery, so the DC side of the system. Looking at the figure, after 0.4 [s] the current becomes constant (but there are always some current ripples due to the DC/DC converter's working mode that can be minimized but not deleted, even if in any case they don't create any degrading or aging issue to the battery). The second transient state is heavier and takes 0.6 [s] for the current to reach almost its rated constant value. An important thing that can be noticed is that the profile of the current decreases very quickly when the switch between the two modes is implemented, and this has consequences on the power released by the inductor.

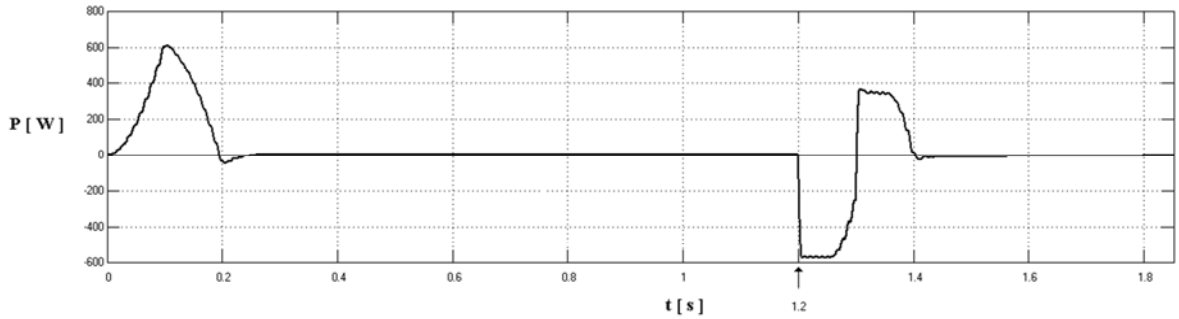

Figure 8.3.13 – Power exchanged by the inductor

The mean power absorbed or released by the inductor can be evaluated through figure 8.3.13. The first transient state produces the charging of the device and the mentioned overshoot determines a little energy release. Since the same transient state is function of the current profile, a constant mean value of the current determines a nil mean value of the power exchanged. The second transient state is characterized by a quick discharging of the energy stored inside the inductor, and the following achievement of a new steady state with a reversed current flow determines a new charging of the inductor, which stores a new quantity of energy. When the current reaches its new steady state no more net flow of power and energy takes place.

The last profile which can be checked is the one of the power flow which interests the battery. The switch from V2G to G2V produces a reverse flow of power, which is no more delivered but now absorbed by the battery. The profile of the current is the symptom that the battery will provide both the states without any problem, and the confirmation comes from figure 8.3.14.

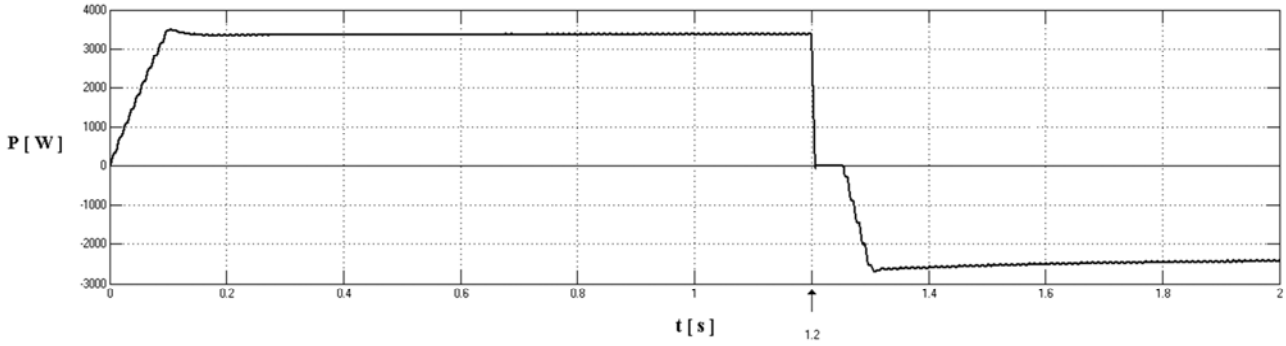

Figure 8.3.14 – Power exchanged by the battery

This chapter has demonstrated how all the switching combinations possible can be implemented by the proposed scheme, producing a fast and free-from-relevant fluctuations transient state, and how the electrical parameters considered are always suitable for the connection of the system to the grid. At the same time, it has been demonstrated that even the battery is always working in conditions that preserve it from any degradation or malfunction. Since the power absorbed from the grid during G2V mode is about 3300 [W] and the power absorbed by the grid during V2G mode is about 2500 [W], the switch between the two modes produces a variation of 5850 [W] in fraction of seconds. This means that the study of the dynamic of the battery charger has been carried out using the worst condition possible, that stresses in the worst way possible the devices of the entire system. As a consequence, the good results found using these input data of the angle phase θ means that every other variation of the angle, with respect to the limit of +13° and -10°, can be considered acceptable.

9 – EV Charging Infrastructures

The electric propulsion depends on the availability of an efficient and reliable energy storage system, the battery. Beside this issue, which can be considered already solved thanks to the growth of this technology, it is necessary to design a proper battery charger, and this has been the principal purpose of this work, already achieved. However, the realization of an adequate device cannot leave aside the concept of proper charging infrastructures, which can guarantee safe connection between the vehicle and the grid according to severe standards. All these standards will basically depend on the power flowing through the system, but also on others important safety factors which deal with the grid.

Focusing on the charging of the battery, two phases can be distinguished. The main charging phase is the one in which the most part of the energy is transferred from the grid to the battery, whilst the final charge phase deals with actions which are able to give balance and stability to the battery. These two different phases can be depicted through fig. 9.1: for the main charge the profile reveals a constant current characteristic, for the final phase instead constant voltage is applied. It can be demonstrated that the final phase can be also neglected without generating any particular disease to the battery, so the assumption will be that all of the energy transferred will take place according to the set of a fixed amount of current. As can be seen, the power absorbed by the battery will increase with the increment of the voltage through the battery: the infrastructure system has to be designed for the maximum peak power applied.

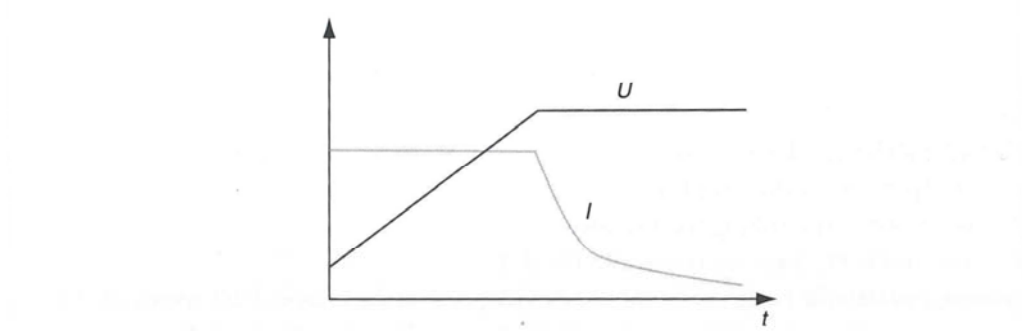

Figure 9.1 – IV charging characteristic

The charging mode duration depends on the energy which flows from the grid to the vehicle, so if the current absorbed by the battery is high, the process will take less time: at the same time, the required infrastructures will be different in function of the power (and the energy) exchanged. It is easy to understand how many factors can influence the design of proper infrastructures for both the safety of the devices and the safety of people. Assuming that the energy required for the full charging of the battery is of about 10 [kWh], the time duration needed for the full charge will depend on the power available: with 2 [kW] available 5 hours would be needed, with 10 [kW] just 1 hour is sufficient. According to the power taken from the grid and the associated charging speed, several power levels defined by appropriate standards can be defined.

The **normal charging mode** is a mode in which the power level is that one typically available in residential installations; the rating of standard power outlets varies from country to country. In most of the European countries the standard outlet is rated 230 [V], 16 [A], so a power of about 3.7 [kW] can be delivered, and as the example above the battery could be charged in less than 3 hours.

Semi-fast charging mode makes use of power levels exceeding those of a standard domestic outlet, available in typical non-residential settings. The three-phase distribution network is used in Europe as a semi-fast charging mode. The most common system uses four wires with a phase voltage of 230 [V] or a line voltage of 400 [V]. In this case, if the three-phase power system is used for charging the battery, considerably high power can be reached even with a low current: with just 16 [A] per phase, indeed, $\sqrt{3} * 400 * 16 * \cos\varphi = 11.1\ [kW]$ which is the amount of power absorbed by the grid. Always considering the total absorption of 10 [kWh] required by the battery, the vehicle is charged in less than 1 hour. The limits on the power flow absorbed by the battery depends, as a consequence, on the power that can be delivered at the AC side, whilst the DC side, so the battery, doesn't present any obstacle to the absorption of higher power level.

These two charging modes deal with power flows which can be absorbed by the grid by a simple connection with the use of the domestic or industrial plant. Since the battery charger is assumed to be on board, V2G and G2V mode are applied by the connection of the vehicle to the domestic socket outlet, which has to present proper safety features. Particular infrastructures, in fact, have to be considered for this (and all the other different) kind of connection: these charging modes are standardized by international standard IEC 61851-1. This standard separates into four different modes all the possible charging strategy adopted, showing all the safety devices that need to be put inside the system.

MODE 1 The mode is referred to the connection of the vehicle to the grid with the use of standardized socket outlets, with current up to 16 [A], so it regulates both normal and semi-fast charging modes already introduced. This mode corresponds to a non-dedicated infrastructure, such as a domestic socket outlet, that allows an easy deliver of the power requested by the grid (V2G) or by the vehicle (G2V). Although the structure is simple, safety concerns have to be taken into account. On the supply side a fuse or a circuit breaker has to be present to protect the system from over currents. Also an earth connection and a residual current device, which switches off the supply if a leakage current greater than a fixed value (for example 30 [mA]) is detected, have to be provided by the manufacturer. The earth connection is particularly important because any fault inside the vehicle would be dangerous for indirect contact. By the way, the issue here stands on the residual current device: in most countries old electric installations are not equipped with it: thanks to this assumption, some countries have decided to left the responsibility to the users, many others have decided not to allow the use of mode 1. In the places where it is tolerated, this mode is the most widespread for private using, thanks to its simplicity and low investment cost, but the problem which deals with the residual current device (that may not be present), with the potential risks that have to be faced in this unlucky situation, has make the manufacturer to try to find valid alternatives.

MODE 2 Even this mode uses standardized socket outlets, but an additional protection is provided: between the vehicle and the plug an in-cable control box with a control pilot conductor is installed. This solution has been adopted by those countries, like the USA, that have refused mode 1 charging. The main disadvantage of this alternative stands on the control box: it protects the downstream cable and the vehicle, but not the plug itself; unfortunately, the same plug is one of the most liable components of the system.

MODE 3 A direct connection of the vehicle to the grid is here applied by the use of dedicated electrical vehicle supply equipment. The IEC standard requires a control pilot protection between the equipment connected to the supply and the electric vehicle. The control pilot protection is a device which mainly has to verify, in any instant during the connection, that the vehicle is properly connected to the grid, that the protective earth conductor is unharmed, whether the system is charging or discharging the battery. The important advantage coming from this mode stands on the fact that safety is reached even when the vehicle is not connected: when no vehicle is connected to the socket outlet, the socket is dead, and power is delivered only when the plug is correctly inserted and the earth circuit is checked. The connection process checks at first the earth connection and at last the pilot connection, the disconnection follows the opposite situation, so the earth connection is the last to be broken. Besides safety advantage, this sequence ensures that the current is interrupted at the contactor and not at the power electronics contacts, prolonging the life of the accessories.

MODE 4 This mode is defined as the indirect connection of the vehicle to the supply network, utilizing an off-board battery charger, where the equipment is permanently kept connected to the AC power supply, and the situation deals whit DC charging stations. As the charger is located off-board, a connection is necessary to allow the charger to be informed about the type and the SOC of the battery, so it is able to furnish the right voltage and current.

Now that the four modes are introduced, the connection of the cable between the vehicle and the charging outlet can be realized in three different ways, as defined by the same standard IEC 61851-1.

CASE A Cable and plug are permanently connected with the vehicle; this case is generally found only in very light vehicles (Fig. 9.2)

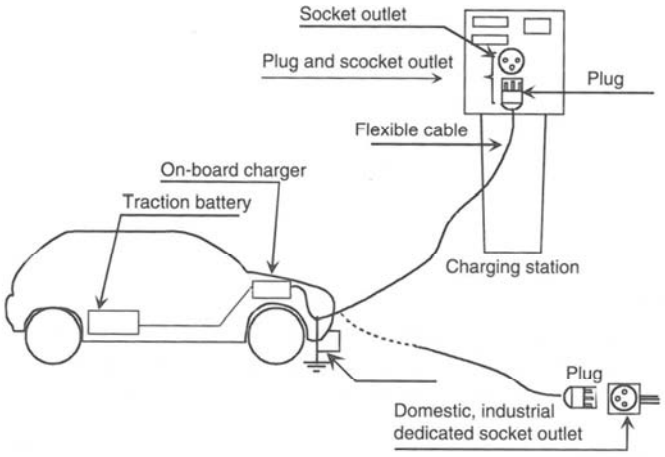

Figure 9.2 - Case A connection [6]

CASE B The cable assembly is detachable and connected to the vehicle with a connector. This is the most common case for normal and semi-fast charging. (Fig. 9.3)

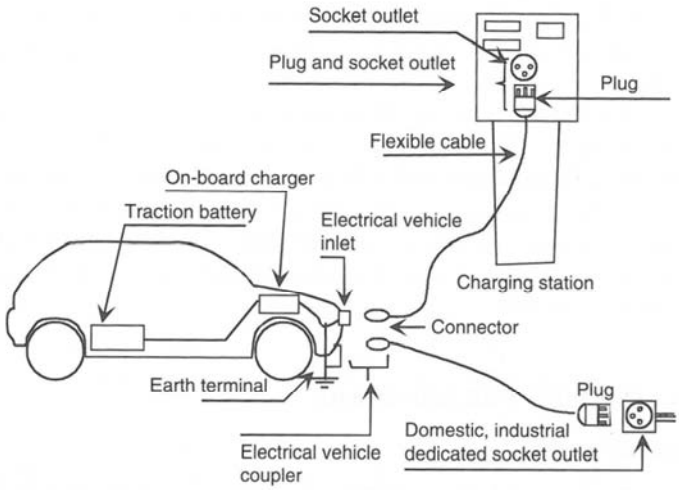

Figure 9.3 – Case B connection [6]

CASE C The cable and vehicle connector are permanently connected to the supply equipment. This arrangement is typically used for fast charging (Mode 4) so that drivers do not have to carry heavy cables around. Public charging stations using this case are however at the higher risk of copper theft. (Fig. 9.4)

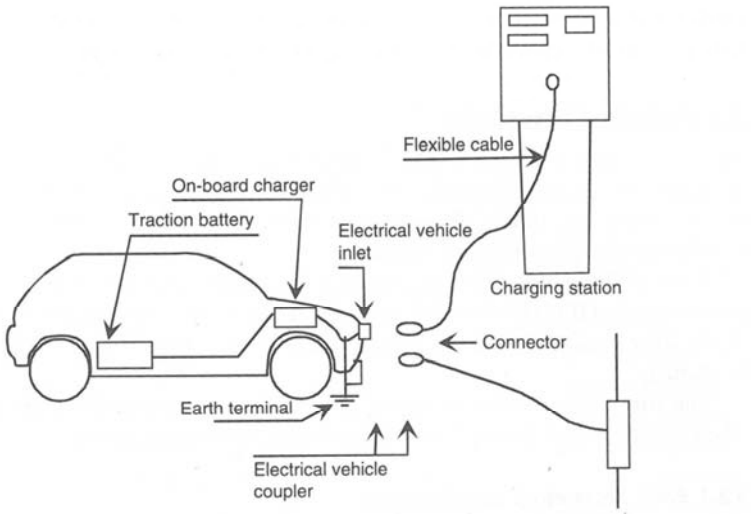

Figure 9.4 – Case C connection [6]

For mode 1 and 3 standard plugs and sockets can be used considering only phase, neutral and earth contacts. In most of the countries, this will usually be the standard domestic plugs, typically rated 10-16 [A]. These domestic plugs are not really suitable for the charging and discharging mode operations, which is characterised by energy flow applied for long times at near rated current and frequent operation including disconnections under rated load. This leads to a shorter lifetime of the accessories and to contact problems which can produce dangerous situations. In this case a better alternative is to use industrial plugs and sockets as defined by the IEC 60309-2. These plugs are widely used for industrial equipment and they are designed for functioning in a way which is comparable to EV charging and discharging mode. The application of the control pilot already introduced necessitates the introduction of specific accessories dedicated only to EV usage; such plugs and sockets are described in the IEC 62196 standard.

Nowadays the coupling technology is growing up quickly, pushed by the widespread of EV technology. A connector accommodating both mode 1 and mode 3 charging has been proposed: it uses particular contacts in such a way that an EV's battery can be refilled in mode 1 with a non-dedicated outlet and in mode 3 on a public charging station.

From the battery point of view, even battery connectors are standardized, and functional requirement can be found on EN 1175-1 standard. Usually the connectors required don't have to be equipped with auxiliary contacts, and the maximum current is fixed at 350 [A] DC. Although these connectors can be found for external connections, their use for mode 4 charging is not advisable, as they are designed neither for the higher battery voltage levels nor for connecting to cable assemblies. Furthermore, they lack earth conductors and are not designed to break a load.

10 – The Practical Realization of a Battery Charger

This chapter deals with the practical realization of the AC/DC converter, which is the heart of the power conversion from AC to DC and vice versa. In this section the laboratory operations for the realization of both the circuitry and the control of the system are exposed, showing how each electronic device works inside the system. The first part deals with the explanation of the electronic devices used, the second part deals instead with the introduction to the dSPACE tool, necessary for the achievement of a proper control system. Before starting the dissertation, the next fig. 10.1 is reported to show the H-bridge topology which will be implemented as a basic circuitry.

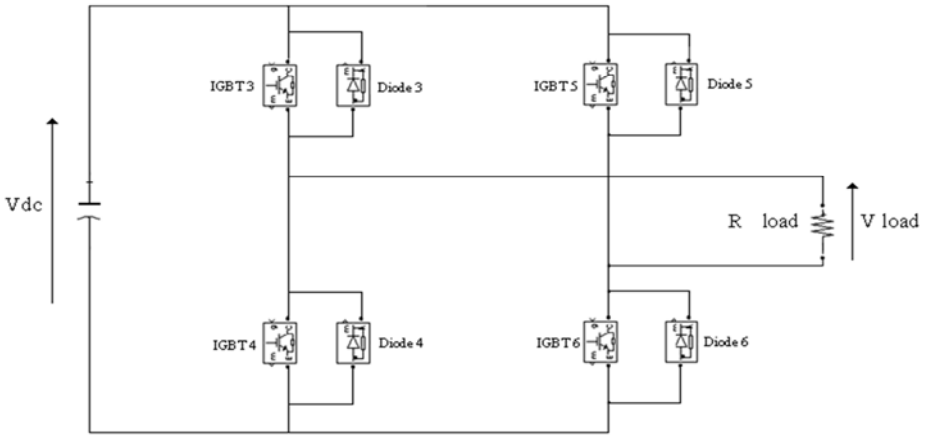

Figure 10.1 – H-bridge topology

The first step consists in the piloting of the circuit with a pure resistive load at its AC side and a DC electrical source which simulates the DC/DC converter and battery system. As a consequence of this, there will be the creation of an alternate sinusoidal voltage through the resistance (the converter acts as an inverter) but the opposite power flow from the load to the DC source can't be produced, since the inductor and the AC power supply are still not inserted. Once verified the correct functioning of the device, the following step will be that of a correct connection of the device to the grid, in such a way to produce bidirectional power flow to simulate V2G and G2V modes.

10.1 – Electronic Devices

The switching device selected is the IGBT - Insulate Gate Bipolar Transistor-, because it can easily work till 70 [kHz] (when the working frequency established for this work is of 20 [kHz]). Also the characteristic is the most indicated for high frequency inverters. The following figure (Fig. 10.1.1) depicts the scheme of the device, taken from the datasheet of the product, with three different pins. Pin 1, which is the gate, corresponds to the pin in which the firing signal has to be applied for making the IGBT conducting. Pin 2 corresponds to the collector, where the current flows inside the device, whilst pin 3 is the emitter, where the current flows out of it. The presence of the freewheeling diode allows the reverse current flow, which won't be possible with the use of the only IGBT.

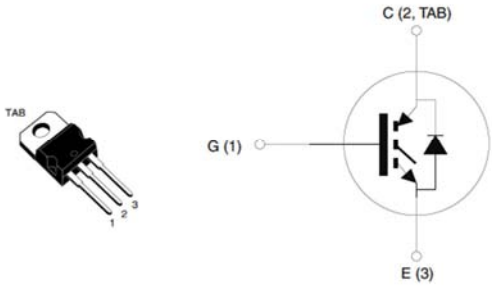

Figure 10.1.1 – IGBT and freewheeling diode scheme

The IGBT will be switched on by the application of a positive voltage of a few volts (over 3.75 [V]) between the emitter and the gate. With reference to the circuit of fig.10.1, IGBT4 and IGBT6 have grounded emitter or, in any case, it is connected to the low voltage of the DC power supply. This means that if the input signal will be applied to the gate, it will surely produce the switching on of the IGBT.

A different case can be found with reference to the upper devices, so with regards to IGBT3 and IGBT5; these two devices present a possible floating potential emitter, due to the dynamic of the switching circuit. This is a problem, since the application of the input signal to the gate will not ensure a positive voltage between the same gate and the emitter, in order to fire the device, and the same device won't work properly. This is because the gate signal is referred to the ground and not to the potential of the emitter.

As a consequence another sort of device is required to complete the H bridge scheme: the **IGBT gate driver**.
Its scheme is reported in fig. 10.1.2, and the important effects of this application are here exposed.
The two depicted input sides are characterised by a low input (LIN) and a high input (HIN); the output side by a low output (LO) and a high output (HO); this driver is able to decouple inputs and outputs in such a way to fire in the proper way the bottom and the upper IGBT (although is not necessary to decouple the low input in this case) avoiding the issue which was affecting the circuitry before. The upper IGBT is properly fired because a virtual earth (named V_S in the scheme) is connected to its emitter. Of course V_S does not present nil potential, but the device guarantees that the voltage between HIN and nil potential (input) is the same between HO and V_S (output).

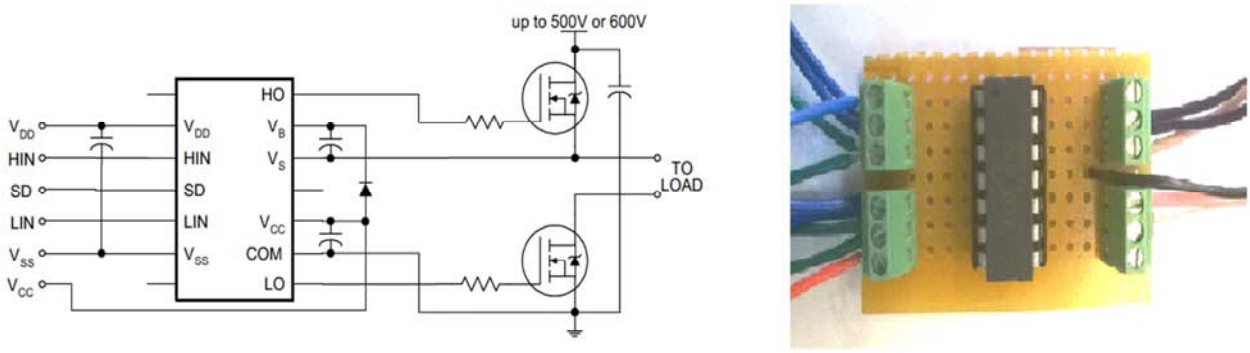

Figure 10.1.2 – Scheme and realization of the IGBT Gate Driver

Now that this issue is solved, before realizing the circuitry of the AC/DC converter by the use of the four IGBTs, a very important thing to do is the introduction of dead times, in such a way to avoid short circuits between the

upper and the bottom switching devices of the same leg. A diode and a capacitor are the device used for introducing a small delay when the gate signal input fires the IGBT, whilst when the gate signal turns to zero no delay is applied. The practical realization of the circuit is depicted by fig. 10.1.3. The four IGBTs are fixed on a heat sink, in order to avoid the overheating of the system.

Figure 10.1.3 – The H bridge circuitry

Now that the circuitry is complete, each leg's work is checked. This inspection is realised at first through the application of the series of two capacitors in parallel with the DC supply. A resistor is grafted between the upper and the bottom IGBTs of the selected leg and the middle point between the two capacitors (in this way an half bridge is created). The two switching devices are then fired by two complementary square waves, and these two firing signals and the voltage through the resistor are measured by an oscilloscope and exposed in fig. 10.1.4. As can be seen the yellow and the green profiles are the gate impulses for firing respectively the upper and the bottom IGBTs, whilst the voltage through the resistor (load) is a square wave with nil mean value.

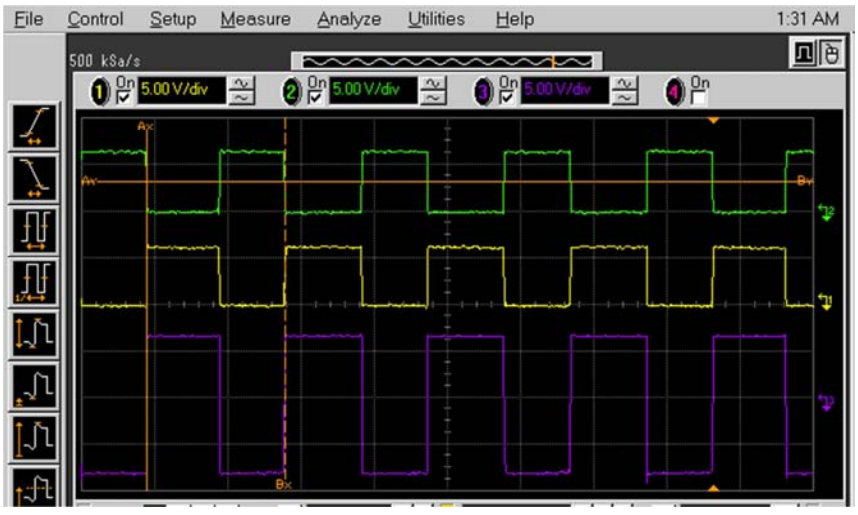

Figure 10.1.4 – Gate inputs for upper (yellow) and lower (green) IGBTs and voltage through the load (violet)

The last important control can be made with regards of the dead times, in order to be sure that effectively no short circuit risks are present. Figure 10.1.5 shows the detail of the two firing signals during the switch.

Figure 10.1.5 – Dead times verification

When this verification is made for both of the legs, this means that the circuitry is correct and the first part is successfully complete: the proper H bridge will be easily completed through the connection of the load between the two legs of the AC/DC converter, whilst the gate signal which fires the upper IGBT of one leg will fire the bottom IGBT of the other leg. If these connections are made and 50% duty cycle square wave signal is applied for the firing of the switching devices, the voltage through the load which can be appreciated is that of a square wave with nil mean value, and whose amplitude is doubled with respect to the amplitude measured in the previous case considered. In this way the first part, dealing with the realization of the circuit and the investigation about the fact that it is effectively working properly, is concluded.

Instead of applying a pure resistive load, the series of an inductive load and an AC source in series with the resistor is applied, in order to model the same grid. After implementing the control strategy, the bidirectional power flow is achieved.

10.2 – Control Strategy: the dSPACE platform

For the achievement of a proper control when the circuit is connected to the grid, an interface which has to be able to fire properly the IGBTs of the AC/DC converter has to be used (since until now a simple signal generator has been used).

The Simulink model already built can be used as the signal source for the proper control of the device: these digital signals from the Simulink model have to be extracted and transformed into analogic signals (DAC conversion). In this way, the results achieved through the model can be reproduced in the real circuit, in a sort of work in parallel.

The dSPACE tool (DS 1103 PPC Controller Board) [16] is an interface specifically designed for the development of high- speed multivariable digital controllers and real time simulations. The controller board is designed to meet the requirements of modern rapid control prototyping, and the application of a Real Time Interface (RTI) makes this tool fully programmable from the Simulink block diagram environment. The application of dSPACE as an interface between the Simulink program already made and the hardware of the system gives the possibility to reproduce the digital data of the program as analogical data to control the real circuit. The AC/DC converter will be directly piloted with the same gate signals that pilot the Simulink's AC/DC converter. If the connection between "master" (Simulink model), "slave" (dSPACE platform) and the real H bridge is conducted properly, the system will run and the results are exposed in fig.10.2.1.

As can be seen, the waveforms of the gate inputs are exactly the waveforms produced according to SPWM elaboration. The load is still a resistor (as a consequence the sine wave current is not yet present). The carrier frequency is 2 [kHz]: higher frequencies exported by the Simulink model will not be successfully implemented, and this depends on the speed of the platform which is not that high for this kind of applications. The waveform produced (violet profile) is measured by a differential probe according to a 20:1 voltage ratio: that is why the signal doesn't appear as high as it should be, considering a DC source of 60 [V].

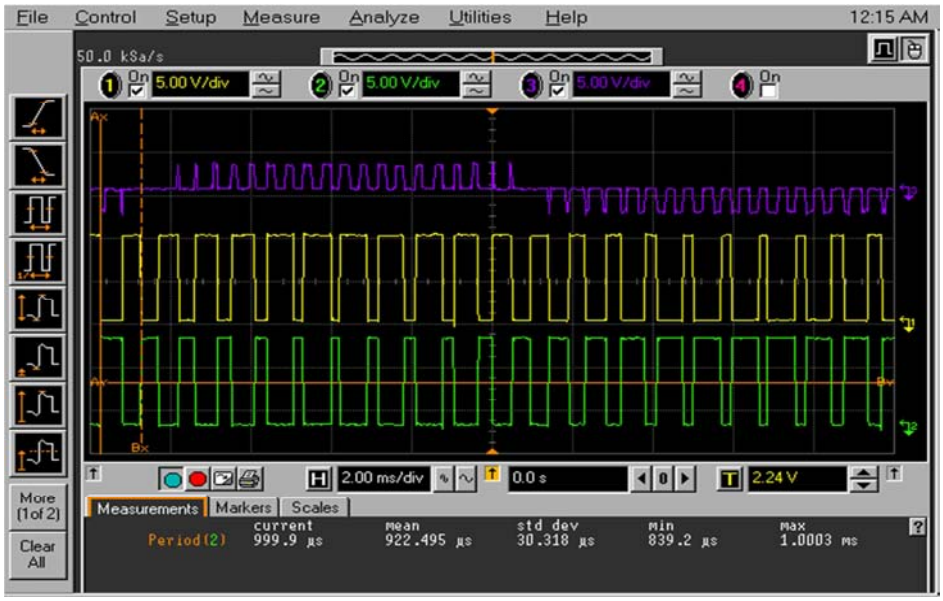

Figure 10.2.1 – Voltage through the load (R) when SPWM technique is applied (violet profile). Yellow and green profiles are the gate signals for the 4 IGBTs

The application of an inductor in series (the AC source is not yet applied: the load is still non active) with the resistor improves the profile of the current through the load. In fact, the series of the RL load, whether the inductor is high enough, will ensure a current characterised by a sinusoidal waveform. This verification is achieved by measuring the voltage through the resistor: this voltage should effectively be a sine wave, and it is (Fig. 10.2.2).

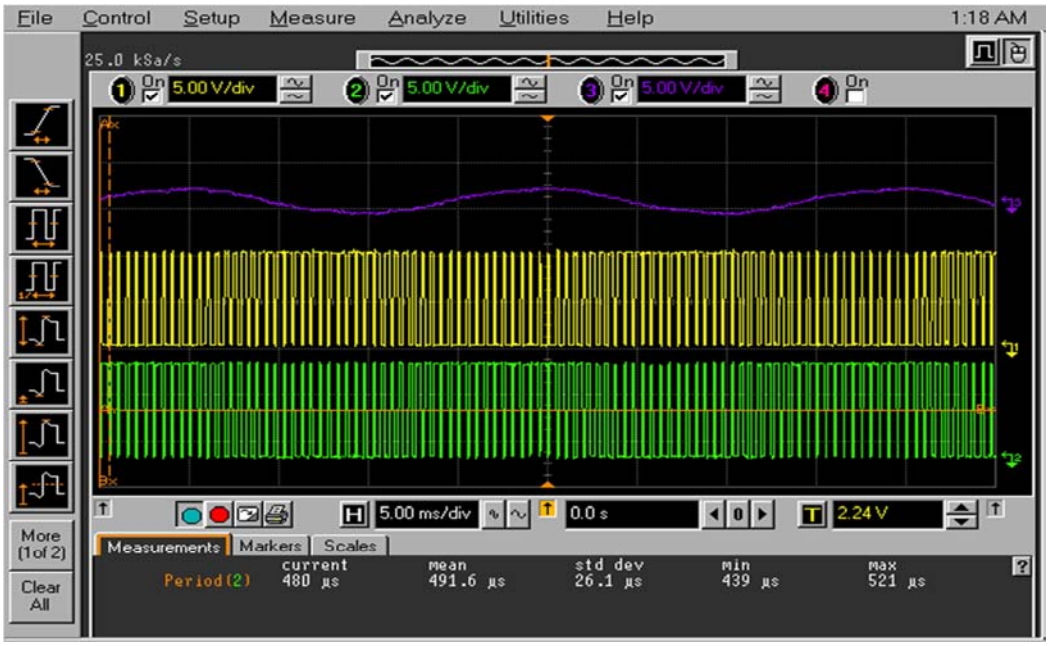

Figure 10.2.2 – Voltage through the resistor (and current through the load) when an RL load is applied (violet profile)

Now that the H bridge is working properly, the **connection of the circuit to the grid** can be done. The RL load already used can be replaced by the application of the AC source to the battery charger (in this way the model of the grid is not necessary; the series of ideal AC source and RL load is represented by the direct connection to the same grid), through the use of a single phase transformer for safety reasons. The idea is that of using the dSPACE platform not only to export data from the model, but also to import external data in it, realizing the conversion from analogic to digital (ADC), and this is fundamental to achieve the synchronization of the battery charger.

The sinusoidal voltage of the grid can be acquired by the use of the same transformer, which can act as an amplitude reducer without modifying the phase (fig.10.2.3). This signal is imported inside the Simulink model environment and then modified, since a certain delay (positive or negative) can be applied on it. The delayed signal obtained can be then used as the reference signal for the SPWM generator. In this way the AC/DC converter creates a sine wave in correspondence of its output which is characterized by a fixed delay with respect to the sine waveform of the grid voltage, and as a consequence the active power flow for the charging or the discharging of the battery is achieved.

The dSPACE tool is running a real time simulation in which there is a contemporary flow of digital data and analogic data. ADC conversion is necessary to monitor the grid sine wave and get the synchronization, whilst at the same time DAC conversion produces the control of the battery charger, firing properly the switching devices (anyway, this process is based on the synchronization data acquired through ADC). The manual variation of the delay (positive or negative) induces the variation of the sine wave produced by the AC/DC converter, so active power will be easily controlled.

Figure 10.2.3 – Single phase transformer, the primary winding connected to the grid (upper wire) and the secondary winding connected to the AC/DC converter and the dSPACE platform as an analogic signal source.

The two following pictures (fig.10.2.4 and 10.2.5) show the two possible situations for charging and discharging purposes. As it can be seen the violet sine wave is the one produced by the AC/DC converter, whilst the purple one is the grid waveform. The amplitude difference between the two waveforms is nil although the oscilloscope depicts two different amplitudes; indeed the two signals are reduced by the use of probes with different voltage ratios.

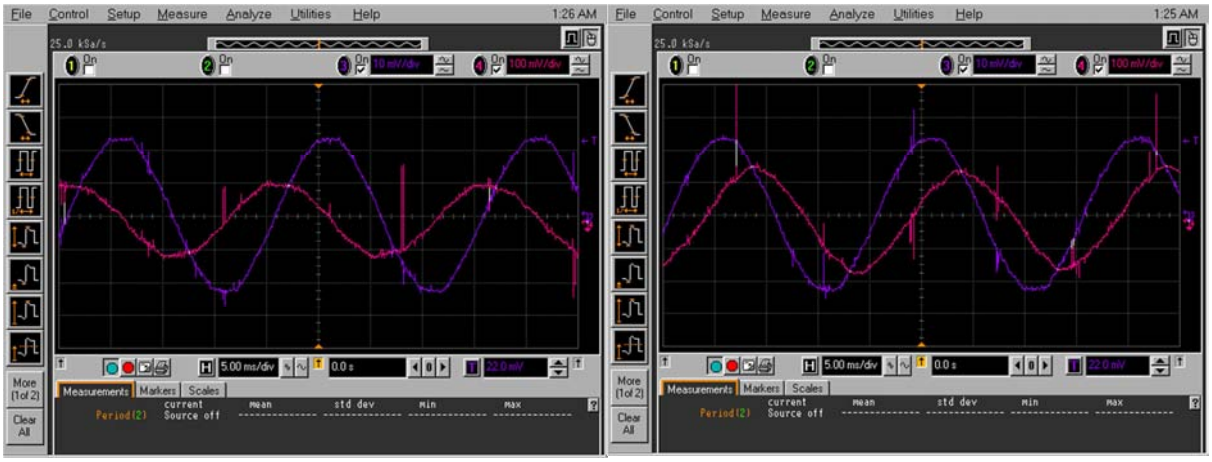

Figure 10.2.4 / 10.2.5 – The profiles on the left depict the AC/DC converter's waveform which lags the grid's waveform and the battery is charged. The profiles on the right depict the AC/DC converter's waveform which leads the grid's waveform and the battery is discharged.

To be sure that the system is working well it is possible to check the current through the battery at the DC side and verify that the sign of the current changes with the variation of the phase angle. With respect to fig. 10.2.4 and fig. 10.2.5, the currents flowing through the battery will be depicted in fig. 10.2.6 and 10.2.7, according to

the dynamic of the system for charging and discharging mode. Figure 10.2.8 shows instead the global configuration of the system working.

Figure 10.2.6 / 10.2.7 – The picture on the left shows a negative current, so a current which is absorbed by the battery, according to the conventions used. The picture on the right shows a positive current, which means the discharging of the battery.

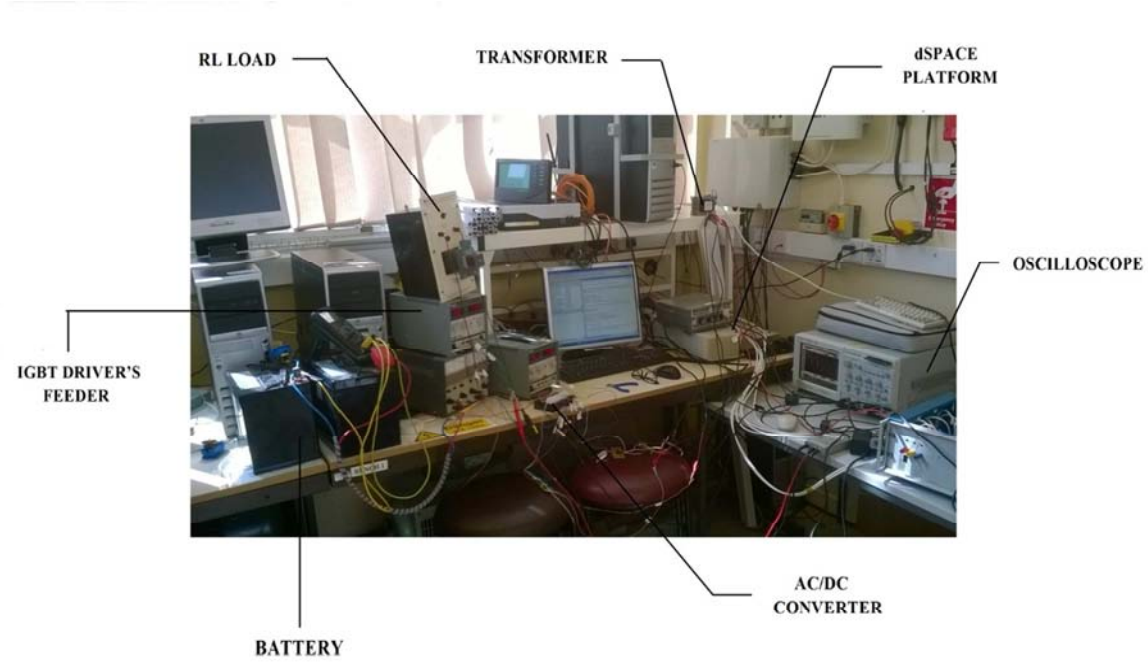

Figure 10.2.8 – Wide shot of the entire system

Final Remarks and Future Works

The design and the realization of the bidirectional battery charger lead to the configuration of a system which matches the requirements pointed out in the introduction. Chapters 5,6 and 8 show indeed how each steady state and transient state that can interest the system (static and dynamic conditions) is suitable for the connection of the EV to the grid, and the consequent achievement of a bidirectional active power flow. The dissertation has demonstrated how this power flow can be successfully produced at first through the implementation of the control strategy using the Simulink platform, whilst the second step is that of the practical realization of the device. The active power flow can be modulated for grid ancillary services whether the smart controller used is able to communicate with the grid manager for instance with an internet protocol (IP). In this work the grid manager is substituted by a block inside the Simulink program, that can be manually set.

The application of the DC/DC converter equipped with a control which is based on the capacitor voltage value is a choice which lead to the possibility to implement a reactive power exchanged control in parallel with the active power control. This is the most important future work that can be done for amplifying the capabilities of the device in terms of ancillary services.

Nowadays the most important application that the bidirectional battery charger can join stands on the system composed by electric vehicles and domestic renewable plant (PV, wind turbine), because the electrical mobility spread has not reached such a level to convince the same grid manager to open to a massive application of V2G/G2V mode yet. Waiting for this scenario to become real, the bidirectional battery charger can handle the power flow produced by the renewable plant in such a way to absorb the energy produced instead of releasing it to the grid, in case of generation higher than absorption. Also the possibility to produce an islanding configuration can be perceived, obviously applying the proper electrical protections.

In this way the customer saves money, power losses are reduced, and the main idea of taking the most advantages from the renewable plant in which the customer invests can be fully achieved, since the self-consumption is maximized.

Appendix 1 - AC/DC and DC/DC Converters' Alternatives and AC/DC Converter's Advanced Control Techniques

In this section some valid alternatives are exposed, both from the topology (AC/DC converter and DC/DC converter) and from the control strategy point of view, in order to justify the original choices taken. The exploration of different options is very important, since it gives the possibility to evaluate strengths and weaknesses of each alternative in order to pick the best model for the selected objective.

1.1 - The AC/DC converter

Different topologies can be faced as an alternative to full bridge converter. **Multilevel power converters** [15] are AC/DC converters that, starting from the same concept of a simple H bridge, are developed for the achievement of higher power quality standard. They need multiple DC sources for synthesizing a staircase voltage waveform, and the commutation of switching devices aggregate these multiple DC sources (DCS), in order to reach high quality voltage in output. The following fig.1.1.1 shows a bidirectional multilevel converter, the cascaded H bridge, that can be used as an alternative of the original H bridge [11].

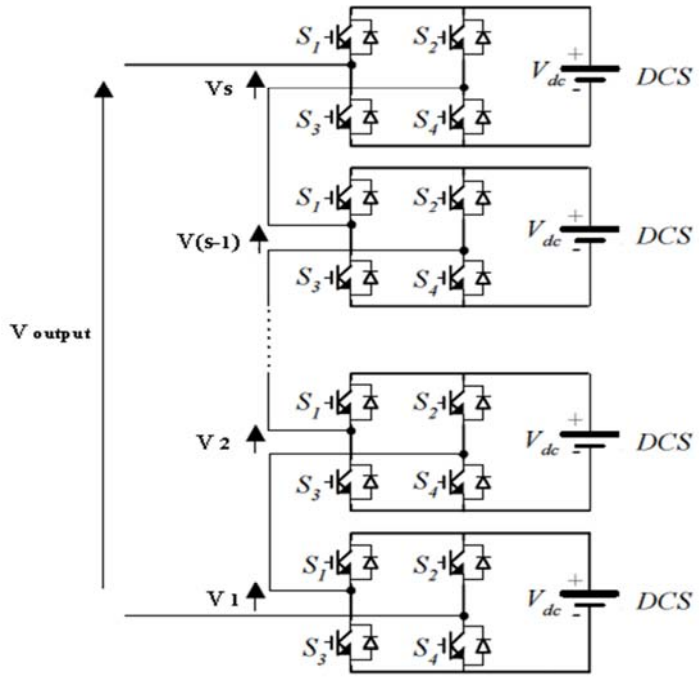

Fig. 1.1.1 – Multilevel converter: cascaded H bridge with s DCS

Each DC source (DCS) is connected to a single phase full bridge converter, and it can generate three different voltage outputs, +Vdc, 0, -Vdc, according to different combinations of the switching devices. The AC output of each converter is connected in series with the others, so the voltage amplitude of the waveform is given by the sum of the converters' outputs. The number of the voltage levels l that the waveform can assume is defined as

$$l = 2s + 1 \tag{1.1}$$

where s is the number of the DC sources. Thanks to this configuration, the waveform produced can be very similar to a sine wave, and the more high is the number of sources, the more the waveform is close to a sine wave and the presence of harmonics is decreased. This configuration is traditionally used for static VAR generation and as an interface with renewable sources, but it has been recently proposed also for EVs purposes. The system indeed can be proposed as the main traction drive of the vehicle, but it can also charge batteries taking the power from an AC supply or when regenerative braking can be applied. From the control point of view, PWM techniques can be properly modified and used in this converter. The most popular techniques use several triangular carrier signals and one reference signal: besides sinusoidal PWM (SPWM) and third harmonic injection PWM (THPWM), also sub harmonic PWM (SHPWM), which is a more advanced technique and it is suitable only for multilevel configuration, can be applied.

The following fig. 1.1.2 a), b) shows a simulation which uses **SPWM** on a cascaded multilevel converter with ten separate 60 [V] DC sources (which means 21 levels). The reference signal is centred in the middle of the carrier signals set (ten different triangular carrier signals, with the same peak to peak amplitude and the same frequency, but each of them with its mean value, different from the others).
When the reference (control) signal is maximum, all the single H bridges produce a voltage equal to +Vdc. When there is a zero crossing, all the "upper" converters (controlled by triangular signal over the zero value) produce positive voltage and all the "lower" produce negative voltage, with the result of zero voltage in output. It can be noticed that in this control scheme the zero output is not allowed for each single converter, which output can be either +Vdc or –Vdc. Zero state can be enabled creating two triangular signal carriers per single H bridge converter, but this is not the case considered.

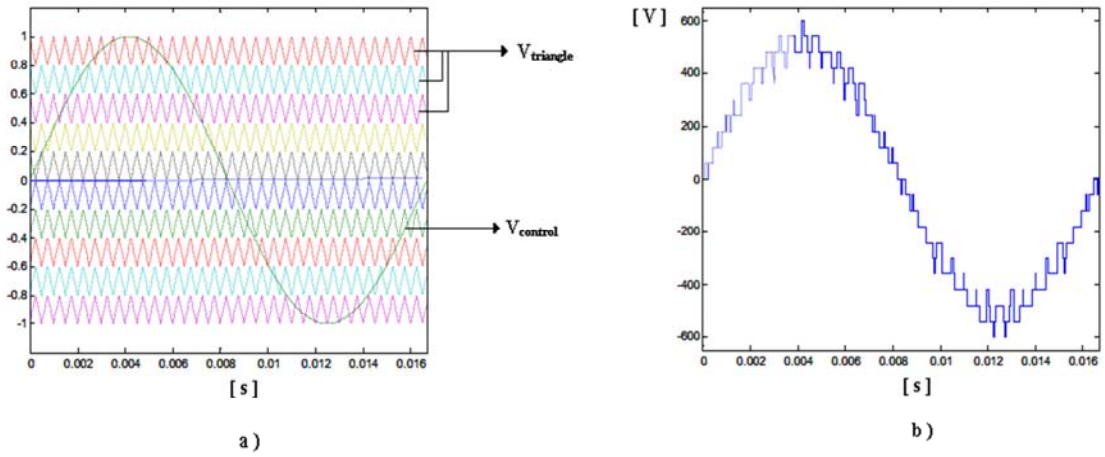

Figure 1.1.2 – a) comparison between the triangular signal of each one of the ten H Bridges and the control signal; b) the 21 levels output voltage waveform

An important alternative is the sub harmonic PWM (**SHPWM**): the principle used is the one already studied for SPWM; when a low modulation index is demanded, the converter will not make use of all its levels, and if the index becomes very low, the converter operates as a traditional converter.

One way to make use of the multiple levels, even during low modulation periods, is to rotate the level usage in the converter after each control signal's period is finished: this can reduce the stresses on some of the inner levels by making use of those outer voltage levels that otherwise wouldn't be used. For modulation indices less than 0.5, the level usage can be so efficiently rotate that the switching frequency can be even doubled (period of the triangular signal carriers halved) and still keep the thermal losses within the limits of the system.

The most important advantage of multilevel converters is surely the production of a high standard output waveform, because harmonic content is limited; at the same time, the H bridge cascade makes the process quick and cheap. The topology needs separate DC sources, required for each single circuit; the voltage of the DC sources can be lower than the voltage required for an equivalent H bridge, but the presence of more than one battery increases the cost of the system. Even the control becomes more expensive, because every battery has to be monitored during charging and discharging, especially during charging mode. In this case, the charging of the battery is the charging of a series of battery, and the characteristic of each one is able to influence the whole process. The losses can be reduced for each switch, but this configuration uses definitely more switching devices than the traditional H bridge. These are the reasons why better performance on voltage and current ripples and harmonic limitations are advantages that don't compensate completely the disadvantage of the application on EVs, even because good results can be anyway ensured by the use of a simple H bridge converter.

1.2 – The AC/DC Control Strategy

Besides the already mentioned SPWM and SHPWM, some different techniques which can achieve better results can be applied for three phase AC/DC converter. SVM technique represent an alternative frequently used, whilst there are some other advanced technique whose usage is not widespread.

The space vector modulation (**SVM**) deals with three phase converter and uses a space vector representation of the converter's AC side voltage. Eight possible switching states are allowed, six of them are active and two non-active. The six active states divide the plane into six sectors. The reference vector, which identifies an output voltage, is obtained by switching on for the proper time two adjacent vectors. In this way, the vector can be implemented by different switch sequences step by step during its rotation, and the non-active vectors can decrease the modulation index. With respect to carrier based PWM (techniques which use a carrier signal), here there aren't separated modulators for each phase, and the reference vector is sampled with fixed clock frequency. A calculation block is used for calculating times of application of the active vectors, and the residual sampling time is reserved for the non-active vectors.

The **random PWM** is another alternative which concentrates on harmonic problems. In fact, apart from the fundamental frequency, all the other components (harmonics) are generally unwanted. The traditional method to alleviate this problem is to insert filters, but random PWM can be an alternative to this remedy. This technique can be implemented simply through the introduction of some modifications of the control circuitry, and it's based on the idea of "randomization": the power carried by discrete frequency components, associated with the "traditional" PWM, is partially transferred into the continuous density spectrum. This means that spectrum originally consisting of narrow band harmonics is mapped into a spectrum whose power is better distributed over the frequency range.

All these techniques can be successfully implemented to the converter, which can produce an output voltage which is useful for feeding the motor or for the connection to the grid, respecting all power quality standards. In this work the requirements allow the use of the carrier base PWM (SPWM), which will be the technique used for the control of the bidirectional AC/DC converter: all the target will be matched properly.

1.3 – The DC/DC converter

Some different techniques have been introduced for getting more advantages from the DC/DC converter's topology. **Interleaved techniques** are used to reduce I/O ripples and to increase the power capacity of the boost converter; in particular, an interleaved DC/DC converter suitable for charging and discharging mode can reduce current and voltage ripples, minimize size and weight of the inductor, improve reliability of power electronic system, and may decrease system losses. As can be seen from fig.1.3.1, two arms composed by a switching device and an inductor can be grafted in parallel for the design of this new DC/DC converter topology, creating a system which is very similar with respect to bidirectional boost converter [19].

This new topology simply splits in two or more arms in parallel the simple bidirectional boost converter configuration [17]. Even the way in which the converter runs is the same because it works with the same principles, but an important difference is now pointed out. During the discharging of the battery, for instance, so when the active power flows from the battery to the grid (V2G mode), IGBT 2 and IGBT 4 are switched off whilst IGBT 1 and IGBT 3 commute. These two commuting switching devices don't work with the same phase (both open or both close), but they present 180° phase difference of driving pulses in a cycle; in this way the fluctuation of input power supply is reduced. For particular applications even more than two arms can be applied. Many other topologies can be used in the field of electric vehicles, for example interleaved coupled inductor boost DC/DC converter [18], clamp mode coupled inductor DC/DC converter, but these are not bidirectional, as they work only as boost converter. These kinds of applications can be found mostly on fuel cell electrical vehicles [20], and the lack of bidirectionality makes them not suitable for the purposes of this work.

Bidirectional interleaved solution fits very well with high voltage ratios (output voltage over input voltage), because in this working field conventional converters are subjected to losses which make their efficiency not acceptable for required standards. This can be a good path to follow for the future, when the voltage of the batteries is expected to grow up more and the standard requirements for power quality in the grid is expected to become even more rigorous.

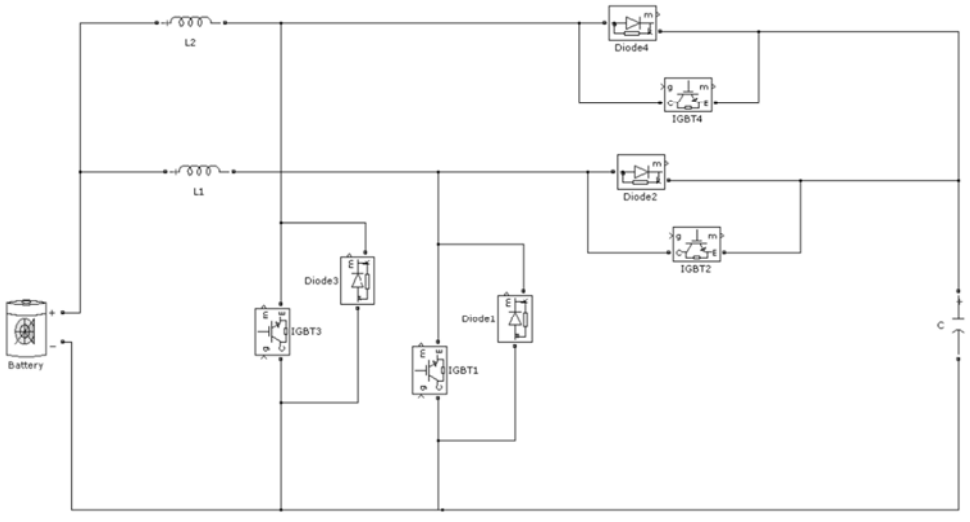

Fig. 1.3.1 - Bidirectional interleaved boost converter

An alternative to conventional or interleaved bidirectional boost topology is brought by the **dual active bridge converter (DAB)** depicted in fig. 1.3.2. The dual active bridge uses eight switching devices and presents a topology which is suitable for high power bidirectional power flow applications. The converter exposed provides high power density and fast control; however, when operations over a wider 2:1 voltage range is required, device

stresses become very high. The principle of operation is that of a transformer: considering V2G mode, the input voltage is transformed from a continue value to an alternate value and thanks to the inductive coupling, an alternate voltage is generated to output side, which is then rectified. This output voltage will be the voltage through the capacitor, so the voltage at the DC side of the AC/DC converter. The principle is that of a transformer, but since it differs from bidirectional boost converters, some difference has to be pointed out: at first when the total amount of power losses is calculated, the thermal ones produced by the switching devices are not the only ones to be considered; even the leakage inductance of the transformer leads to non-negligible losses. Several changes can be made on the original structure to prevent device stresses, particularly if the application deals with ultra-capacitors, which is a problem that leads to low life time and high electrical losses.
Once overcome electrical stresses on switching devices, the achievement of modified configurations is useful for high power applications, such as charging and discharging of ultra-capacitors, but not optimized for being the interface between the battery and the AC/DC converter. If the converter needs to manage the voltage of the battery and the voltage of the DC link, the achievement of good results with DAB [16] converter passes through some more improvements, which are not only electric. For instance, whether the working frequency is fixed to 50/60 Hz, the transformer can produce a considerable weight increase once installed in the vehicle: an optimized DAB consists in two high frequency H bridges coupled with a high frequency transformer; this situation is analysed in the following paraghaph.

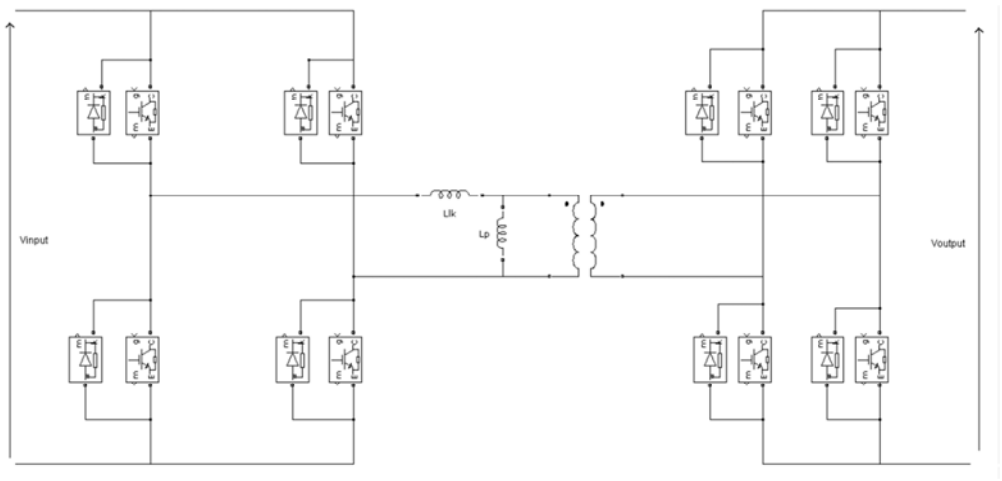

Fig. 1.3.2 – DAB converter with LFT or HFT

Two on board DC/DC bidirectional converter's topologies are shown; several advantages and disadvantages can be investigated. For the LFT (low frequency transformer) the existing hardware present on the EV can be theoretically used: for example the windings of the electrical machine can be, if properly designed, used during charging; however, the additional weight must be accounted in terms of extra power required during traction mode, because the core of the transformer can represent a non-negligible weight. The HFT provides a lighter solution and avoid the issue of malfunctions affecting the drive system of the EV.

All these different DAB topologies present a relevant disadvantage, which is the fact that many devices are involved. Power losses are not negligible (each switch can be less stressed and can also produce less thermal loss, but the total number of switches piloted can be eight: a conventional bidirectional boost converter can suffer from more voltage and currents stresses and its commutating switch may produce more thermal losses, but the switch is just one instead of eight). The fact that many devices are used means that this DC/DC converter may be more expensive and complex with respect to topologies considered before, and at the same time the

reliability of the system decreases because a more difficult control and the failure's probabilities inevitably increase.

The real advantage of this topology and the reason why this model is spreading even if it's not really performing doesn't stand on the real performance of the converter, but on its safety. In fact, manufacturers are trying to pull up the voltage of the batteries produced in order to improve capacity and increase the total energy that can be stored in them. This can be dangerous, because in event of failure of the safety protections or short circuits, relevant electric shock risks can occur. DAB topologies can free from this risk because galvanic isolation between the battery and the circuit is ensured; in this way there is no way for the battery to energize accidentally the circuit, even if for any reason any device fails. The galvanic isolation is an important issue which has been always taken in consideration, but the high costs and the lack of alternatives (galvanic isolation can be ensured only by the use of a transformer) have convinced manufacturers not to apply it on electric vehicles.

Acknowledgements

Now all is done. Years and years of study now they come to an end. The last word of this chapter is already written, a new life is coming.

If I think about these last 24 years, that lead me to this moment, the only feeling that I have is gratitude. When I was a child I hated maths, but my father persuaded me about the importance of this subject: beside its objective necessity in the world of today, maths is the synthesis of a series of rules to be respected, which don't restrain the fantasy or the freedom, but on the contrary they exalt it: the essence of how problems have to be faced, more than escaped. Growing up I started living a life full of happy days and sad days: my mother has always been next to me, and there is nothing better than someone you can share feelings with: nobody, no matter the age, should feel alone for a second; and I've never been. My sister has been the partner (and the victim) of my youth, always present as any sister should be.
All my relatives has always been the best background, and I shared with them many beautiful days.
The friends, Real Friends, are those who have never left: life can put barriers through us, but True Friendship never ends; typing down some names is wasting time, a Friend has no doubt whether I am writing about him/her or not.

This work has been realised during my Erasmus experience in the city of Newcastle upon Tyne at the University of Northumbria (22 Feb-24 Jul 2014); it has been my first experience abroad and I managed to complete it thanks to many helpful people: professor Ghanim Putrus, Edward, Laith among the others; not only scientific support, I felt as a part of their team and my presence important for them. A particular acknowledgement goes to Professor Turri, who gave me the possibility to realise this project, so important for me and my professional and personal growth, which is just started.

Honestly, the citation I put at the beginning of the work talks about Love: the one which is always present, no matter the distances or the circumstances. I took this choice because if this is just a lie, neither Shakespeare nor I have ever written: this work is based on a network of relation which gave me the possibility to reach this point, starting from so far away in the past, when I was just a child. But if this ideal network is just an illusion, all my efforts are based on nothing, and also all my aspirations and my objectives are something that is empty, cold, with any final aim… But I know, this is not the case.

References

[1] G. Putrus, P. Suwanapingkarl, D. Johnston, E. Bentley, M. Narayana, *"Impact of Electric Vehicles on Power Distribution Networks"*

[2] A. Emadi, Y. J. Lee, K. Rajashekara, *"Power Electronics and Motor Drives in Electric, Hybrid Electric, and Plug-In Hybrid Electric Vehicles"*

[3] S. Haghbin, S. Lundmark, O. Carlson, M. Alakula, *"A Combined Motor/Drive/Battery Charger Based on a Split Windings PMSM"*

[4] K. Khan, S. Haghbin, M. Leksell, O. Wallmark, *"Design and Performance Analysis of a Permanent-Magnet Assisted Synchronous Reluctance Machine for an Integrated Charger Application"*

[5] S. Lacroix, E. Laboure, M. Hilairet, *"An Integrated Fast Battery Charger for Electric Vehicle"*

[6] G. Pistoia, *" Electric and Hybrid Vehicles"*, UK, ELSEVIER, 2010

[7] Letendre, Denholm, Lilienthal, *"Electric&Hybrid Cars: New Load, or new Resource?"* 2006

[8] S. S. Hosseini, A. Badri, M. Parvania, *"The Plug-in Electric Vehicles for Power System Applications: the Vehicle to Grid (V2G) Concept"*

[9] M. Kisacikoglu, B. Ozpineci, L. M. Tolbert, *"EV/PHEV Bidirectional Charger Assessment for V2G Reactive Power Operation"*

[10] N. Mohan, T. Undeland, W. Robbins, *"Power Electronics: Converters, Applications, and Design"*USA, Media Enhanced Third Edition, 2003

[11] B. Singh, B. N. Singh, A. Chandra, K. Ah-Haddad, A. Pandey, D. P. Khotari, *"A Review of Single Phase Improved Power Quality AC-DC Converters"*

[12] H. Chen, X. Wang, A. Khaligh, *"A Single Stage Integrated Bidirectional AC/DC and DC/DC Converter for Plug-In Hybrid Electric Vehicles"*

[13] M. Hedlund, *"Design and construction of a Bidirectional DCDC converter for EV applications"* UPTEC, February 2010

[14] J. Zhang, *" Bidirectional DC-DC Power Converter Design Optimization, Modelling and Control"*

[15] M. Malinowski, K. Gopakumar, J. Rodriguez, M. A. Perez, *"A Survey on Cascaded Multilevel Inverters"*

[16] www.dspace.com

[17] S. Dwari, L. Parsa, *"A Novel High Efficiency High Power Interleaved Coupled Inductor Boost DC/DC Converter for Hybrid and Fuel Cell Electric Vehicle"*

[18] S. Han, D. Divan, *"Bi-Directional DC/DC Converters for Plug-in Hybrid Electric Vehicle (PHEV) Applications"*

[19] O. F. Ruiz, I. Cervantes, *"Averaged Modelling of Transformer-Coupled Interleaved Boost Converters"*

[20] G. Calderon-Lopez, A.J. Forsyth, D. R. Nuttall, *"Design and Performance Evaluation of a 10-kW Interleaved Boost Converter for a Fuel Cell Electric Vehicle"*